COUNTER WEAPON CONTROL

THESIS

Brian J. Roadruck

AFIT-ENG-MS-15-M-056

DEPARTMENT OF THE AIR FORCE
AIR UNIVERSITY

AIR FORCE INSTITUTE OF TECHNOLOGY

Wright-Patterson Air Force Base, Ohio

AFIT-ENG-MS-15-M-056

COUNTER WEAPON CONTROL

THESIS

Presented to the Faculty

Department of Electrical Engineering

Graduate School of Engineering and Management

Air Force Institute of Technology

Air University

Air Education and Training Command

in Partial Fulfillment of the Requirements for the

Degree of Master of Science in Electrical Engineering

Brian J. Roadruck, A.S.E.E., A.S.A.S, B.S.E.E.

March 2015

AFIT-ENG-MS-15-M-056

COUNTER WEAPON CONTROL

THESIS

Brian J. Roadruck, A.S.E.E., A.S.A.S, B.S.E.E.

Committee Membership:

Meir Pachter, PhD
Chair

Richard Cobb, PhD
Member

Maj Matthew Dillsaver
Member

Table of Contents

Page

Page

AFIT-ENG-MS-15-M-056

Abstract

Active target defense is an area of exploration as strategic planners seek to protect an airborne target from an attacker. Current counter measures include electronic warfare (i.e. jammers) and diversionary measures (chaff or flares). An additional defensive measure proposed is the employment of a defender missile. In an active target defense scenario, a target is defended from an attacker with a defending missile. In this scenario, the target seeks to escape, the attacker strives to capture the target, and the defenders goal is to intercept the attacker before the latter reaches the target. The target and defender cooperate such that when the defender intercepts the attacker, the target-attacker separation is maximized while the attacker strives to minimize said distance. Approaches based on optimal control theory have been proposed to develop guidance strategies for the target-defender team assuming the attacking missiles control law is known. These approaches model the target defense scenario as a one-sided optimal control problem. In previous work, the target defense scenario has also been modeled as a two sided optimization problem, whereby linear quadratic differential game theory is applied. In our work, pursuit-evasion differential game theory is applied to the target defense scenario. The targets, attackers, and the defenders positional information is assumed to be known to the players. With positional information, a computational efficient method of strategy synthesis can be derived applying a differential game theory approach. We demonstrate that when non-optimal strategies are employed by one of the players, e.g. LOS guidance, the outcome will favor the players that employ the optimal strategy given by the solution of the pursuit-evasion differential game.

AFIT-ENG-MS-15-M-056

Dedication

I would like to acknowledge Dr. Pachter as my advisor on this research project, Maj Dillsaver and Dr. Cobb as my committee members. It is through their guidance I was able to produce results that will further research efforts into solving optimal control problems with differential game theory. I wish to thank Capt. Carr for his efforts and time in providing optimal control theory results I was able to include in this research. I also wish to thank my fellow ANT-lers, as I could not have hoped to have a better group of classmates. Everything is awsome when you are part of a team. I feel honored and privileged to have shared the AFIT experience with you. To Capt. Kawecki and Capt. Jones, thank you guys for being the sanity check and sounding boards that kept me on track. And finally to my family, thank you for being there. And to my beloved bride, thank you for understanding the time I needed to complete the experience here at AFIT.

List of Figures

Figure Page

List of Tables

COUNTER WEAPON CONTROL

I. Introduction

Active target defense is an area of interest to the Air Force. Optimal control theory has been employed to obtain strategies for both a defending missile and the target aircraft to protect it from missile attack. Most of the scenarios considered in the literature are two agent events consisting of the attacker and target, with one assumption being a predictable trajectory for either the target or the attacker. In practical applications, such a trajectory is not always predictable. In this work, it is assumed that a target has a defender intercepting the attacker, resulting in an active target defense scenario with three agents: the Target, the Attacker, and the Defender. The research presented in this thesis explores an alternative method to optimal control theory by taking advantage of positional information and differential game theory to develop strategy formulations for all three agents. Expected benefits are to develop an analytic solution that exploits positional data that is obtainable from radar data.

Protecting a high value target from adversaries is a goal of any target defense scenario. In the early days of warfare, the active target defense scenario would be about defending a castle attack. In this scenario, the target castle is static: the defenders are initially inside and somewhat static as they are to repel the attack; the attackers are somewhat static in that the siege engines are not easy to move. The distance from the siege engines to the castle walls would be a variable to be optimized. The defenders' goal is to maximize the distance the attackers can be from the walls, ren-

dering the siege engines ineffective. The attacker's goal is to minimize the angle, to give the siege engines maximum effect. The scenario is a zero-sum game as one side will control the distance to their advantage, and the strategies of all agents becomes fixed once the siege begins.

As technology progressed, targets became mobile. An example of mobile target are battleships of WW II, such as the Bismark. Before the final battle of the Bismark, the ship was maneuvering to avoid incoming torpedoes of British aircraft. For this scenario, the Bismark is a mobile target, the German gunners of the Bismark are the static defenders and the British aircraft are mobile attackers. The attackers had to adjust their strategy to be in the correct place to release the torpedoes and score a hit on the Bismark. The Bismark strategy is to maneuver so the attackers do not have a constant bearing to release the torpedoes. For the torpedoes to hit the Bismark, the attackers would predict the trajectory of the ship and release the torpedoes based the future position of the ship. The torpedoes had no ability to make heading changes in response to the maneuvers of the Bismark. Fifteen British torpedo bombers attacked the Bismark with torpedoes. Of the torpedoes launched at the Bismark, only two hit: the predicted trajectory of the ship was correct for the two hits, and thus the attackers scored a low hit ratio.

In more modern times, fighter aircraft could possibly be equipped with anti-air missiles. Ground-based anti-air missiles are capable of hitting airborne targets at an altitude of 30 thousand feet or more, as seen in the 1990's in Iraq. For this scenario, both the target and attacker are mobile. The counter-measures employed by the target are electronic countermeasures and flares. In this scenario, the target is an evader, the attacker is a pursuer and there is no defender other than the countermeasures. An

additional defensive option is to launch a defender missile to intercept the attacking anti-air missile. Then the scenario changes from a two agent pursuit-evasion problem to a three agent problem.

1.1 Problem Statement

The goal of this work is to provide a method of deriving guidance laws for the three agent scenario by applying differential game theory. The guidance laws will be developed based on positional information provided by an assumed radar system giving each agent situational awareness of the other agents. The developed guidance laws will be capable of using the positional information to calculate an optimal strategy to be taken by the agents. The optimal strategy will be tested against sub-optimal strategies to verify the optimal strategy is the best choice for the agents.

1.2 Motivation

Active target defense system exists for armored vehicles. An example of one of such systems is the Trophy Active Protection System [9]. This system is designed to counter the threat of anti-armor threats such as anti-tank missiles or Rocket Propelled Grenades. The Air Force Office of Scientific Research is interested in basic research into adversarial interactions where differential game theory and probabilistic modeling can be employed to synthesize guidance laws [6]. The goal is to develop a computationally efficient method of deriving optimal guidance laws based on positional information. Developed guidance laws would be able to utilize positional data from radar systems to track and intercept threats. The goal is to develop systems that can be fitted to existing aircraft ranging from attack aircraft, military transports and commercial aviation. Military aviation would benefit as active defense systems

are additional countermeasures to threats. Commercial aviation would benefit from active defense systems to counter potential threats since some air routes pass through conflict zones.

1.3 Scope

The scope of the research is to develop target and defender guidance laws based on differential game theory. The outcome of this research is to validate the fundamental geometry of the guidance laws. High fidelity flight dynamics are not within the scope of this research. After the guidance laws are verified, future research will include layering of flight dynamics and additional environmental effects.

1.4 Organization

Chapter I introduces the subject and provides a brief historical perspective. Chapter II highlights the development of guidance laws as employed by the agents in the active target defense scenario. Chapter III discusses the mathematical formulation of the strategies employed by the agents, and an overview of the optimal control theory analysis tool. Chapter IV presents the results of the simulations and the results from the optimal control theory analysis tool. Chapter V presents the conclusions of the simulations, a comparison between differential game theory solutions and optimal control theory solutions, and directions for future research.

II. Background

2.1 Introduction

This chapter provides a highlight of the development of some common guidance laws for pursuit-evasion games. The highlights cover the early research breakthroughs, followed by refinements to guidance laws for optimal control modeling. As part of the refinement exploration, additional tools for solving pursuit-evasion games were developed and modeled as differential equations leading to differential game theory.

Pursuit-evasion games have a zero sum outcome, that is the pursuer captures the evader, or the evader escapes. Early research in pursuit-evasion scenarios led to the development of Proportional Navigation (PN) guidance, which in steady state amounts to collision course navigation. PN guidance laws are based on the assumption that the attacker's velocity is greater than the target's velocity, and both have constant velocities as explored in "Homing and Navigation Courses of Automatic Target-Seeking Devices" by Yuan.[22]. The goal was to derive navigation laws that a pursuer would employ to capture an evader. A key assumption is that the target is moving on a fixed course, making the analysis of the engagement's kinematics easier. The simulations show the attacker following a curved trajectory that results in the attacker homing in on the target. One of the conclusions of Yuan is that there is a speed ratio critical to successful capture. The larger the ratio of attacker velocity to target velocity, the larger the tangential curve. If the attacker's velocity is more than twice that of the target's velocity, the attacker's turn radius becomes large enough to be impractical for a successful capture.

The issue of an accelerating target is also a subject of study. In a real-world application, the target will not be moving in a predictable fashion as it executes maneuvers to evade the attacker. This led to the development of Augmented Pro-

portional Navigation (APN) as discussed by Garber in "Optimum Intercept Laws for Accelerating Targets" [7]. The effect of target acceleration is considered as part of the attacker's guidance law. A target that has a changing course was also addressed by implementation of an outer feedback loop in PN guidance laws. The addition of a feedback loop yielded the optimal guidance law as noted in "Optimal Intercept Guidance for Short-Range Tactical Missiles" by Cottrell [5]. All three guidance laws were developed using optimal control theory. PN has received much attention in terms of exploration for opportunities to refine the guidance law formulation discussed by Baba and Yamaguchi in "Generalized Guidance Law for Collision Courses" [2]. An assumption made in formulating these guidance laws is a predictable target trajectory as discussed in "Differential Games and Optimal Pursuit-Evasion Strategies" by Ho and Bryson [8].

Optimal control theory synthesized optimal strategies in two agent pursuit-evader scenarios. Anderson examined formulations of the two body scenario in "Comparison of Optimal Control and Differential Game Intercept Missile Guidance Laws" [1]. To derive an optimal strategy for Target (T), it is assumed the Attacker's (A) guidance law is known. Conversely, to derive an optimal strategy for A, it is assumed T's guidance law is known.

Optimal control theory can minimize or maximize a variable provided the other conditions are known or assumed. In a pursuit-evasion scenario implementing optimal control theory solutions, a given scenario is solved where A minimizing or T maximizing the Attacker-Target (A-T) distance. Shima in "Optimal Cooperative Pursuit and Evasion Strategies Against a Homing Missile" [19] demonstrated optimal control theory application to pursuit-evasion scenarios involving two agents. The attacker has the goal of capturing T, therefore the optimization problem entails minimizing the A-T distance. The assumption made is T follows a predictable trajectory thereby

making the problem one sided. The same scenario is also considered for T, where the distance is maximized. To solve the problem as a one sided problem, A is assumed to be following a predictable course.

Optimal control theory has been applied to three agent pursuit-evader scenarios as explored by Boyell in "Counterweapon Aiming for Defense of a Moving Target" [3]. The assumptions are (1) A's guidance law is known, and (2) T and (3) a Defender (D) are working in a cooperative fashion. The goal of the team is to have T avoid capture by A. For this scenario, the optimal strategy is for T to evade A, and D to intercept A. In "Optimal Cooperative Pursuit and Evasion Strategies Against a Homing Missile" by Shima [19], the scenario investigated is A is homing in on T, and T is luring A into the range of D where D can intercept A. Under this construct, there are one of two end results can occur. The first one is the T-A interception event, and the second one is the D-A interception event. Here, T is evading A, and D is pursuing A. The goal for T, is minimizing the D-A distance, whereas in a one on one engagement T would seek to maximize the T-A distance. Additional exploration of the problem is examined by Prokopov in "Linear Quadratic Optimal Cooperative Strategies for Active Aircraft Protection" [15].

Shima also examined a three agent problem where there is an A, and a D-T team. The D-T team is considered to have a goal of minimizing the D-A distance. Ratnoo,et.al also explored a solution for the D-T team in the three body problem where the defender follows a Command to Line Of Sight (CLOS) in "Line-of-sight Interceptor Guidance for Defending an Aircraft" [16]. For CLOS guidance, T is tracking both A and D. Ratnoo et.al further refined the LOS exploration in "Guidance Strategies Against Defended Aerial Targets" [17]. Additional exploration and refinement of CLOS was investigated by Yamasaki, et.al in "Modified Command to Line-of-Sight Intercept Guidance for Aircraft Defense" [21].

Applying optimal control theory to analyze pursuit-evasion scenarios can lead to some high-level mathematics depending on what is being optimized (time to capture, energy expenditure, or miss distance). In pursuit-evasion scenarios, both agents have goals that are in direct opposition to each other. For example, the attacker's strategy is to minimize the distance to the target, and the target's strategy is to maximize the distance to the attacker. Oyler implemented differential game theory in "In Pursuit-Evasion Games in the Presence of a Line Segment Obstacle" [12]. In the article, the author solves for the optimal strategy with differential game theory. Optimal solutions can be found for minimizing or maximizing. Given the agents have situational awareness of the opposition, the problem entails a minimization and a maximization. Minimizing and maximizing simultaneously, the problem becomes two-sided. Optimal control theory may not the best tool for a two-sided problem and does not guarantee capturability in the face of intelligent opposition [8]. The application of differential game theory can address two-sided optimization problems and its big advantage is it does not require prior knowledge of any one agent's trajectory or strategy.

Differential game theory allows differential equations to model the attendant dynamics of the agents playing the game. Isaccs has analysis of pursuit-evader different games involving two agents [10]. Game analysis included scenarios such as torpedo and a ship, dog fighting aircraft or a missile intercepting an aircraft. Pursuit-Evasion games are non-cooperative in nature as each player has goals that are in opposition as discussed by Bressan in "Noncooperative Differential Games. A Tutorial" [4].

By using differential equations, the cost/payoff function can be set to zero (i.e.: distance from Pursuer to Evader at end of game), and the resulting equation can then be minimized for one agent and simultaneously maximized for the other. The output of the solutions result in strategies for each side. The strategies developed are the moves the agents can make to achieve their respective objectives. These games

have a payoff quantity, and if both agents have selected strategies that yield the best payoff for the respective agents, then optimal strategies were chosen. The payoff under optimal play reached a min-max. The min-max is when a minimum for one agent and a maximum for the other has been reached at game conclusion. When non-optimal strategies are selected, the payoff will favor one agent more than the other.

An alternative approach to solving a pursuit-evasion scenario involving three agents is proposed by Rusnak in "The Lady, the Bandits, and the Body-Guard Game" [18]. The goal of the Lady and the Body-guard is to maximize the distance to the Bandits. The Bandits' goal is to minimize the distance to the Lady. The proposed game scenario is the Lady and the Body-Guards are one cooperative team and the Bandits are an opposing cooperative team. The two teams have non-cooperative goals, as the game is zero sum. An exploration of this concept was explored by Perelman,et.al in "Cooperative Differential Games Strategies for Active Aircraft Protection from a Homing Missile" [14]. Currently, the literature supporting three body pursuit-evasion games are modeled in DGT with predicted trajectories, and not with positional information.

Differential game theory has a few differences over optimal control theory. PN and APN do not have a feedback loop, and optimal control theory is suited to solving open-loop problems. Differential game theory requires feedback, as the strategies need to be identified with feedback control laws [8]. Optimal control theory does not guarantee a conclusion to the game, whereas differential game theory will have conclusion to the game. Optimal Control theory can solve for a minimum or maximum solution. In differential game theory, two sided pursuit-evasion games can be solved by finding a minimum and a maximum simultaneously. The motion of the agents are described in the non-rotating Euclidean space, or realistic space, by kinematic

equations. The kinematic equations can be reduced in degree in a rotating frame called the reduced state space. As the pursuit-evader game takes place, the agents have heading information to achieve their respective goals. The headings, or strategies are synthesized in the reduced state space, and executed in the realistic space.

2.2 Summary

Early exploration of pursuit-evasion games lead to development of guidance laws with modeling to find optimal solutions based in optimal control theory. As higher fidelity models were explored, modified guidance laws developed. Additional tools for solving pursuit-evasion games resulted in differential game theory.

III. Methodology

3.1 Introduction

In this chapter, the methodology for strategy synthesis of the agents is presented. First, the formulation of the problem is discussed. Next, the strategies of the agents are presented. Third, the Apollonius circle is presented as part of the formulation of strategies. The fourth topic is the optimization process. The fifth topic are the cases where the target is static is presented. Finally, the setup the Optimal Control Theory (OCT) problem solver solutions is discussed.

3.2 Formulation

The problem is formulated with the assumption engagement beginning Beyond Visual Range (BVR). The agents playing the active target defense game are the Target (T) aircraft, an Attacking (A) missile, and a Defending (D) missile protecting the target aircraft. It is assumed that D will intercept A during the game at the intercept point I. The goals for each agent are as follows: A seeks to minimize the distance between the intercept point I where he is intercepted by D, and T; D seeks to maximize the distance between said intercept point I and T; T, with a goal of escape, seeks to maximize the distance between A and T at the instant of interception of A by D at intercept point I. Both D and A have a capture circle. When A is in D's capture circle, the simulation ends as A has been intercepted. Likewise, when T falls in A's capture circle, the simulation ends as T is intercepted by A. At BVR, flight dynamics and environmental effects are neglected. Thus, it is assumed the agents are modeled as point masses. There is a velocity difference between A and T with the assumption A's velocity is higher than T's velocity. The velocity ratio α is defined as

$$\alpha = \frac{v_T}{v_A} \tag{1}$$

where v_A is the velocity of the attacker and v_T is the velocity of the target. Thus, v_A is normalized, and v_T, which is less than v_A, is $0 < \alpha < 1$. If $v_T \geq v_A$, then there is no need for D or consequently the target defense game, as T can always escape. It is here assumed that the velocities of A and D, are the same: $v_A = v_D$. The active target defense game occurs in realistic space that is the non-rotating two dimensional Euclidean plane (x,y). Within the realistic space, a reduced state space exists and is designated as (X,Y). The reduced state space is constructed such that its x-axis is a line segment connecting the points A and D, the y-axis is the orthogonal bisector of the segment $\overline{AD}$, and the origin O of the reduced state space (X,Y) is the midpoint of the segment $\overline{AD}$. Thus, the position of A in the (X,Y) reduced state space is A=(A_X,0), the position of D =($-A_X$,0) since the bisector is midway between A and D, the starting point for A is mirrored by D along the X axis, and the position of T=(T_X, T_Y). The attacker, defender and target coordinates in the realistic plane (x,y) are designated as A=(A_x, A_y), D=(D_x, D_y) and T=(T_x, T_y), respectively. Figure 1 shows the realistic space and the reduced state space.

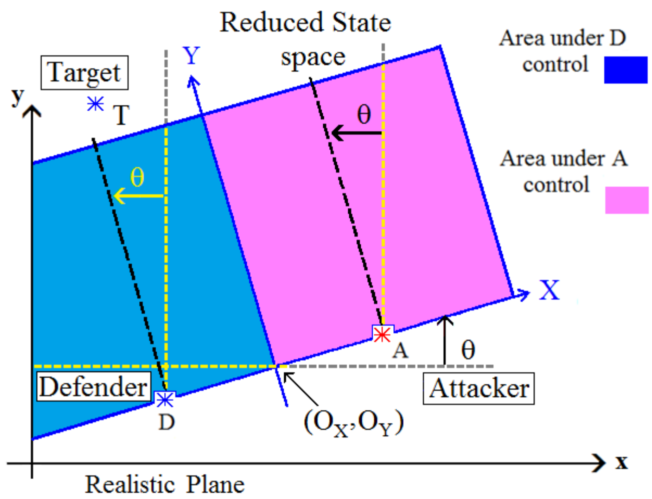

Figure 1. Frame rotation

The origin of the local frame at O is at the midpoint of the segment $\overline{AD}$ and its X-axis is aligned with the $\overline{AD}$ segment. Agents A and D have areas of control, namely points in the plane which can be reached by A before D (as shown in Figure 1) and, vice versa, the points in the plane which D can reach before A. In the reduced space, the boundary of the areas controlled by A and D is the orthogonal bisector of the segment $\overline{AD}$ because $v_A = v_D$. It defines the Y-axis of the local frame whose origin O is at the midpoint of the segment $\overline{AD}$; the X-axis of the reduced state space connects points A and D. Thus, the origin of the reduced state space (X,Y) in the realistic space (x,y) is

$$(O_X, O_Y) = \left(\frac{A_x + D_x}{2}, \frac{A_y + D_y}{2}\right) \tag{2}$$

The reduced state space (X,Y) is rotated by an angle θ relative to the realistic space plane (x,y):

$$\sin\theta = \frac{A_y - D_y}{\sqrt{(A_x - D_x)^2 + (A_y - D_y)^2}} \tag{3}$$

$$\cos\theta = \frac{A_x - D_x}{\sqrt{(A_x - D_x)^2 + (A_y - D_y)^2}} \tag{4}$$

The transformation for translation and rotation of the reduced state space (X,Y) relative to the realistic space (x,y) is

$$X = (x - O_x)\cos\theta + (y - O_y)\sin\theta \tag{5}$$

$$Y = -(x - O_x)\sin\theta + (y - O_y)\cos\theta \tag{6}$$

By inserting the expressions for $\sin\theta$, $\cos\theta$ and the position of the reduced state space origin O in the realistic space

$$\begin{aligned} X = {} & \left(x - \frac{A_x + D_x}{2}\right)\left(\frac{A_x - D_x}{\sqrt{(A_x - D_x)^2 + (A_y - D_y)^2}}\right) \\ & + \left(y - \frac{A_y + D_y}{2}\right)\left(\frac{A_y - D_y}{\sqrt{(A_x - D_x)^2 + (A_y - D_y)^2}}\right) \end{aligned} \tag{7}$$

$$\begin{aligned} Y = {} & \left(x - \frac{A_x + D_x}{2}\right)\left(\frac{A_y - D_y}{\sqrt{(A_x - D_x)^2 + (A_y - D_y)^2}}\right) \\ & + \left(y - \frac{A_y + D_y}{2}\right)\left(\frac{A_x - D_x}{\sqrt{(A_x - D_x)^2 + (A_y - D_y)^2}}\right) \end{aligned} \tag{8}$$

Figure 1 shows the rotation angle between the reduced state space and the realistic space. Since the reduced state space X-axis connects A and D, $A_Y = D_Y = 0$ by construction. The bisector being halfway between A and D means that the agents A and D are located one half the distance to the bisector. Thus, the positions of A and D in the reduced state space are

For A:

$$A_X = \frac{1}{2}\sqrt{(A_x - D_x)^2 + (A_y - D_y)^2} \tag{9}$$

$$A_Y = 0 \tag{10}$$

For D:

$$D_X = -\frac{1}{2}\sqrt{(A_x - D_x)^2 + (A_y - D_y)^2} \tag{11}$$

$$D_Y = 0 \tag{12}$$

For T:

$$\begin{aligned} T_X = {} & \left(T_x - \frac{A_x + D_x}{2}\right)\left(\frac{A_x - D_x}{\sqrt{(A_x - D_x)^2 + (A_y - D_y)^2}}\right) \\ & + \left(T_y - \frac{A_y + D_y}{2}\right)\left(\frac{A_y - D_y}{\sqrt{(A_x - D_x)^2 + (A_y - D_y)^2}}\right) \end{aligned} \tag{13}$$

$$
\begin{aligned}
T_Y = &-\left(T_x - \frac{A_x + D_x}{2}\right)\left(\frac{A_y - D_y}{\sqrt{(A_x - D_x)^2 + (A_y - D_y)^2}}\right) \\
&+ \left(T_y - \frac{A_y + D_y}{2}\right)\left(\frac{A_x - D_x}{\sqrt{(A_x - D_x)^2 + (A_y - D_y)^2}}\right)
\end{aligned} \tag{14}
$$

3.3 Strategies

The goal for A is to get to T, and D's goal is to prevent A getting to T by intercepting A. Hence, the equal speed of agents A and D will meet at point I on the orthogonal bisector of the segment $\overline{AD}$ as shown in Figure 2. The intercept point I is on the Y axis and its vertical distance (noted as Y in Figure 2) is the distance from the origin O to the intercept point I. The optimal choice of Y will be discussed in the following sections. The strategies of each agent are specified in terms of heading in the reduced state space. Figure 2 shows the strategies in the reduced state space.

$$\text{For A}: \quad \psi_A = \arctan \tfrac{A_X}{Y} \tag{15}$$

$$\text{For D}: \quad \psi_D = \arctan \tfrac{A_X}{Y} \tag{16}$$

$$\text{For T}: \quad \psi_T = \arctan \tfrac{T_Y - Y}{-T_X} \tag{17}$$

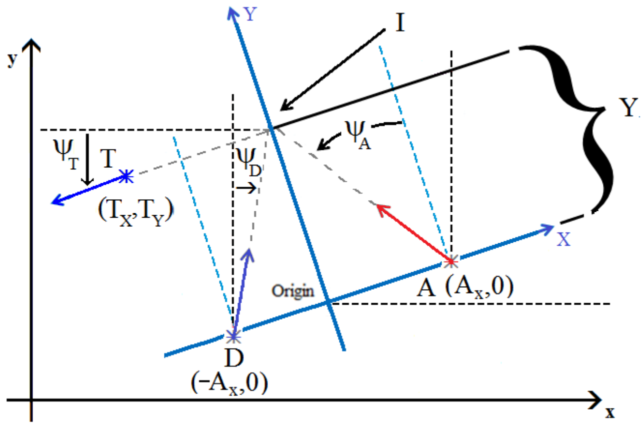

Figure 2. Strategies in reduced state space

The simulations are performed in the realistic space. The realistic strategies are expressed as the reduced state space heading with the rotation and translation between the spaces included. Figure 3 shows the strategies in the realistic space.

$$\text{For A}: \quad \phi_A = \arctan \tfrac{A_X}{Y} + \theta \tag{18}$$

$$\text{For D}: \quad \phi_D = \arctan \tfrac{A_X}{Y} - \theta \tag{19}$$

$$\text{For T}: \quad \phi_T = \arctan \tfrac{T_Y - Y}{-T_X} + \theta \tag{20}$$

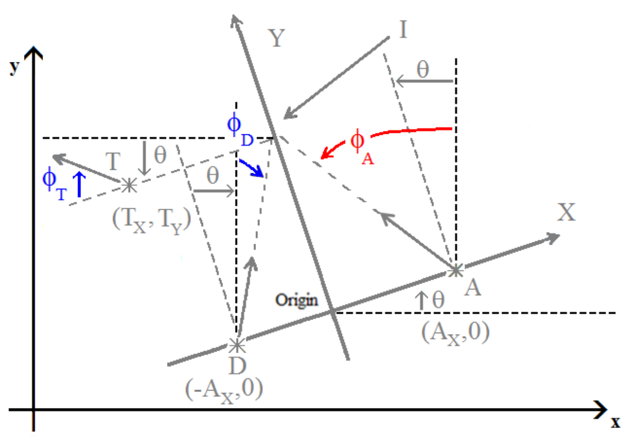

Figure 3. Strategies in the realsitic space

It is noted that as the strategy defined as an arc-tangent function composed of

an X component and a Y component in the reduced state space, the Y component is the aim point that impacts the heading to be taken by any agent. Assuming the strategy of A is such that Y=T_Y, the state feedback (sub-optimal) strategies for the A, D, and T agents in the realistic plane (see Figure 3) are

$$\phi_A = \arctan \frac{A_X}{T_Y} + \arctan(\frac{A_y - D_y}{A_x - D_x}) \tag{21}$$

$$\phi_D = \arctan \frac{A_X}{T_Y} - \arctan(\frac{A_y - D_y}{A_x - D_x}) \tag{22}$$

$$\phi_T = \arctan \frac{T_Y - Y}{-T_X} + \arctan(\frac{A_y - D_y}{A_x - D_x}) \tag{23}$$

For the simulation, the only inputs to the dynamic equations are the initial positions. Each time step is built with the inputs being the previous time step, and ends at game conclusion. The dynamics in the realistic plane are therefore

$$\dot{x}_A = -\sin\Big(\phi_A(A_x, A_y, D_x, D_y, T_x, T_y)\Big), x_A(0) = x_{A0} \tag{24}$$

$$\dot{y}_A = \cos\Big(\phi_A(A_x, A_y, D_x, D_y, T_x, T_y)\Big), y_A(0) = y_{A0} \tag{25}$$

$$\dot{x}_D = \sin\Big(\phi_D(A_x, A_y, D_x, D_y, T_x, T_y)\Big), x_D(0) = x_{D0} \tag{26}$$

$$\dot{y}_D = \cos\Big(\phi_D(A_x, A_y, D_x, D_y, T_x, T_y)\Big), y_D(0) = y_{D0} \tag{27}$$

$$\dot{x}_T = -\alpha\cos\Big(\phi_T(A_x, A_y, D_x, D_y, T_x, T_y)\Big), x_T(0) = x_{T0} \tag{28}$$

$$\dot{y}_T = \alpha\sin\Big(\phi_T(A_x, A_y, D_x, D_y, T_x, T_y)\Big), y_T(0) = y_{T0}, 0 \le t \le t_f \tag{29}$$

where the game duration t_f is

$$t_f = \sqrt{A_{X0}^2 + Y^2} \tag{30}$$

and where

$$A_{X0} = \frac{1}{2}\sqrt{(A_{x0} - D_{x0})^2 + (A_{y0} - D_{y0})^2} \tag{31}$$

Having obtained the A, D, and T trajectories (as shown in Figure 3) in the realistic space (x,y), their respective representation in the reduced state space can be obtained, namely $A_X(t), T_X(t)$, and $T_Y(t)$, where $0 \leq t \leq t_f$. Shown in Figure 4, and Figure 5 are the trajectories when Y=T_Y.

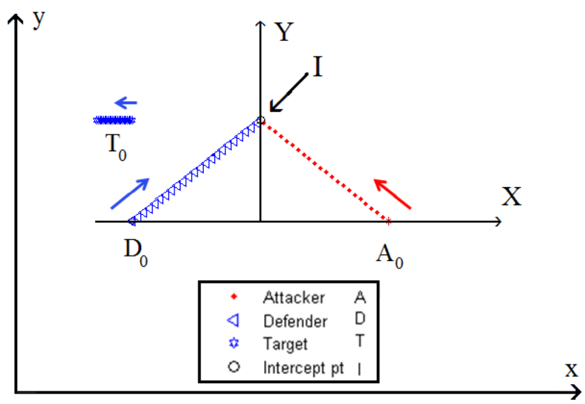

Figure 4. Reduced state space aligned with the realistic space. Agent A operating with sub-optimal strategy, Y=T_Y

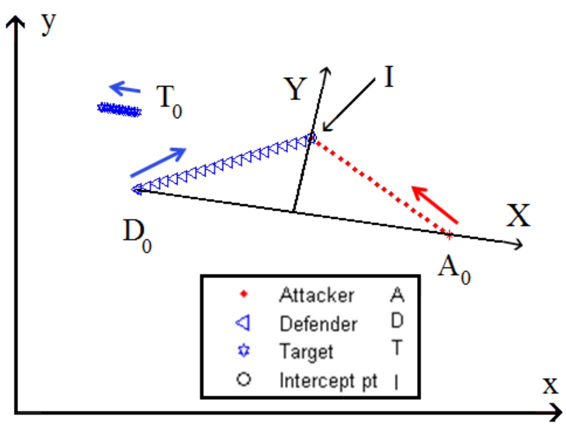

Figure 5. Reduced state space not initially aligned with the realistic space. Agents T, D, employ sub-optimal strategy Y=T_Y and A employ LOS strategy

Figure 6 and Figure 7 show trajectories when A chose a Line Of Sight (LOS)

strategy and T and D chose sub-optimal strategy Y=T_Y.

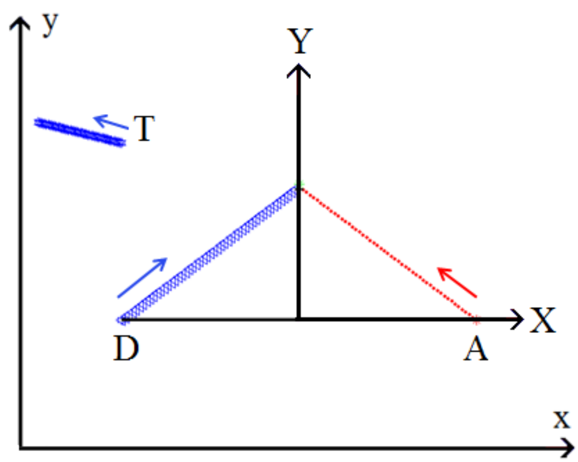

Figure 6. Reduced state space not initially aligned with the realistic plane. T, D, and A operating with sub-optimal strategy.

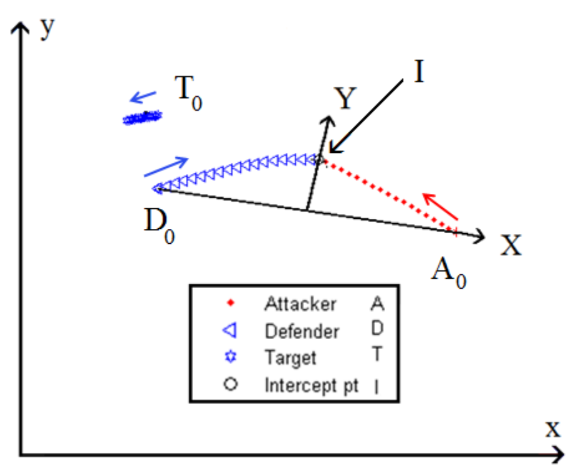

Figure 7. Reduced space initially aligned with the realistic plane. T and D employing sub-optimal strategy, A employing LOS strategy.

3.4 Apollonius Circle

The next case considered is where initially T is on the side of A. As before, A seeks to minimize and D seeks to maximize the distance between T and the point I on the orthogonal bisector of $\overline{AD}$ where D intercepts A.

If A and T take a head on collision course, they would collide at point P as shown in Figure 8. Since both A and T have moved over the same time duration, the ratio of distances can be expressed as a ratio, and this ratio is equal to the speed ratio α.

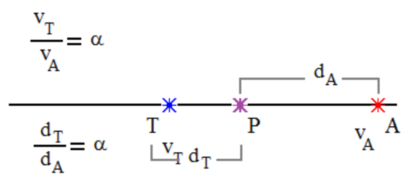

Figure 8. A and T approaching with a head-on collision course

If T evades A, and A pursues T, A will capture T at point P shown in Figure 9 as the dotted line. Again, the ratio of distances is still maintained as α.

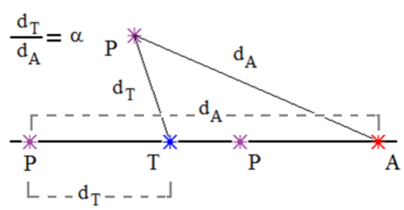

Figure 9. T evading A

If T selects a different escape route, A will catch T at point P shown in Figure 9 as the solid line. The ratio of distances is still maintained. All the points selected where the ratio of distances are maintained as α, the resulting figure is a circle as shown in Figure 10, which is the definition of an Apollonius circle [11].

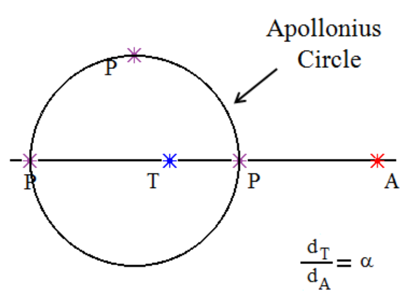

Figure 10. T evading A

A solution to the target defense differential game exist if and only if the Apollonius circle, which is based on the segment $\overline{AT}$ and the speed ratio α, intersects the orthogonal bisector of $\overline{AD}$, as shown in Figure 11. This imposes a lower bound $\overline{\alpha}$ on the speed ratio such that it is required that $1 > \alpha > \overline{\alpha}$. The critical speed ratio $\overline{\alpha}$ corresponds to the case where the Apollonius circle is tangent to the orthogonal bisector of $\overline{AD}$. Also, if α=1, T always escapes and there is no need for D. The center P of the Apollonius circle is on the collinear line through points A and T is at a distance of $\frac{\alpha^2}{1-\alpha^2}$d from T and its radius is $\frac{\alpha}{1-\alpha}$d, where the A-T separation d= $\sqrt{(A_X - T_X)^2 + (T_Y)^2}$. Hence, in the reduced state space the following holds,

$$
\begin{aligned}
P_X =& \frac{1}{1-\alpha^2}T_X - \frac{\alpha^2}{1-\alpha^2}A_X \\
P_Y =& \frac{1}{1-\alpha^2}T_Y
\end{aligned}
\tag{32}
$$

which yields the coordinates of the center of the Apollonius circle in the reduced state space:

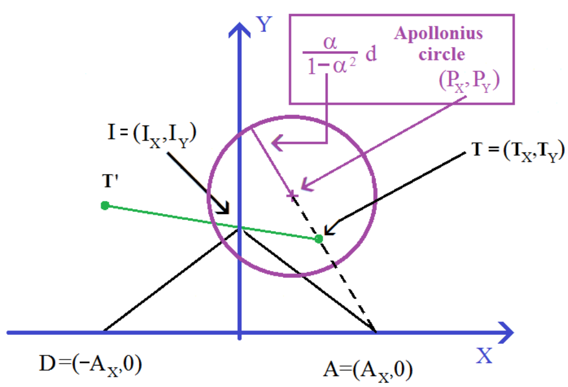

Figure 11. Apollonius circle in reduced state space

Given the position ($A_X > 0$) of A, and the position (T_X, T_Y) of T the critical

speed ratio $\overline{\alpha}$ is the solution of the quadratic equation in α^2

$$T_X - \alpha^2 A_X = \alpha\sqrt{(A_X - T_X)^2 - T_Y^2} \tag{33}$$

which is derived from

$$P_X = \frac{\alpha}{1-\alpha^2} d \tag{34}$$

Solving for $\overline{\alpha}$ yields

$$\overline{\alpha} = \frac{\sqrt{(A_X + T_X)^2 + T_Y^2} - \sqrt{(A_X - T_X)^2 + T_Y^2}}{2A_X} \tag{35}$$

If $T_Y > 0$, $\bar{\alpha} < 1 \Rightarrow \quad \exists \quad 1 > \alpha \geq \bar{\alpha}$

If T_Y =0, $\bar{\alpha} = \begin{cases} \frac{T_X}{A_X} < 1, & \text{if} \quad A_X > T_X \\ 1, & \text{if} \quad A_X \leq T_X \end{cases}$

$\bar{\alpha} < 1$, except if T_Y=0 and $T_X \geq A_X$

If the assumption $1 > \alpha \geq \bar{\alpha}$ is made, then a solution to the target defense differential game of max-min the A-T separation at the instant of interception of A by D exists; otherwise if $\alpha \leq \bar{\alpha}$, D will not be able to intercept A before A captures T, and invariably T will be captured by A. If $\alpha \geq 1$, T always escapes and D is not needed, therefore no differential target defense game can take place. Hence, the standing assumption

$$1 > \alpha > \bar{\alpha}$$

3.5 Optimization

The cost /payoff function gives the Y coordinate on the orthogonal bisector that is best aim point for the players to achieve their respective goals. For A, the cost/payoff function is the optimal aim point for A to get as close to T by game conclusion. For T, the cost/payoff function is the aim point for T to move as far away from A as possible by game conclusion. The strategies for the players are shown in Figure 2 and defined as

For A:

$$A_X = \frac{1}{2}\sqrt{(A_x - D_x)^2 + (A_y - D_y)^2} \tag{36}$$

$$A_Y = 0 \tag{37}$$

For D:

$$D_X = -\frac{1}{2}\sqrt{(A_x - D_x)^2 + (A_y - D_y)^2} \tag{38}$$

$$D_Y = 0 \tag{39}$$

For T:

$$\begin{aligned} T_X = &\left(T_x - \frac{A_x + D_x}{2}\right)\left(\frac{A_x - D_x}{\sqrt{(A_x - D_x)^2 + (A_y - D_y)^2}}\right) \\ &+ \left(T_y - \frac{A_y + D_y}{2}\right)\left(\frac{A_y - D_y}{\sqrt{(A_x - D_x)^2 + (A_y - D_y)^2}}\right) \end{aligned} \tag{40}$$

$$T_Y = -\left(T_x - \frac{A_x + D_x}{2}\right)\left(\frac{A_y - D_y}{\sqrt{(A_x - D_x)^2 + (A_y - D_y)^2}}\right) + \left(T_y - \frac{A_y + D_y}{2}\right)\left(\frac{A_x - D_x}{\sqrt{(A_x - D_x)^2 + (A_y - D_y)^2}}\right) \tag{41}$$

the cost/payoff function is the Y component of the heading formulation. Attacker chooses his aim point I on the orthogonal bisector of $\overline{AD}$ to minimize the cost/payoff function

$$J(Y) = \alpha\sqrt{A_X^2 + Y^2} \pm \sqrt{(Y - T_Y)^2 + T_X^2} \tag{42}$$

which is the I-T separation at time t_f when D intercepts A at point I on the orthogonal bisector of $\overline{AD}$. In order to minimize the cost/payoff function, it is differentiated with respect to Y and set to 0

$$\text{J(Y)'} = \alpha\frac{Y}{\sqrt{A_X^2+Y^2}} \pm \frac{T_Y-Y}{\sqrt{T_X^2+(T_Y-Y)^2}} = 0 \tag{43}$$

Rearranging

$$\text{J(Y)'} = \alpha\frac{Y}{\sqrt{A_X^2+Y^2}} = \mp\frac{T_Y-Y}{\sqrt{T_X^2+(T_Y-Y)^2}} \tag{44}$$

Square both sides to remove the square root:

$$\alpha^2\frac{Y^2}{(A_X+Y^2)} = \frac{(T_Y-Y)^2}{(T_Y-Y)^2+T_X^2} \tag{45}$$

The final equation results in a quartic equation in the unknown Y, where $Y \geq 0$:

$$(1-\alpha^2)Y^4-2(1-\alpha^2)T_YY^3+\left[(1-\alpha^2)T_Y^2 + A_X^2 - \alpha^2T_X^2\right]\ Y^2-2A_X^2T_Y(Y)+A_X^2T_Y^2 = 0 \tag{46}$$

The quartic equation (Eq. 46) provides four solutions [20]. The solution are in two

combinations: one combination with two real and two imaginary solutions; the other has four real solutions. In the four real solution combination, the values needed are the real positive minimum and positive maximum. When α =1, the equation becomes a quadratic equation in Y

$$\left(1 - \frac{T_X^2}{A_X^2}\right) Y^2 - T_Y(Y) + T_Y^2 = 0 \quad \text{provided} \quad |T_X| \neq A_X, \tag{47}$$

however, if $\alpha = 1$, there is no target defense differential game as A and T have the same velocity and T can always escape. The quartic equation always has a real solution $0 < Y < T_Y$ and an additional real solution $Y > T_Y$, provided that $T_X \neq 0$. If T_X =0, then $Y = T_Y$ is a repeated real root of the quartic equation. Since A_X is defined as the one half the distance between D and A, if $A_X = 0$ then the conclusion is the game has ended as D has intercepted A. It is noted that that both A and D have a capture radius (r) > 0, and therefore the minimum value for A_X is 2 r .

Three separate cases are considered where:

1. T is on the side of D, where T_X <0
2. T is on the side of A ,where T_X >0
3. T is on the orthogonal bisector $\overline{AT}$,where T_X =0

Case 1.

The objective of T is to get to D territory. In the case where T is initially on the side of D, where T_X <0, the cost/payoff function is constructed as shown in Figure 12. The I-T separation distance is added to the distance T will travel during the game since T is initially in D territory.

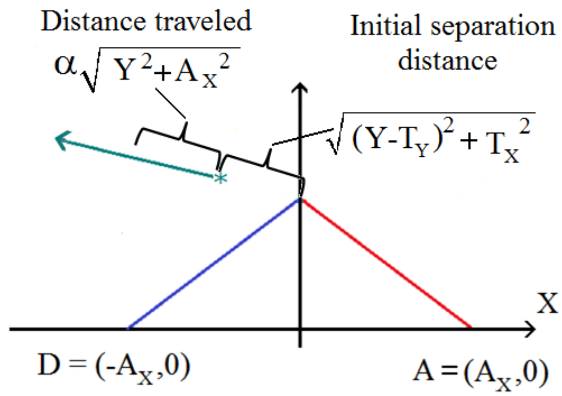

Figure 12. Visulation of the cost/payoff function when in D territory

Thus the cost/payoff function is

$$J(Y) = \sqrt{(T_Y - Y)^2 + T_X^2} + \alpha\sqrt{A_X^2 + Y^2} \tag{48}$$

It is the I-T separation at time t_f when D intercepts A at point I on the orthogonal bisector $\overline{AD}$. Its first derivative in Y is

$$\frac{dJ}{dY} = \frac{(Y - T_Y)}{\sqrt{T_X^2 + (Y - T_Y)^2}} + \alpha\frac{Y}{\sqrt{A_X^2 + Y^2}} \tag{49}$$

and the second derivative in Y is

$$\frac{d^2J}{dY^2} = \frac{T_X^2}{[T_X^2+(Y-T_Y)^2]^{\frac{3}{2}}} + \alpha\frac{A_X^2}{(A_X^2+Y^2)^{\frac{3}{2}}} \tag{50}$$

Attacker is choosing Y to minimize the cost/payoff function J(Y). Hence, the solution Y of the quartic equation must satisfy $\frac{d^2J}{dY^2} > 0$. In view of Eq (49), we know:

$$\frac{1}{\sqrt{T_X^2 + (Y - T_Y)^2}} = -\alpha\frac{1}{\sqrt{A_X^2 + Y^2}}\left(\frac{Y}{Y - T_Y}\right) \tag{51}$$

Inserting Eq (51) into Eq (50) yields:

$$\frac{d^2J}{dY^2} = \frac{1}{(A_X^2 + Y^2)}^{3/2} \left[\alpha A_X^2 - \alpha^3 \left(\frac{Y}{Y - T_Y} \right)^3 T_X^2 \right] \tag{52}$$

so

$$\frac{d^2J}{dY^2} > 0 \quad \text{iff} \quad \frac{1}{\alpha^2} \left(\frac{A_X}{T_X} \right)^2 > \left(\frac{Y}{Y - T_Y} \right) \tag{53}$$

The solution to the quartic equation (Eq. 46) yields four possible solutions. Imaginary are solutions not relevant and can be discarded. Since T is on the D side of bisector $\overline{AD}$, the solution needs to be a positive minimum at T_Y. Hence, the solution $Y < T_Y$ of the quartic equation yields $\frac{d^2J}{dY^2} > 0$ and there is a minimum at $Y < T_Y$. Inserting Eq (51) into Eq (48) yields:

$$J(Y) = \frac{1}{\alpha} \sqrt{A_X^2 + Y^2} \left(\frac{Y - T_Y}{Y} \right) + \alpha \sqrt{A_X^2 + Y^2} \tag{54}$$

so the cost/payoff function becomes

$$J(Y) = \frac{1}{\alpha} \sqrt{A_X^2 + Y^2} \left[\frac{T_Y}{Y} - (1 - \alpha^2) \right] \tag{55}$$

Figure 13 shows there is no need for the Apollonius circle as T is on the side of the bisector $\overline{AD}$ under control of D; D intercepts A before A can capture T. The resulting expected strategies under optimal play have different trajectories than what is shown in Figure 4

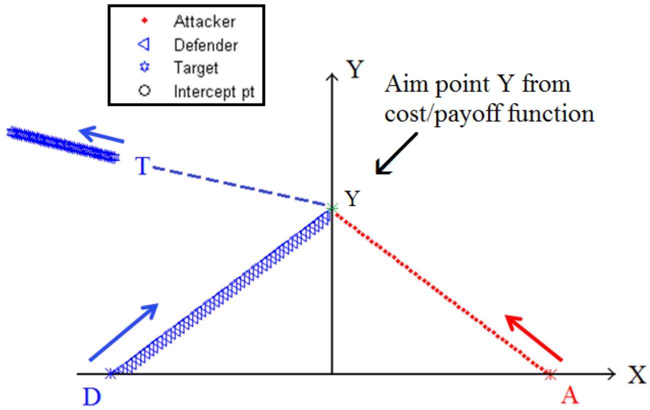

Figure 13. Expected behavior under optimal play for agents in reduced state space

Case 2.

Given the initial condition where T starts on the orthogonal bisector of $\overline{AD}$, A should pick Y = T_Y to minimize the separation distance. If A selects Y $< T_Y$, the diagram is

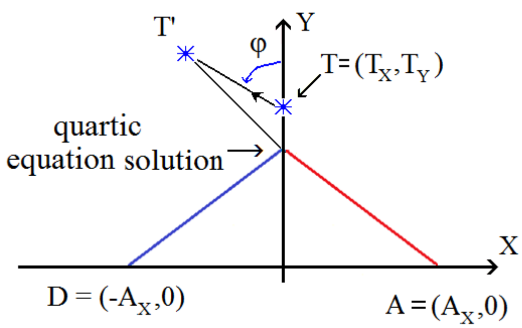

Figure 14. Mobile Case 2

An examination of the diagram shows a triangle formed by T's starting position T, to T's final position T', and the solution Y of the quartic equation, as shown in Figure 14.

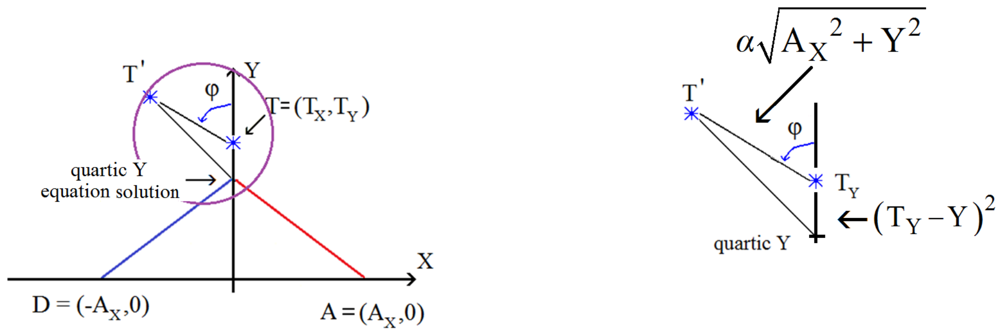

Figure 15. Mobile Case 2 triangle zoom

The information on the triangle is the distance from Y to T_Y, the distance on the Y axis from T to T', and the angle φ-the course of T as shown in Figure 15. The application of the Law of Cosines solves the triangle, yielding the optimal Y. The Law of Cosines is

$$c^2 = a^2 + b^2 - 2ab\cos\varphi \tag{56}$$

where $a = \left(\alpha\sqrt{A_X^2 + Y^2}\right)$ and $b = (T_Y - Y)$. The angle that is known is not the inside angle, but the outside angle φ, leading to the last term in the Law of Cosines to be positive rather than negative. Thus, cost/payoff function becomes

$$\left(J(Y)\right)^2 = \left(\alpha\sqrt{A_X^2 + Y^2}\right)^2 + (T_Y - Y)^2 + 2\alpha\sqrt{A_X^2 + Y^2}\,(T_Y - Y)\cos\varphi \tag{57}$$

Since A has chosen the aim point to be T_Y, T chooses φ to maximize J(Y), thus $\varphi^* = 0$ so the cosine for φ is 1, and the cost/payoff function is now

$$J(Y)^2 = \left(\alpha\sqrt{A_X^2 + Y^2}\right)^2 + (T_Y - Y)^2 + 2\alpha\sqrt{A_X^2 + Y^2}\,(T_Y - Y) \tag{58}$$

rearranging

$$J(Y)^2 = (T_Y - Y)^2 + 2\alpha\sqrt{A_X^2 + Y^2}\,(T_Y - Y) + \left(\alpha\sqrt{A_X^2 + Y^2}\right)^2 \tag{59}$$

and simplifying to a quadratic expression

$$J(Y)^2 = \left[(T_Y - Y) + \left(\alpha \sqrt{A_X^2 + Y^2} \right) \right]^2 \tag{60}$$

Taking the positive square root, the cost/payoff function becomes

$$J(Y) = \left((T_Y - Y) + \alpha \sqrt{A_X^2 + Y^2} \right) \tag{61}$$

The plot of the cost/function is shown in Figure 16, observation leads to a conclusion the minimum point is located at T_Y.

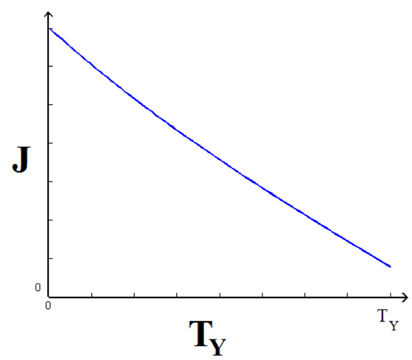

Figure 16. Case where A chooses Y> T_Y

Next, assume A chooses $Y > T_Y$ so the situation is

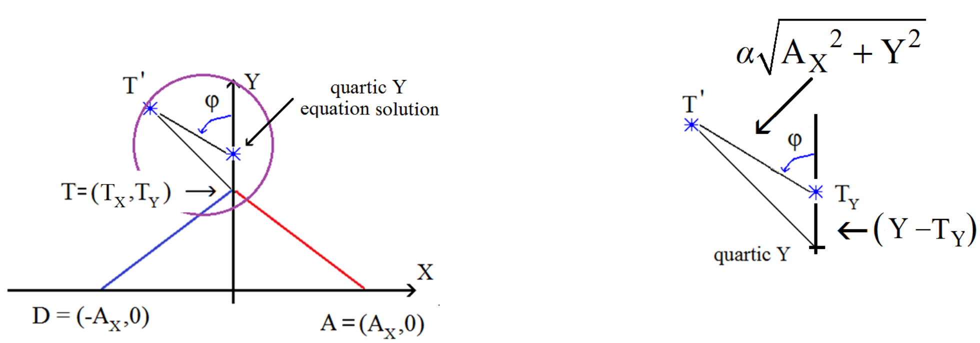

Figure 17. Mobile Case 2

T chooses ϕ to maximize the cost/payoff function J(Y), thus $\varphi^* = \pi$

The cosine for φ is -1, and the equation is now

$$J(Y)^2 = \left(\alpha\sqrt{A_X^2 + Y^2}\right)^2 + (Y - T_Y)^2 - 2\alpha\sqrt{A_X^2 + Y^2}\,(Y - T_Y) \tag{62}$$

applying the Law of Cosines and rearranging yields

$$J(Y)^2 = (Y - T_Y)^2 - 2\alpha\sqrt{A_X^2 + Y^2}\,(Y - T_Y) + \left(\alpha\sqrt{A_X^2 + Y^2}\right)^2 \tag{63}$$

and simplifying to a quadratic expression

$$J(Y)^2 = \left[(T_Y - Y) - \left(\alpha\sqrt{A_X^2 + Y^2}\right)\right]^2 \tag{64}$$

Taking the positive square root, the cost/payoff function becomes

$$J(Y) = \left((Y - T_Y) - \alpha\sqrt{A_X^2 + Y^2}\right) \tag{65}$$

The plot of the cost/function is shown in Figure 18, observation leads to a conclusion the minimum point is located at T_Y.

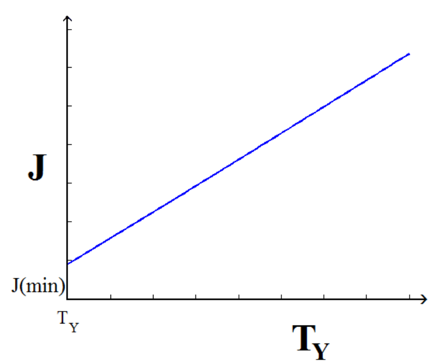

Figure 18. Case where A chooses Y$< T_Y$

The best value A can select in this case is $Y = T_Y$. It is A's optimal choice. Hence

the optimal strategy of A is $Y = T_Y$. This is also the solution of the quartic equation when T_X=0.

To determine T's strategy, a limiting approach will be pursued. Let $X_T = \epsilon(\ll 1)$ for when T_X =0 the solution of the quartic equation is Y=T_Y. The quartic equation is solved where $T_X = \epsilon$ and setting $Y = T_Y + \delta, |\delta| \ll 1$. This will allow for determination of T's optimal heading φ^*. Here δ is the distance from the solution Y of quartic equation when $T_X = 0$ to T_Y and ϵ is the x distance from the reduced state space of the Y-axis to T_Y, as shown in Figure 19.

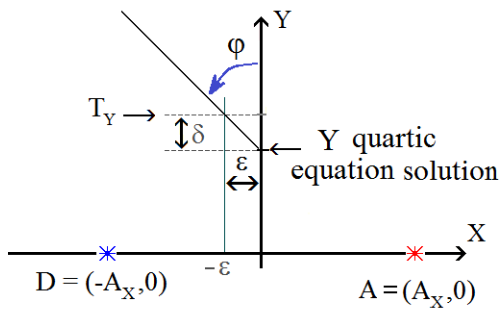

Figure 19. $\tan\phi^* = \frac{\delta}{\epsilon}$

In original quartic equation,

$$(1-\alpha^2)Y^4 - 2(1-\alpha^2)T_Y Y^3 + \left[(1-\alpha^2)T_Y^2 + A_X^2 - \alpha^2 T_X^2\right] Y^2 - 2A_X^2 T_Y(Y) + A_X^2 T_Y^2 = 0 \tag{66}$$

which it the same from Eq. 46, Y is replaced with $(T_Y + \delta)$ and solved for δ.

Substitution:

$$\begin{aligned}\left(1-\alpha^2\right)(T_Y+\delta)^4 - 2\left(1-\alpha^2\right)T_Y(T_Y+\delta)^3 \\ + \left[\left(1-\alpha^2\right)T_Y^2 + A_X^2 - \alpha^2\epsilon^2\right](T_Y+\delta)^2 - 2A_X^2 T_Y(T_Y+\delta) + A_X^2 T_Y^2 = 0\end{aligned} \tag{67}$$

After expanding all terms and neglecting δ terms that are power three or higher ≈ 0, the equation in δ becomes

$$\begin{aligned}\left(1-\alpha^2\right)\left(T_Y^4 + 4T_Y^3\delta + 6T_Y^2\delta^2\right) - 2\left(1-\alpha^2\right)T_Y\left(T_Y^3 + 3T_Y^2\delta + 3T_Y\delta^2\right) + \\ \left[\left(1-\alpha^2\right)T_Y^2 + A_X^2 - \alpha^2\epsilon^2\right](T_Y^2 + 2T_Y\delta + \delta^2) \\ - 2A_X^2T_Y^2 - 2A_X^2T_Y\delta + A_X^2T_Y^2 = 0\end{aligned} \tag{68}$$

The terms can be grouped by powers of δ yielding

$$\begin{aligned}\left[\left(1-\alpha^2\right)T_Y^4 - 2\left(1-\alpha^2\right)T_Y^4 + \left(1-\alpha^2\right)T_Y^4 + A_X^2T_Y^2 - \alpha^2\epsilon^2T_Y^2 - 2A_X^2T_Y^2 + A_X^2T_Y^2\right] \\ \left[+4\left(1-\alpha^2\right)T_Y^3\delta - 6\left(1-\alpha^2\right)T_Y^3\delta + 2\left(1-\alpha^2\right)T_Y^3\delta + 2A_X^2T_Y\delta - 2\alpha^2\epsilon^2T_Y\delta - 2A_X^2T_Y\delta\right] \\ \left[+6\left(1-\alpha^2\right)T_Y^2\delta^2 - 6\left(1-\alpha^2\right)T_Y^2\delta^2 + \left(1-\alpha^2\right)T_Y^2\delta^2 + A_X^2\delta^2 - \alpha^2\epsilon^2\delta^2\right] = 0\end{aligned} \tag{69}$$

where black are the δ^0 terms, blue are the δ^1 terms, and red is the δ^2 terms.

After cancellations

$$-\alpha^2\epsilon^2T_Y^2 - 2\alpha^2\epsilon^2T_Y\delta + \left(1-\alpha^2\right)T_Y^2\delta^2 + A_X^2\delta^2 - \alpha^2\epsilon^2\delta^2 = 0 \tag{70}$$

and since $\delta \ll 1$ and $\epsilon \ll 1$ then $\delta^2\epsilon^2 \approx 0$

$$-\alpha^2\epsilon^2T_Y^2 + \left(1-\alpha^2\right)T_Y^2\delta^2 + A_X^2\delta^2 = 0 \tag{71}$$

Solving for δ yields

$$\delta^2 = \frac{\alpha^2\epsilon^2T_Y^2}{\left(1-\alpha^2\right)T_Y^2 + A_X^2} \tag{72}$$

taking the positive square root

$$\delta = \frac{\alpha\epsilon T_Y}{\sqrt{\left(1-\alpha^2\right)T_Y^2 + A_X^2}} \tag{73}$$

so with a limiting approach, δ and ϵ and are established, φ^* can be defined as

$$\varphi^* = \text{atan}\left(\frac{\delta}{\epsilon}\right) \tag{74}$$

Substituting δ into the equation yields

$$\varphi^* = \text{atan}\quad \frac{\frac{\alpha\epsilon T_Y}{\sqrt{(1-\alpha^2)T_Y^2+A_X^2}}}{\epsilon} \tag{75}$$

and after simplification

$$\varphi^* = \text{atan}\quad \frac{\alpha}{\sqrt{\left(1-\alpha^2\right) + \frac{A_X^2}{T_Y^2}}} \tag{76}$$

Case 3.

In the case where T initially starts in A territory, i.e. $T_X > 0$, T will have to travel from A territory to D territory. Thus, I-T separation distance is subtracted from the distance T will travel during the game, as shown in Figure 20.

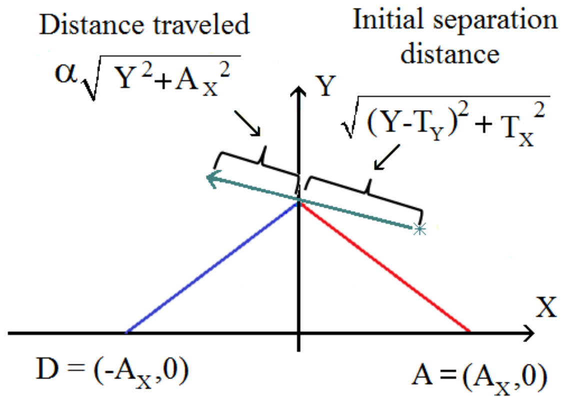

Figure 20. Visulation of the cost/payoff function when in A territory

and the cost/payoff function is then

$$J(Y) = \alpha\sqrt{A_X^2 + Y^2} - \sqrt{(Y - T_X)^2 + T_X^2} \tag{77}$$

The first derivative in Y is

$$\frac{dJ}{dY} = \alpha\frac{Y}{\sqrt{A_X^2 + Y^2}} - \frac{(Y - T_Y)}{\sqrt{(Y - T_X)^2 + T_X^2}} \tag{78}$$

the second derivative in Y is

$$\frac{d^2J}{dY^2} = \alpha\frac{\sqrt{A_X^2 + Y^2} - \dfrac{Y^2}{\sqrt{A_X^2 + Y^2}}}{A_X^2 + Y^2} - \frac{\sqrt{(Y - T_Y)^2 + T_X^2} - \dfrac{(Y - T_Y)^2}{\sqrt{(Y - T_Y) + T_X^2}}}{(Y - T_Y)^2 + T_Y^2} \tag{79}$$

Simplifing:

$$\frac{d^2J}{dY^2} = \alpha \frac{A_X^2}{\left[A_X^2 + Y^2\right]^{3/2}} \frac{T_X^2}{\left[\left(Y - T_Y^2\right) + T_X^2\right]^{3/2}} \tag{80}$$

T is choosing Y to maximize the cost/payoff function J(Y). The solution Y of the quartic equation is such that $\dfrac{d^2J}{dY^2} < 0$.

In view of Eq (78) it is known that

$$\frac{1}{\sqrt{\left(Y - T_Y\right)^2 + T_X^2}} = \alpha \frac{Y}{Y - T_Y} \frac{1}{\sqrt{A_X^2 + Y^2}} \tag{81}$$

Inserting Eq (81) into Eq (79) yields:

$$\frac{d^2J}{dY^2} = \alpha \frac{1}{\left(A_X^2 + Y^2\right)^{3/2}} \left[A_x^2 - \alpha^2 \left(\frac{Y}{Y - T_Y}\right)^3 T_x^2\right] \quad \Rightarrow \quad \frac{d^2J}{dY^2} < 0 \tag{82}$$

This holds true if and only if:

$$\frac{1}{\alpha^2} \left(\frac{A_X}{T_X}\right)^2 < \left(\frac{Y}{Y - T_Y}\right)^3 \tag{83}$$

The solutions to the quartic equation (Eq.66) provides two real positive values. One value is greater than T_Y and one is less than T_Y. Hence, the real solution $Y < T_Y$ of the quartic equation does not fulfill the role of yielding a maximum and the second real solution $Y > T_Y$ of the quartic equation is the candidate solution. Thus, it is T who as before chooses Y to maximize the cost/payoff function J(Y).

Inserting Eq (81) into Eq (77) yields:

$$\frac{1}{\alpha^2} \left(\frac{A_X}{T_X}\right)^2 < \left(\frac{Y}{Y - T_Y}\right)^3 \tag{84}$$

$$J(Y) = \frac{1}{\alpha}\sqrt{A_X^2 + Y^2}\left(\alpha^2 - 1 + \frac{T_Y}{Y}\right) \tag{85}$$

as before. Since now $Y > T_y$ and J(y)> 0, this solution of the quartic equation must satisfy $T_Y < Y < \dfrac{1}{1-\alpha^2}T_Y$.

In Figure 21, the initial starting conditions are shown with the reduced state space. T starts on the side of the bisector $\overline{AD}$ under control of A, the Apollonius circle intersects the bisector and therefore T avoids capture by A as seen in Figure 22. The zoomed in portion (see Figure 23) shows the final positions of A, D, and T (noted as A', D' and T' at game termination). The zoomed-in portion also shows the Apollonius circle intersecting the orthogonal bisector of $\overline{AD}$. The final position of T is across the bisector, and D intercepts A on the orthogonal bisector $\overline{AD}$. The conclusion is T evades capture by A courtesy of D who intercepted A.

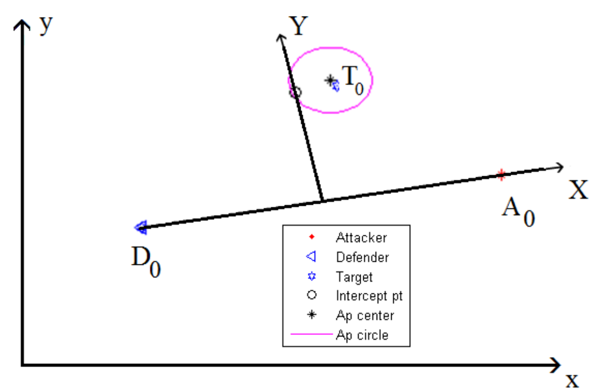

Figure 21. Reduced state space not aligned with realistic plane and Apollonius circle intersects orthogonal bisector. All agents employing optimals strategies.

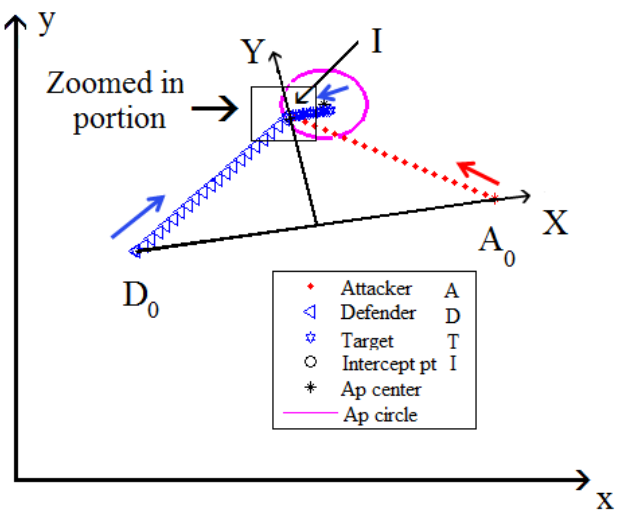

Figure 22. Plotted trajectories at conclusion of game.

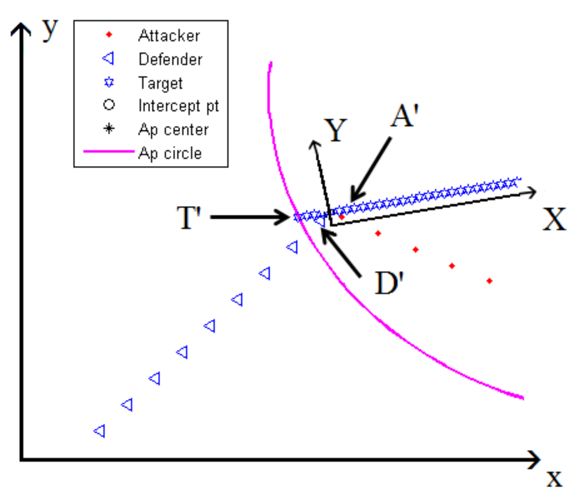

Figure 23. Zoomed in section near where Apollonius circle intersection the orthogonal bisector of $\overline{AD}$.

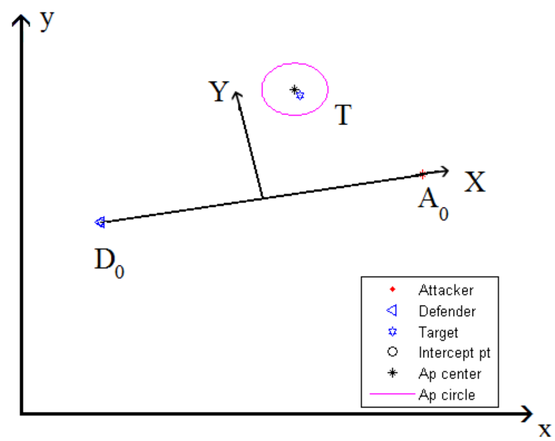

Figure 24. The Apollonius circle does not intersect the orthogonal bisector. The reduced state space and realistic plane not in alignment

In Figure 24, T starts on the side under the control of A. The Apollonius circle does not intersect the bisector $\overline{AD}$, and T cannot avoid capture by A before D intercepts A.

3.6 Static Target

The final condition to be considered will be when T is a static target. Since T is static, the velocity is 0, thus the quartic equation goes from Eq. 86, which it the same from Eq. 46,

$$(1-\alpha^2)Y^4 - 2(1-\alpha^2)T_Y Y^3 + \left[(1-\alpha^2)T_Y^2 + A_X^2 - \alpha^2 T_X^2\right] Y^2 - 2A_X^2 T_Y(Y) + A_X^2 T_Y^2 = 0 \tag{86}$$

to

$$(1-0^2)Y^4 - 2(1-0^2)T_Y Y^3 + \left[(1-0^2)T_Y^2 + A_X^2 - 0^2 T_X^2\right] Y^2 - 2A_X^2 T_Y(Y) + A_X^2 T_Y^2 = 0 \tag{87}$$

Substituting Y=T_Y yields

$$Y^4 - 2Y^4 + Y^4 + A_X^2 Y^2 - 2A_X^2 Y^2 + A_X^2 Y^2 = 0 \tag{88}$$

which reduces to 0, so the conclusion is that T_Y=Y.

3.7 Optimal Control Theory

At the Air Force Institute of Technology, students have access to an Optimal Control Theory (OCT) solver called GPOPS and available within Matlab^{TM} software. GPOPS solves optimal control problems with numerical methods [13]. Numerical method analysis techniques are computationally intensive because successive approximations are continually tested until the approximation falls within a previous set of bounding conditions. GPOPS implements the dynamic equations from Section 3.3 and solves for an optimal control given some objective function. The objective function is defined as an equation to maximize the final separation distance between A and T, and is equivalent to the cost/payoff function. GPOPS is also given the sub-optimal strategies for the players and solves for the control to be optimized. The results from OCT solution will be presented to draw a comparison between the two methods of solving the active target defense scenario. Discussion of OCT and the functionality GPOPS program are not within scope of this thesis. For more in-depth discussion of GPOPS refer to ”GPOPS-II: A MATLAB Software for Solving Multiple-Phase Optimal Control Problems Using hp-Adaptive Gaussian Quadrature Collocation Methods and Sparse Nonlinear Programming” by Patterson and Rao [13].

3.8 Summary

For this chapter, the formulation of the of strategy formulation was discussed. The chapter started with formulation of the problem. The second point covered was the strategy synthesis for the agents. Third, formulation of the Apollonius circle was discussed. The cost function was introduced and the optimization process was analyzed. The cases where T is a static target were presented. Finally, the OCT approach to implementation the active target defense scenario was discussed.

IV. Results

4.1 Introduction

The contents of this chapter contain the results of the active target defense game simulations constructed from the mathematics presented in Chapter III. First, the simulation assumptions are defined. Second, to verify that the Chapter III discussion provides a viable solution, the simulations cover the three possible starting locations for a mobile Target (T). These starting positions are: T is in Defender (D) territory (Case 1); T is on the orthogonal bisector of $\overline{AD}$ (Case 2); T is in Attacker (A) territory where the Apollonius circle intersects the orthogonal bisector of $\overline{AD}$ (Case 3 see Figure 25).

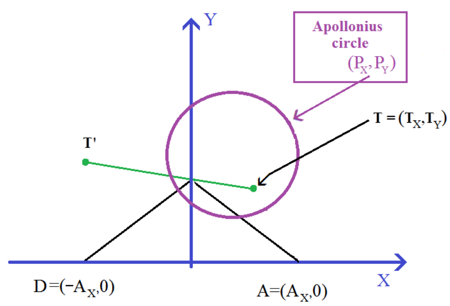

Figure 25. Apollonius circle intersecting orthogonal bisector of $\overline{AD}$

In addition to the above three cases and additional two cases are presented. Case 4 is presented simulating when T is in A territory where the Apollonius circle does not intersect the orthogonal bisector of $\overline{AD}$. Case 5 to be presented are simulations for when T is stationary. For each case simulation, D and A initial positions remain constant, and the initial conditions also put the reduced state space and the realistic plane in alignment. In the Appendix, the plots of additional testing of simulations where initial conditions involving translation and rotation of the reduced space relative to the realistic plane are listed. Rotations and translations demonstrate the

robustness of the mathematics as well as the implementation of the simulations. Finally, the last set of results to be presented is the case where a suite of initial positions and selected scenarios are simulated with Optimal Control Theory (OCT) and Differential Game Theory (DGT). The goal is to compare the I-T separation distances with both methodologies.

4.2 Simulation Assumptions

The outcome of the simulations is to demonstrate the fundamental geometry in deriving the optimal strategies is sound, with some assumptions. The velocities of A and D are constant during the simulations, equal and normalized to 1 and the T velocity is also constant and when scaled is 0.4. The type of motion exhibited by the agents is simple motion, and all agents are assumed to have perfect, noise free data inputs. The coordinate systems for the reduced space and realistic plane are unit-less, and the initial engagement range is considered to be Beyond Visual Range (BVR). At BVR, flight dynamics are neglected. The time base is also unit-less, and the time division in the simulations are 0.2 of a time unit. Agents D and A have a capture radius of 0.4. The strategies for the agents in reduced state space are

$$\text{For A}: \quad \psi_A = \arctan \tfrac{A_X}{Y} \tag{89}$$

$$\text{For D}: \quad \psi_D = \arctan \tfrac{A_X}{Y} \tag{90}$$

$$\text{For T}: \quad \psi_T = \arctan \tfrac{T_Y - Y}{-T_X} \tag{91}$$

Each case simulation runs a combination of strategy scenarios. In the first scenario, all agents are following the optimal strategy where Y is the solution to the quartic equation. In the second scenario, T and D implement optimal strategies and A's strategy is the sub-optimal strategy where Y=T_Y such that T_Y is the Y component

of the coordinates of T. A third scenario is where T and D are employing optimal strategies and A takes a Line -Of -Sight (LOS) approach to T. The fourth scenario, D and T chose a sub-optimal strategy where Y=T_Y, and A chooses the optimal strategy. The fifth scenario is where A and D are following optimal strategies and T follows a sub-optimal strategy where Y=T_Y. The sixth scenario is where A and T employ optimal strategies and D follows a sub-optimal strategy where Y=T_Y. For the final scenario, T follows the optimal strategy whereas A and D follow the Y=T_Y strategy. The strategy combinations are shown in Table 1.

Table 1. Strategy Combinations

	T (target)	D (defender)	A (attacker)
Scenario 1	Y=quartic eq Y	Y=quartic eq Y	Y=quartic eq Y
Scenario 2	Y=quartic eq Y	Y=quartic eq Y	Y=T_Y
Scenario 3	Y=quartic eq Y	Y=quartic eq Y	$\phi_A = \text{atan}\frac{A_x - T_x}{T_y - A_y}$
Scenario 4	Y=T_Y	Y=T_Y	Y=quartic eq Y
Scenario 5	Y=quartic eq Y	Y=T_Y	Y=quartic eq Y
Scenario 6	Y=T_Y	Y=quartic eq Y	Y=quartic eq Y
Scenario 7	quartic Y=Y	Y=T_Y	Y=T_Y

4.3 Mobile Target

The general cost/payoff function is Eq. 92

$$J(Y) = \alpha\sqrt{A_X^2 + Y^2} \pm \sqrt{(Y - T_Y)^2 + T_X^2} \tag{92}$$

and defines the Intercept-Target (I-T) separation at the end of the target defense game. Optimization of the cost/payoff function is covered in Chapter III. The ob-

jective of the simulations is to demonstrate which combinations of strategies favor D and T, and which combinations favor A. The first scenario will establish a baseline as all agents are employing optimal strategies. When the distance is greater than the baseline, then the strategy combinations favor D and T. Conversely, a distance decrease over the baseline means the strategy combinations favor A.

Case 1 Mobile Target.

As discussed in Chapter III, the first case to be simulated is the initial positions where T is on the D controlled side of the $\overline{AD}$ bisector. For comparison of the strategy combinations to be simulated, the starting locations are held constant. By holding the starting locations constant, the final I-T separation distance can be compared. The first starting location are A at (8,0), D at (-8,0), and T at (-8,8), with the realistic plane and reduced state space initially aligned. The resulting trajectories are shown in the realistic plane.

Scenario 1.

In the realistic space, strategies

$$\text{for T: } \phi_T = \arctan \frac{T_Y - Y}{-T_X} + \theta \tag{93}$$

$$\text{for A: } \phi_A = \arctan \frac{A_X}{Y} + \theta \tag{94}$$

and

$$\text{for D: } \phi_D = \arctan \frac{A_X}{Y} - \theta \tag{95}$$

are calculated with the solution of the quartic equation. The solutions have a constant heading as Eq.(94) and (95) have the same result. Since both agents have constant

headings, the resulting motion is straight line motion, therefore the angle of rotation between the reduced state space and realistic plane remains constant. As discussed in Optimization Case 1, the expectation is T should move in a straight line away from point I as shown in Figure 26.

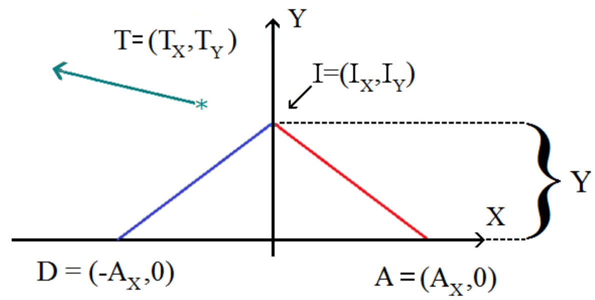

Figure 26. A and T both employing optimal strategies

The results from Scenario 1 reflects the expectation. At the conclusion of the game, the I-T separation distance is 12.3562 units, and the resulting trajectories are shown in Figure 27. The distance for this scenario is the baseline for the other strategy combination distances. The reduced state space and the realistic plane do not have an initial rotation angle since both agents start with the spaces aligned.

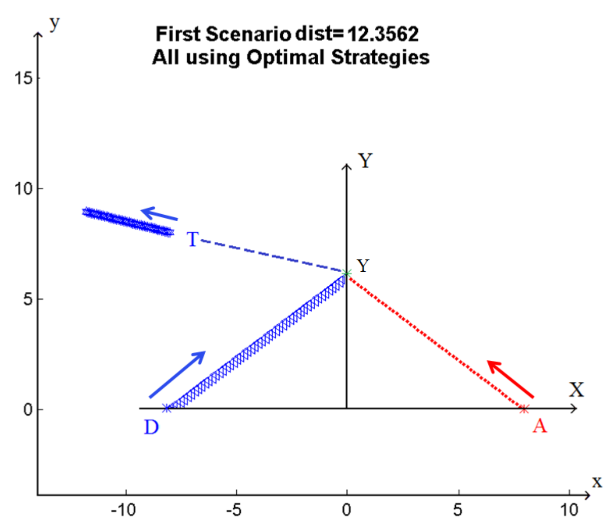

Figure 27. All agents using optimal strategies. Optimal strategy, $\alpha = \frac{2}{5}$

Scenario 2.

T's and D's strategies are calculated with the quartic equation solution Y, and A's strategy is calculated based on Y= T_Y. As A selects a sub-optimal strategy, the expectation is I-T separation distance will increase verses the result from the first scenario. At the end of game, the distance is 13.1065 units which is greater than the 12.3562 units from the baseline. With an increased I-T separation distance, the strategies employed by the agents favor T and D, as expected. Figure 28 shows the initial aim points for A and D. Agent A is initially aiming for the point marked as T_Y and D is aiming for the point is marked as Y. Since A and D have differing strategies, the result is an angle of rotation between the reduced state space and the realistic space. The resulting trajectories are shown in Figure 28.

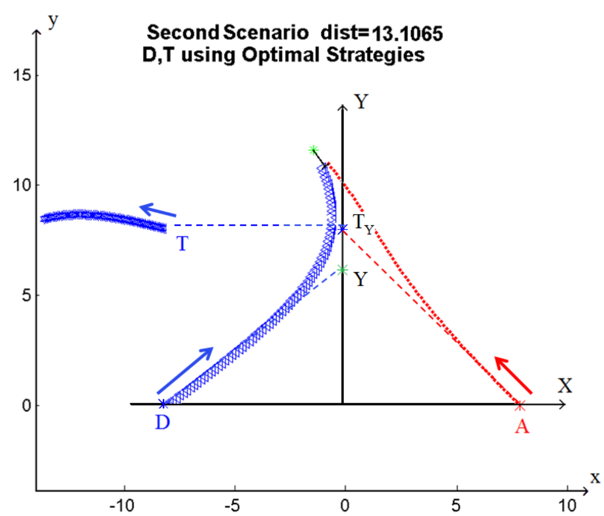

Figure 28. D,T using optimal strategies. A using suboptimal strategy Y=T_Y, and $\alpha = \frac{2}{5}$

Scenario 3.

T and D strategies are calculated with the quartic equation solution Y, and A's LOS strategy is calculated based on realistic plane coordinates for T such that the

resulting strategy is

$$\phi_A = \arctan \frac{A_x - T_y}{T_y - A_y} \tag{96}$$

The expectation is T and D will benefit from the selection of the optimal strategies, and the I-T separation distance will increase verses the result from baseline. At the end of game, the distance is 12.4532 units which is greater than the 12.3562 units from the baseline. The increased I-T separation distance means the strategies employed by the agents favor T and D. The resulting trajectories are shown in Figure 29.

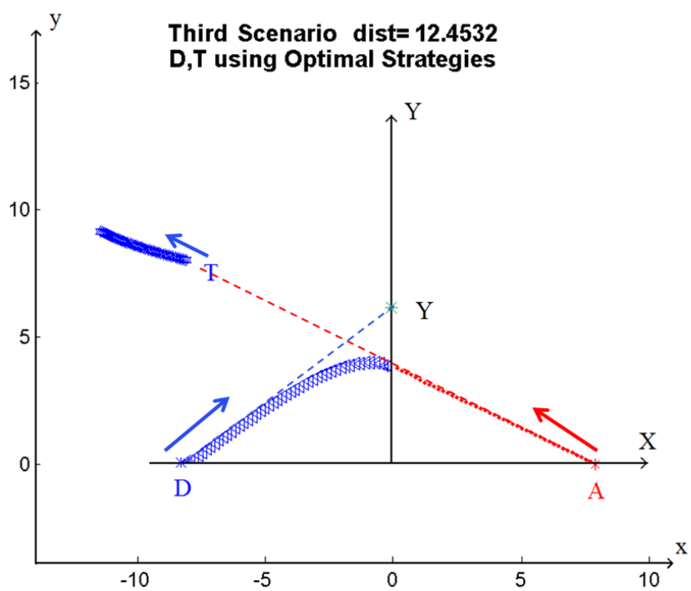

Figure 29. D,T using optimal strategies. A using LOS strategy and $\alpha = \frac{2}{5}$

Scenario 4.

T and D strategies are calculated where Y=T_Y, and A strategy is calculated with the quartic equation solution Y. Since D and T are selecting sub-optimal strategies and A is implementing the optimal strategy, the expectation is the cost/payoff will favor A. The resulting I-T separation distance should be less than what is seen in the baseline. At the end of game, the distance is 12.2231 units which is less than the 12.3562 units from Section 4.3. The decreased I-T separation distance means the

strategies employed by the agents favor A as shown in Figure 30.

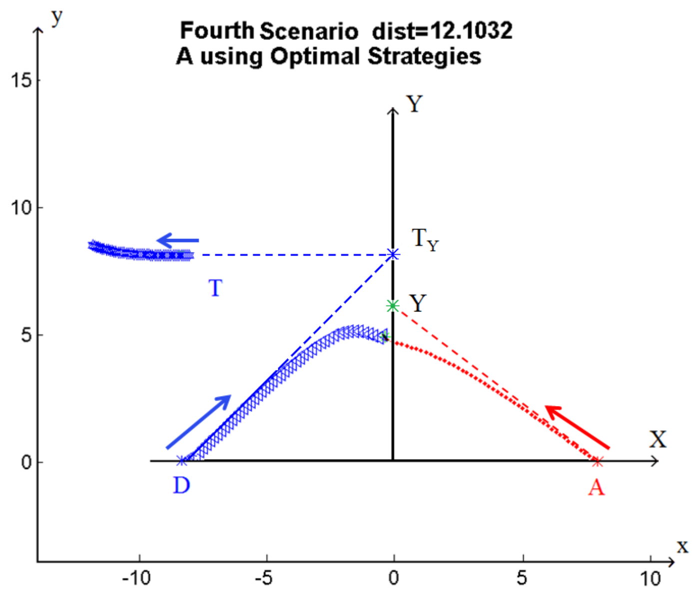

Figure 30. A using optimal strategies. D, T using suboptimal strategy Y=T_Y, and $\alpha = \frac{2}{5}$

Scenario 5.

The starting coordinates for the fifth scenario are the same as the first, A and D strategies are calculated with the quartic equation solution Y, and T strategy is calculated where Y=T_Y. In the scenario, A is implementing the optimal strategy and D is implementing a sub-optimal strategy. The expectation is the I-T separation distance will be less than the baseline result. A second expectation is the I-T separation distance will be greater than the fourth scenario. At the end of game, the distance is 12.2656 units which is less than the 12.3562 units from the baseline and greater than the 12.2231 units from Scenario 4. The resulting trajectories are shown in Figure 31 and, the decreased I-T separation distance means the strategies employed by the agents favor A.

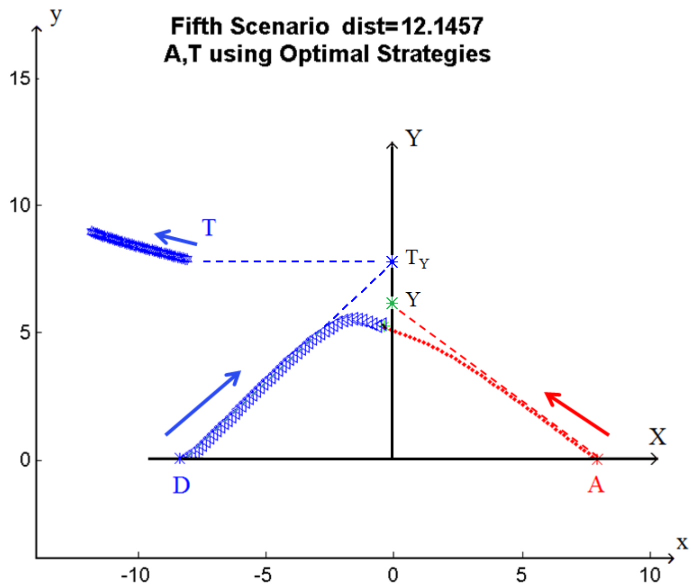

Figure 31. A,T using optimal strategies. D using suboptimal strategy Y=T_Y, and $\alpha = \frac{2}{5}$

Scenario 6.

The starting coordinates for the final scenario are the same as the first, A and T strategies are calculated with the quartic equation solution Y, and T strategy is calculated where Y=T_Y. In the scenario, A and D are implementing the optimal strategy and T is implementing a sub-optimal strategy. The expectation is the I-T separation distance will be less than Section 4.3. At the end of game, the distance is 12.2656 units which is less than the baseline distance. It is also noted the distance is greater than the results from Scenario 4. The resulting trajectories are shown in Figure 32 and, the decreased I-T separation distance means the strategies employed by the agents favor A.

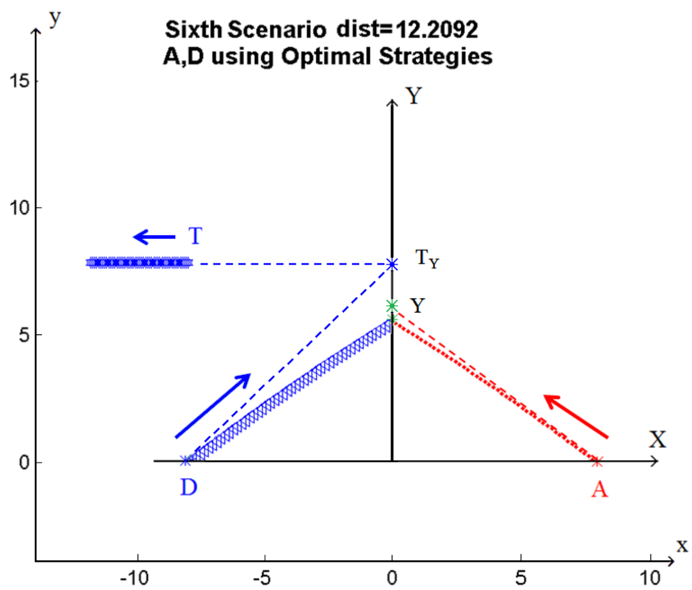

Figure 32. A,D using optimal strategies. T using suboptimal strategy Y=T_Y, and $\alpha = \frac{2}{5}$

Scenario 7.

In Scenario 7, T is employing the optimal strategy and D and A are implementing the sub-optimal strategy where Y=T_Y. With T optimal and D and A sub-optimal, the expectation is the final separation distance will favor the T, D team. When the game concludes, the distance is 12.7581 units which is greater than the 12.3562 units of the baseline. Resulting trajectories are shown in Figure 33 and, increased I-T separation distance means the strategies employed by the agents favor T.

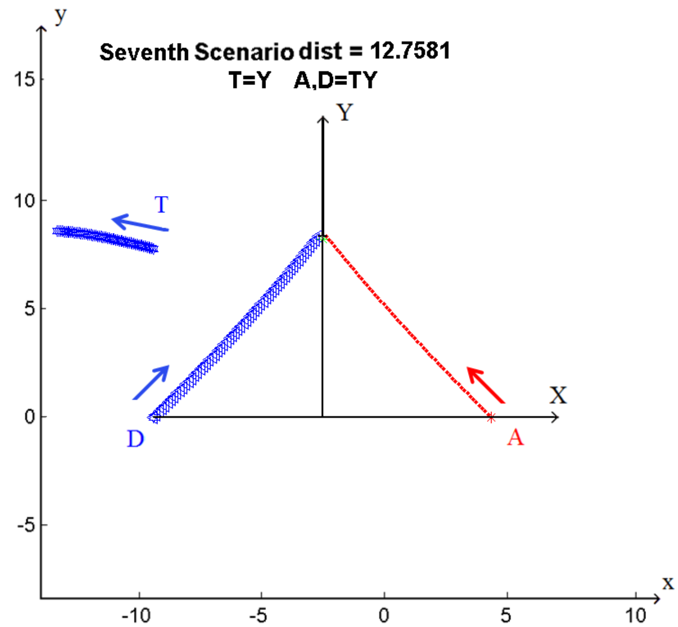

Figure 33. T using optimal strategies. A,D using suboptimal strategy Y=T_Y, and $\alpha = \frac{2}{5}$

The summary of final distances of the I-T separation at the game conclusion are shown in Table 2.

Table 2. Distance summary

Scenario 1	12.3562	T optimal	D optimal	A optimal
Scenario 2	13.1065	T optimal	D optimal	A sub-optimal
Scenario 3	12.4532	T optimal	D optimal	A LOS
Scenario 4	12.1032	T sub-optimal	D sub-optimal	A optimal
Scenario 5	12.1457	T optimal	D sub-optimall	A optimal
Scenario 6	12.2092	T sub-optimal	D optimal	A optimal
Scenario 7	12.7581	T optimal	D sub-optimal	A sub-optimal

Case 2 Mobile Target.

As in the previous section, the starting locations are held constant so the I-T separation distance can be compared. The second starting locations are A at (8,0), D at (-8,0), and T at (0,8), with the reduced state space and the realistic plane initially aligned. It is noted the choice of initial positions places T on the $\overline{AD}$ bisector. The discussion in Chapter III Case 2 covers the formulation of the optimal solution when T is starting on the orthogonal bisector. The resulting trajectories are shown in the realistic plane.

Scenario 1.

In this scenario, T is on the orthogonal bisector $\overline{AD}$. T has an escape route, and D aids T. Agents A and D meet on the orthogonal bisector. The final distance with all agents following the optimal strategy is 4.5820 units and is the baseline for the following scenarios.

The resulting trajectories are shown in Figure 34.

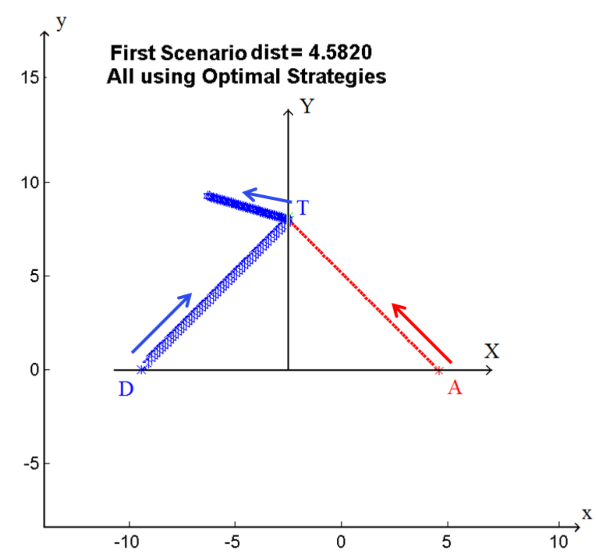

Figure 34. All agents using optimal strategies. Optimal strategy, $\alpha = \frac{2}{5}$

Scenario 2.

In this scenario, T and D are executing the optimal strategy, A is executing a strategy where Y $=T_Y$, or sub-optimal. The final separation distance is 4.8946 units. The outcome is an increased distance from the baseline and similar to the result in Section 4.3. The resulting trajectories are shown in Figure 35.

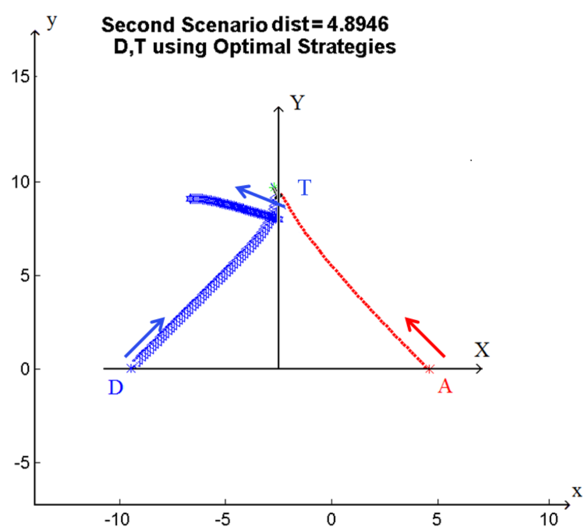

Figure 35. D,T using optimal strategies. A using suboptimal strategy Y=T_Y, and $\alpha = \frac{2}{5}$

Scenario 3.

In this scenario T and D are executing the optimal strategy, A is executing a LOS strategy. The final separation distance is 4.9060 units. The outcome is an increased distance from the baseline and similar to the result in Section 4.3. The resulting trajectories are shown in Figure 36.

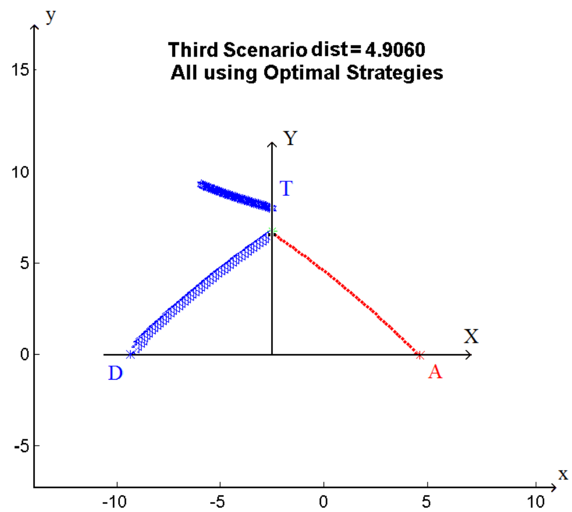

Figure 36. D,T using optimal strategies. A using LOS strategy and $\alpha = \frac{2}{5}$

Scenario 4.

In this scenario T and D are executing a sub-optimal strategy, A is executing the optimal strategy. The final separation distance is 4.5075 units. The outcome is a decreased distance from the baseline and similar to the result in Section 4.3. The resulting trajectories are shown in Figure 37.

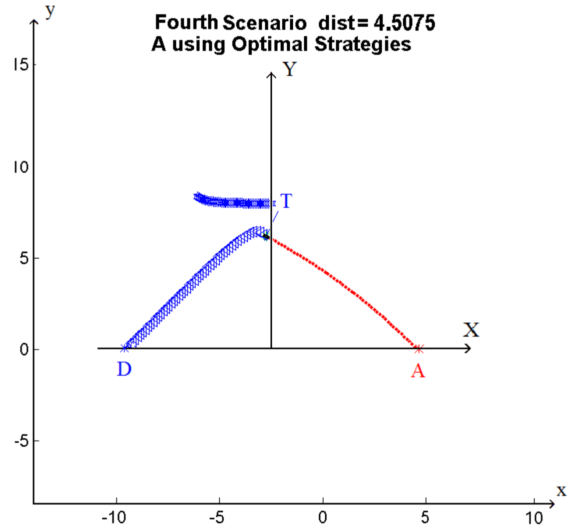

Figure 37. A using optimal strategies. D, T using suboptimal strategy Y=T_Y, and $\alpha = \frac{2}{5}$

Scenario 5.

In this scenario T is executing the optimal strategy, D is executing the sub-optimal strategy $Y = T_Y$, and A is executing the optimal strategy. The final separation distance is 4.4471 units. The outcome is a decreased distance from the baseline and similar to the result in Section 4.3. The resulting trajectories are shown in Figure 37

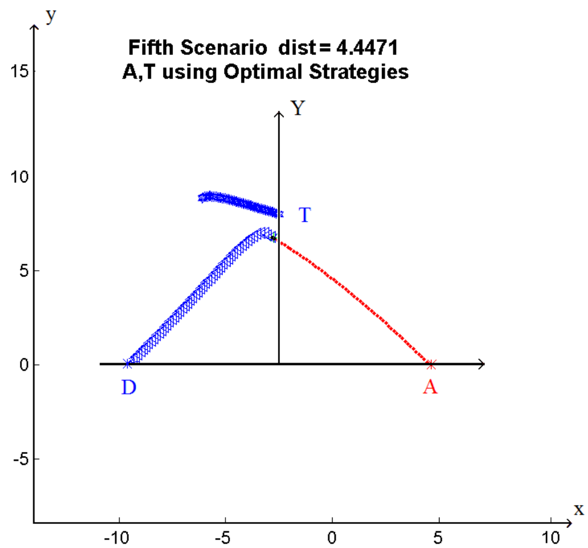

Figure 38. A,T using optimal strategies. D using suboptimal strategy Y=T_Y, and $\alpha = \frac{2}{5}$

Scenario 6.

In this scenario T is executing the sub-optimal strategy, D is executing the optimal strategy, A is executing the optimal strategy. The final separation distance is 4.5106 units. The outcome is an decreased distance from the baseline and similar to the result in Section 4.3. The resulting trajectories are shown in Figure 39.

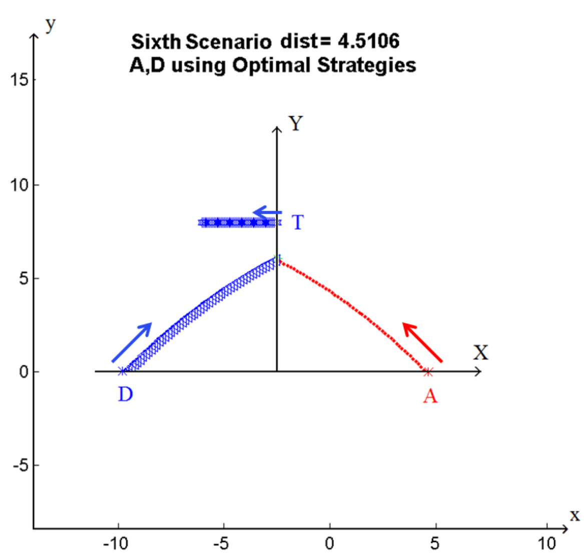

Figure 39. A,D using optimal strategies. T using suboptimal strategy Y=T_Y, and $\alpha = \frac{2}{5}$

Scenario 7.

For Scenario 7, T is employing the optimal strategy and D and A are implementing the sub-optimal strategy where Y=T_Y. With T optimal and D and A sub-optimal, the expectation is the final separation distance will favor the T, D team. At game conclusion, the distance is 4.7612 units which is greater than the baseline. Resulting trajectories are shown in Figure 33 and, increased I,T separation distance means the strategies employed by the agents favor T.

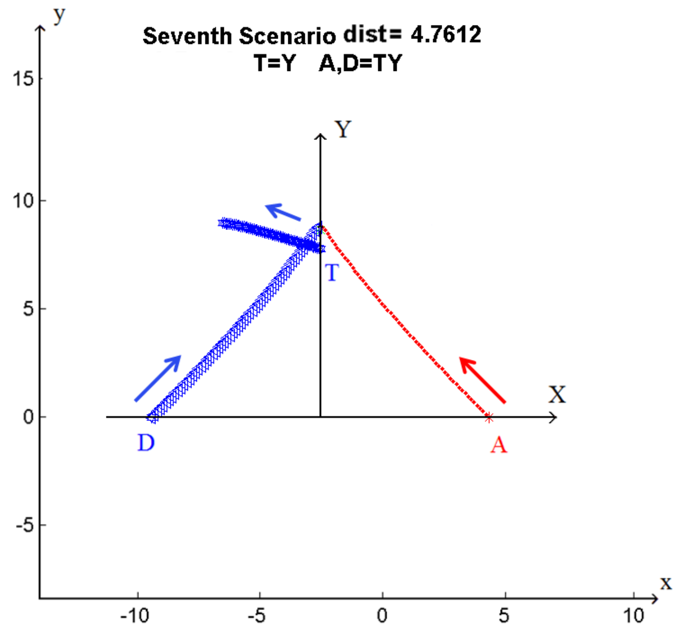

Figure 40. T using optimal strategies. A,D using suboptimal strategy Y=T_Y, and $\alpha = \frac{2}{5}$

For cases where T is on the orthogonal bisector, the results are summarized in Table 3 and follow the trend as seen as Table 2.

Table 3. Distance summary

Scenario 1	4.5820	T optimal	D optimal	A optimal
Scenario 2	4.8946	T optimal	D optimal	A sub-optimal
Scenario 3	4.9060	T optimal	D optimal	A LOS
Scenario 4	4.5075	T sub-optimal	D sub-optimal	A optimal
Scenario 5	4.4471	T optimal	D sub-optimal	A optimal
Scenario 6	4.5106	T sub-optimal	D optimal	A optimal
Scenario 7	4.7612	T optimal	D sub-optimal	A sub-optimal

Case 3 Mobile Target.

The third starting location is A at (8,0), D at (-8,0), and T at (4,8), with the realistic space and reduced state space initially aligned. It is noted the choice of initial positions places T on the A controlled side of the $\overline{AD}$ bisector. The resulting trajectories are shown in the realistic plane. By starting T in A territory, the Apollonius circle intersects the orthogonal bisector of $\overline{AD}$ showing that D can provide T aid.

Scenario 1.

In the scenario, T has an escape route, and D aids T. The final distance with all agents using optimal strategies is 0.8222 units as is the baseline for the following scenarios. The resulting trajectory of T follows the expectation as in Figure **??**. The resulting trajectories are shown in Figure 41.

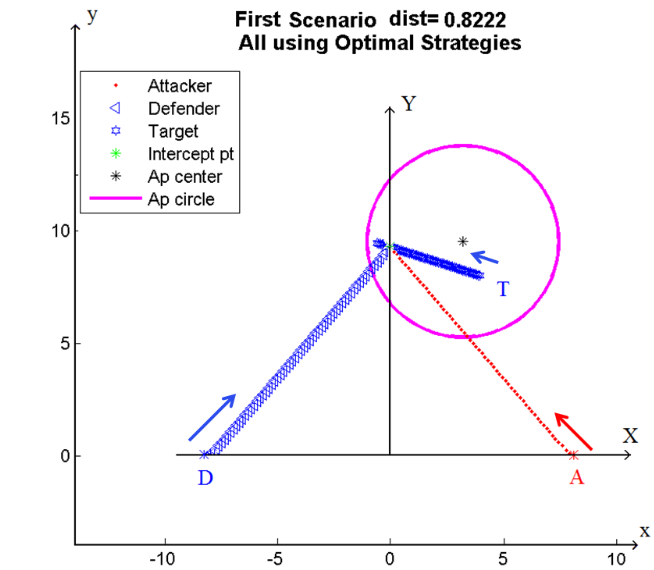

Figure 41. All agents using optimal strategies. Optimal strategy, $\alpha = \frac{2}{5}$

Scenario 2.

The results are similar to Scenario 2 from the previous section such that the optimal strategy favors T and D as the final distance is 0.8314 which is greater than the baseline distance. The resulting trajectories are shown in Figure 42.

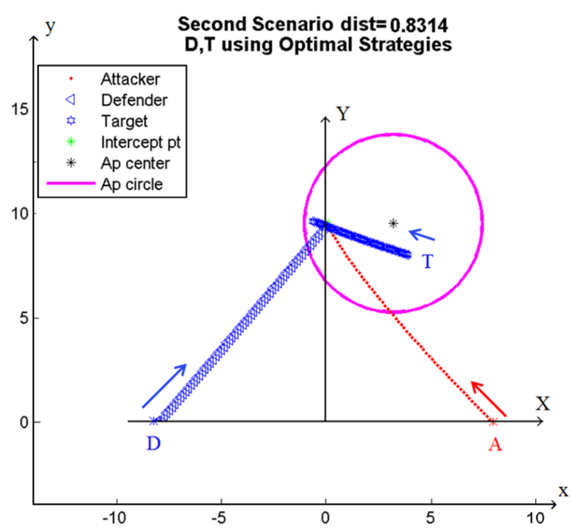

Figure 42. D,T using optimal strategies. A using suboptimal strategy Y=T_Y, and $\alpha = \frac{2}{5}$

Scenario 3.

For the scenario, A is employing the same LOS strategy from Section 4.3 resulting in a curved path. T and D follow the optimal strategies results in an increased separation distance greater than the baseline. The resulting trajectories are shown in Figure 43.

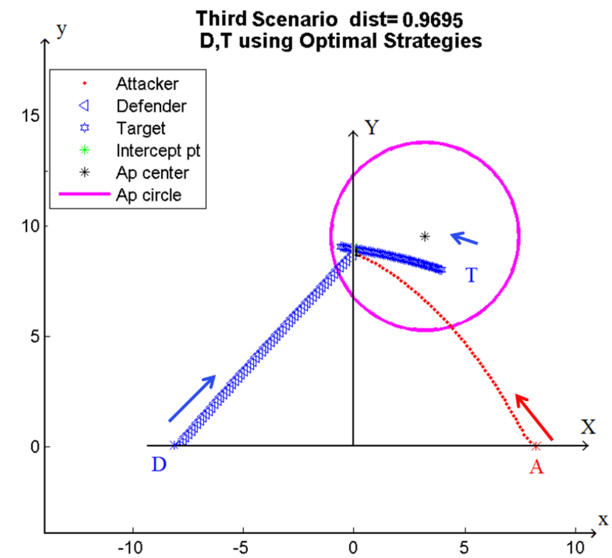

Figure 43. D,T using optimal strategies. A using LOS strategy and $\alpha = \frac{2}{5}$

Scenario 4.

For Scenario 4, T and D chose non-optimal strategies and A chose the optimal strategy. The path the agents follow are shown in Figure 44. The final separation distance is 0.6204 which is less than the baseline.

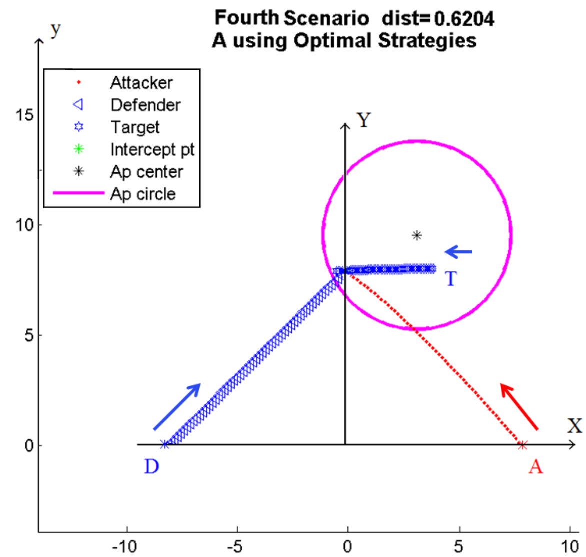

Figure 44. A using optimal strategies. D, T using suboptimal strategy Y=T_Y, and $\alpha = \frac{2}{5}$

Scenario 5.

The resulting trajectories are different than what is seen in Section 4.3. The strategy combination favors A as the distance is less than the baseline. The trajectories are shown in Figure 45.

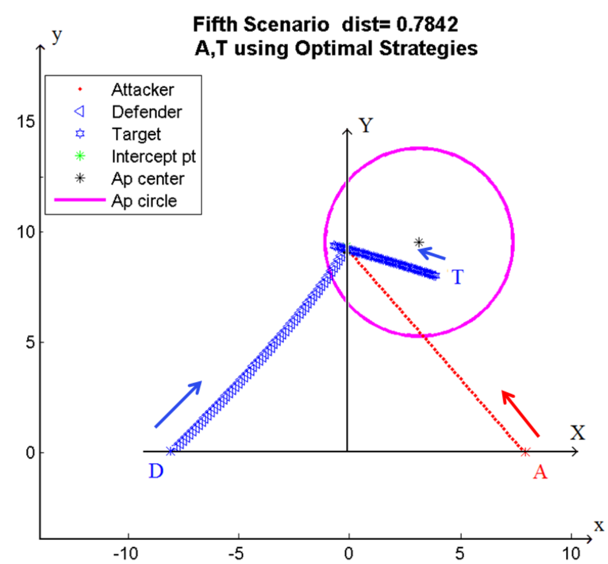

Figure 45. A,T using optimal strategies. D using suboptimal strategy Y=T_Y, and $\alpha = \frac{2}{5}$

Scenario 6.

D and A have selected optimal strategies and T has chosen a non-optimal strategy resulting in a final distance that is less than the baseline. The final separation distance is 0.5651. In the case where T starts in A territory and T chooses a non-optimal strategy, the resulting final I-T separation is less than the baseline. The strategy selections favor A. The resulting trajectories are shown in Figure 46.

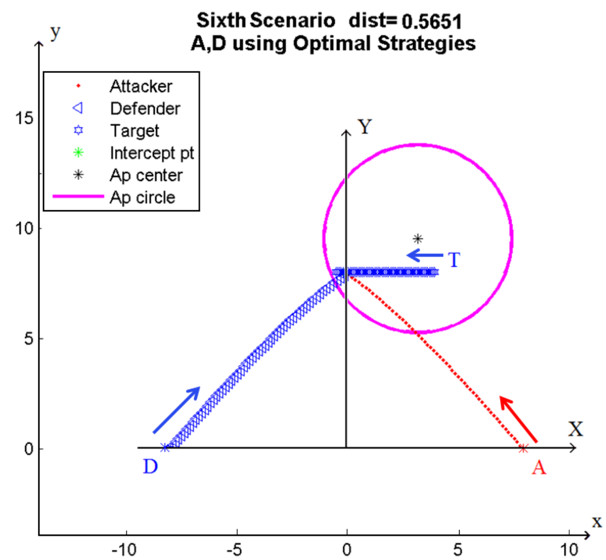

Figure 46. A,D using optimal strategies. T using suboptimal strategy Y=T_Y, and $\alpha = \frac{2}{5}$

Scenario 7.

For Scenario 7, T is employing the optimal strategy and D and A are implementing the sub-optimal strategy where Y=T_Y. With T optimal and D and A sub-optimal, the expectation is the final separation distance will favor the T, D team. At game conclusion, the distance is .8002 units which is less than the baseline. Resulting trajectories are shown in Figure 33 and, decreased I-T separation distance means the strategies employed by the agents favor A. Table 4 contains the results of Case 3.

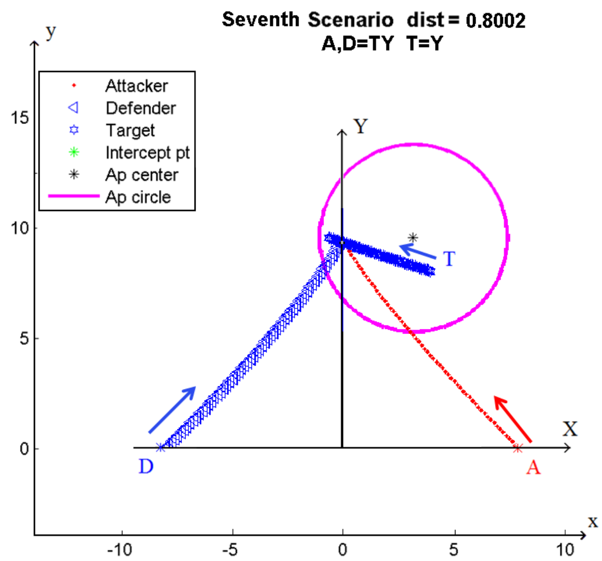

Figure 47. T using optimal strategies. D and A using suboptimal strategy Y=T_Y, and $\alpha = \frac{2}{5}$

Table 4. Distance summary

Scenario 1	.8222	T optimal	D optimal	A optimal
Scenario 2	.8314	T optimal	D optimal	A sub-optimal
Scenario 3	.9695	T optimal	D optimal	A LOS
Scenario 4	.6204	T sub-optimal	D sub-optimal	A optimal
Scenario 5	.7842	T optimal	D sub-optimall	A optimal
Scenario 6	.5651	T sub-optimal	D optimal	A optimal
Scenario 7	.8002	T optimal	D sub-optimal	A sub-optimal

Further investigation into Scenario 7 for this case was pursued. The initial positions for D and A were maintained, and T was given the following initial positions as shown in Table 18.

Table 5. Position summary for Scenario 7 investigation

	T position	D position	A position	Baseline distance	Scenario distance
Bisector	(0,8)	(-8,0)	(8,0)	4.5802	4.7612
A territory	(0.5,8)	(-8,0)	(8,0)	4.1517	4.2677
A territory	(1,8)	(-8,0)	(8,0)	3.6282	3.7749
A territory	(2,8)	(-8,0)	(8,0)	2.6836	2.7895
A territory	(3,8)	(-8,0)	(8,0)	1.7469	1.8126
A territory	(3.5,8)	(-8,0)	(8,0)	1.2333	1.2765
A territory	(3.75,8)	(-8,0)	(8,0)	1.0262	1.0371
A territory	(4,8)	(-8,0)	(8,0)	0.8222	0.8002

Appendix Results.

Part of the strategy formulation in the realistic space involves translation and rotation of reduced state space coordinates relative to the realistic plane. For verification and validation of the mathematics, the agents are placed in different initial locations with rotations and translations. The process begins with rotations in both positive and negative directions. After the rotations are proven, the translations are added. For each starting position of seven scenarios ran, the collected data to determine if any relationships develop . A summary of the positions chosen for simulation are in Table 6. The data results are presented in this chapter, and the figures are located in the Appendix. The results of the simulations are in Table 7.

Table 6. Initial Position summary

Position 1	Position 2	Position 3	Position 4	Position 5
D territory aligned	D territory + rotation	D territory - rotation	D territory + rotation -translation	D territory - rotation - translation
T (-8,8) D (-8,0) A (8,0)	T (-2.25,8) D (-8,-2) A (8,2)	T (-8,8) D (-8,2) A (8,-2)	T (-8,8) D (-8,-2) A (8,0)	T (-8,8) D (-10,0) A (8,-4)

Position 6	Position 7	Position 8	Position 9	Position 10	Position 11
A territory aligned	A territory + rotation	A territory - rotation	A territory + rotation -translation	A territory - rotation - translation	A territory aligned out of range for D
T (0,8) D (-8,0) A (8,0)	T (0,8) D (-6,-2) A (8,2)	T (4,8) D(-8,2) A(8,-2)	T (2,8) D (-8,-2) A (8,0)	T (4,8) D (-8,0) A (8,-2)	T (6,8) D (-8,0) A (8,0)

Table 7. Position distances

	Scenario 1	Scenario 2	Scenario 3	Scenario 4	Scenario 5	Scenario 6	Scenario 7
Position 1	12.3562	13.1065	12.4532	12.1032	12.1457	12.2092	12.7581
Position 2	5.0376	5.2969	5.1255	4.7667	4.9280	4.8290	5.1702
Position 3	13.6476	14.4800	13.6958	13.4669	13.5313	13.4669	13.8980
Position 4	11.6826	12.4337	12.0516	11.5276	11.4990	11.4394	12.2092
Position 5	13.7304	14.6407	13.9675	13.6134	13.6427	13.6134	14.1412
Position 6	4.5802	4.8946	4.7040	4.5075	4.3440	4.5107	4.7612
Position 7	3.2692	3.3936	3.3194	3.0449	3.0869	2.9612	3.3189
Position 8	3.0719	3.2128	3.1405	2.8404	2.7271	2.8404	3.1452
Position 9	1.8742	1.9820	1.9100	1.8398	1.8324	1.7866	1.9106
Position 10	2.3113	2.4791	2.4062	2.0325	2.1974	2.0325	2.4093
Position 11	A captures T	A captures T	A captures T	A captures T	A captures T	A captures T	A captures T

In each initial starting location, Scenario 1 established the baseline distance. For remaining scenarios of each position, the final I-T distances were compared to the baseline distances to develop a pattern. The comparisons were made by

$$\% \text{ difference} = \frac{|\text{Scenario 1 distance} - \text{Scenario N distance}|}{\text{Scenario 1 distance}} * 100 \tag{97}$$

where N is the scenario. The results of the analysis are in Table 19.

Table 8. Position percentages

	Scenario 1	Scenario 2	Scenario 3	Scenario 4	Scenario 5	Scenario 6	Scenario 7
Position 1	0	6.07	0.79	2.05	1.70	1.19	3.25
Position 2	0	5.15	1.74	5.38	2.18	4.14	2.63
Position 3	0	6.10	0.35	1.32	0.85	1.32	1.83
Position 4	0	6.43	3.16	1.33	1.57	2.08	4.51
Position 5	0	6.63	1.73	0.85	0.64	0.85	2.99
Position 6	0	6.86	2.70	1.59	5.16	1.52	3.95
Position 7	0	3.81	1.54	6.86	5.58	9.42	1.52
Position 8	0	4.59	2.23	7.54	11.22	7.54	2.39
Position 9	0	5.75	36.51	1.84	2.23	4.67	1.94
Position 10	0	7.26	4.11	12.06	4.93	12.06	4.24
Position 11	A captures T	A captures T	A captures T	A captures T	A captures T	A captures T	A captures T

Case 4 Mobile Target.

The fourth starting locations is A at (8,0), D at (-8,0), and T at (6,8), with the realistic plane and reduced state space initially aligned. The choice of initial positions places T on the A controlled side of the $\overline{AD}$ bisector. Scenario 1 resulting trajectories are shown in the realistic plane and shown in Figure!48. By starting T in A territory, the Apollonius circle does not intersect the orthogonal bisector of $\overline{AD}$ and shows that T cannot escape A. The choice of strategy will not impact the final outcome of A capturing T as seen in Figure 48. The resulting trajectories and outcome seen in Figure 48 are the same for Scenarios 2 through Scenario 7, and are not presented.

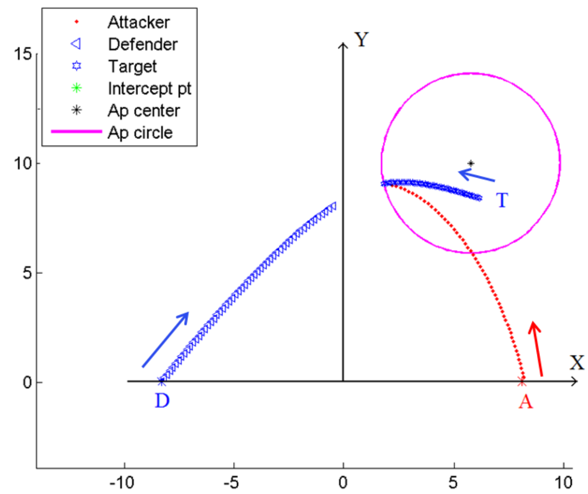

Figure 48. A,D using optimal strategies. T using suboptimal strategy Y=T_Y, and $\alpha = \frac{2}{5}$

4.4 Case 5 Static Target

Case 1 Static Target.

As discussed in Chapter III, when the speed ratio ratio α goes to zero, the quartic equation solution Y is equal to T_Y. For the first case, the static target to be simulated begins with position of T on the D controlled side of the $\overline{AD}$ bisector. For comparison of the strategy combinations to be simulated, the starting locations are held constant. By holding the starting locations constant, the final I-T separation distance can be compared. The starting locations are A at (8,0), D at (-8,0), and T at (-8,8), with the realistic plane and reduced state space initially aligned. The resulting trajectories are shown in the realistic plane.

Note that for Scenario 1 (Figure 49), 2 (Figure 50) ,4 (Figure 52), 5 (Figure 53) and 6 (Figure 54) have similar trajectories and final separation distance, while Scenario 3 (Figure 51) is different as A selects a LOS approach to T. With A not having feedback on D's position, A does not avoid D and is intercepted at a greater

distance than in the other scenarios. The result for Scenario 7 is similar to Scenario 6 and is not presented.

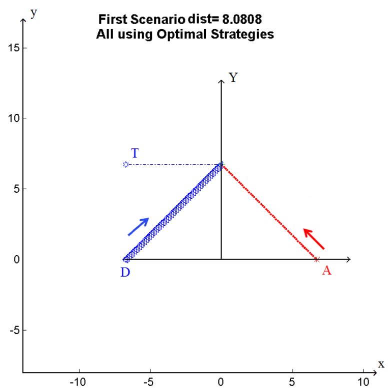

Figure 49. All agents following optimal strategies.

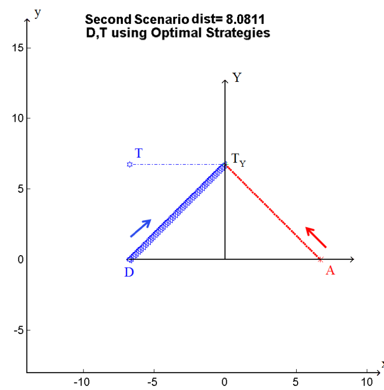

Figure 50. D,T following optimal strategy, A following sub-optimal strategy

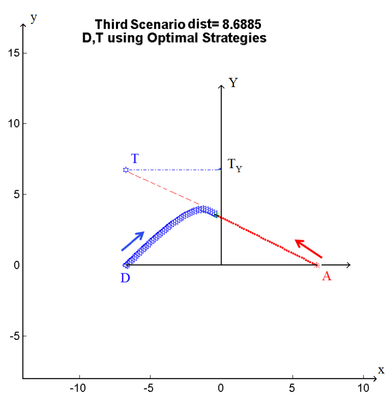

Figure 51. D,T following optimal strategy, A following LOS strategy

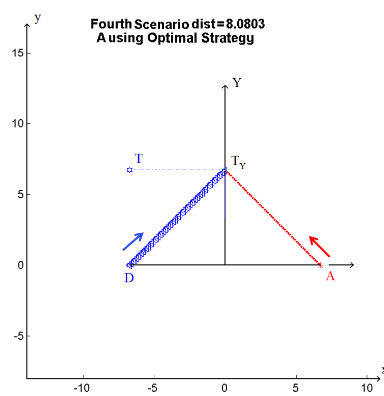

Figure 52. A following optimal strategy, D,T following sub-optimal strategy

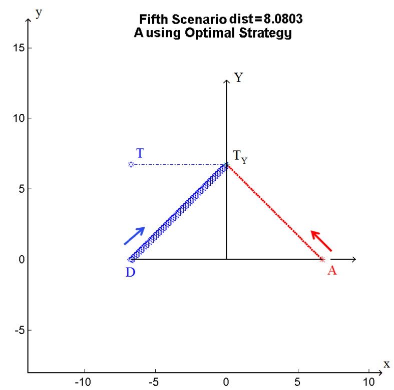

Figure 53. A,T following optimal strategy, D following sub-optimal strategy

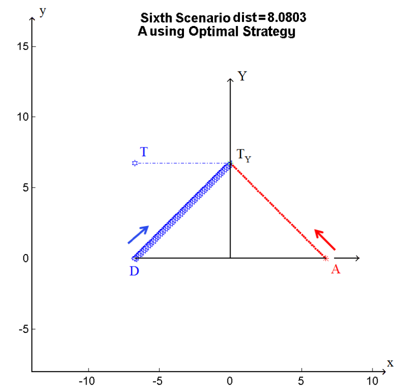

Figure 54. Scenario 6 T in D territory

Case 2 Static Target.

In Case 2, T is on the $\overline{AD}$ orthogonal bisector. As in Case 1, the starting locations are A at (8,0), D at (-8,0), and T is moved to at (0,8), with the realistic plane and reduced state space initially aligned. The resulting trajectories are shown in the realistic plane.

All six scenarios have similar trajectories as shown in Figures 55,56, 57, 58, 59, 60. D has a capture radius and intercepts A, however A also has a capture radius and T is in the capture radius of A at the game conclusion. The conclusion is A wins the game as A has captured T.

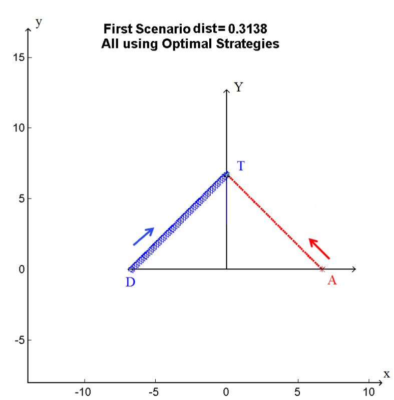

Figure 55. All agents following optimal strategies.

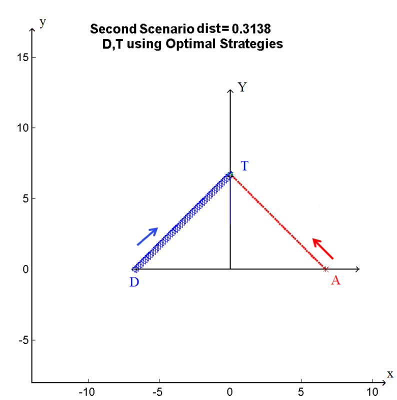

Figure 56. D,T following optimal strategy, A following sub-optimal strategy

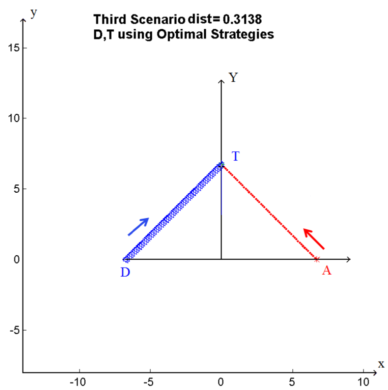

Figure 57. D,T following optimal strategy, A following LOS strategy

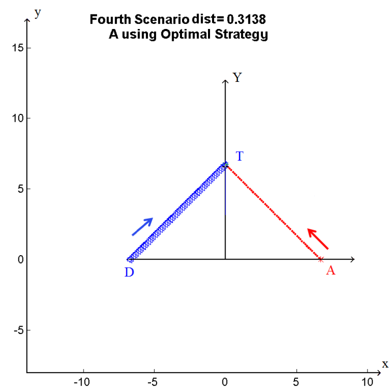

Figure 58. A following optimal strategy, D,T following sub-optimal strategy

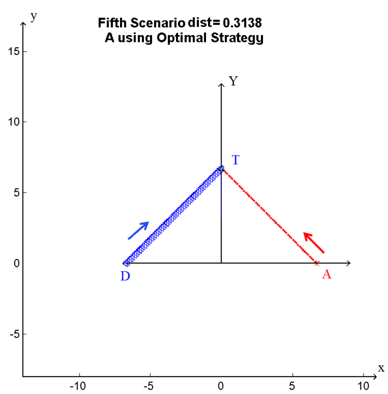

Figure 59. A,T following optimal strategy, D following sub-optimal strategy

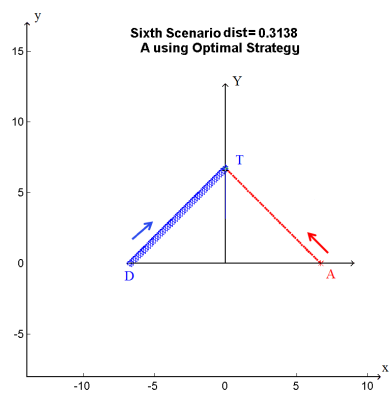

Figure 60. A,D following optimal strategy, T following sub-optimal strategy

Case 3 Static Target.

For Case 3, T is in A territory. As in Case 1, the starting locations are A at (8,0), D at (-8,0), and T is moved to at (4,8), with the realistic plane and reduced state space initially aligned. The resulting trajectories are shown in the realistic space plane. Since T is static, the Apollonius circle does not apply and T is captured in each scenario. D cannot cross the orthogonal bisector of $\overline{AD}$, and thus cannot aid T. Scenario 1 to 6 outcomes are seen in Figures 61,62, 63, 64, 65, 66, have the same outcomes and trajectories and strategy combinations do not impact the final I-T separation distance.

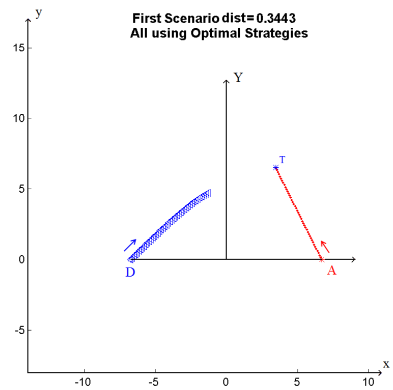

Figure 61. All agents following optimal strategies.

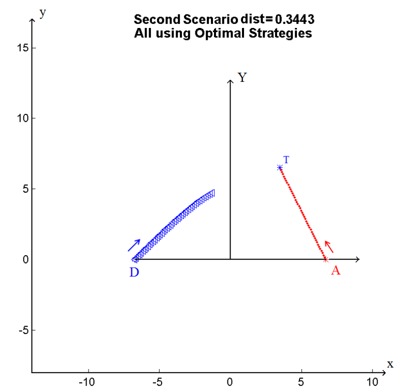

Figure 62. D,T following optimal strategy, A following sub-optimal strategy

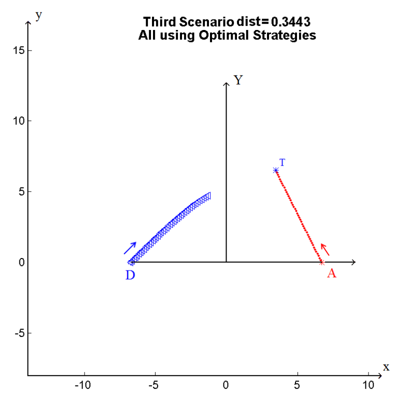

Figure 63. D,T following optimal strategy, A following LOS strategy

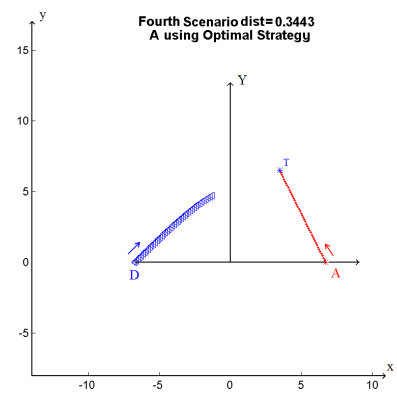

Figure 64. A following optimal strategy, D,T following sub-optimal strategy

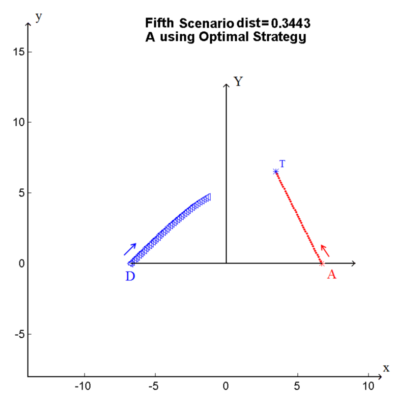

Figure 65. A,T following optimal strategy, D following sub-optimal strategy

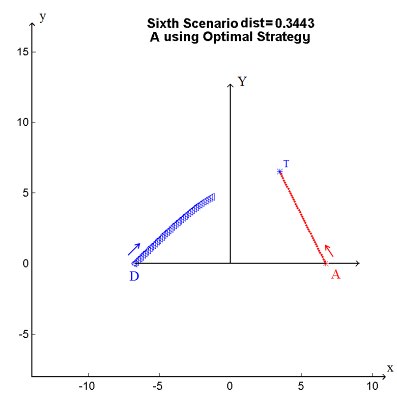

Figure 66. A,D following optimal strategy, T following sub-optimal strategy

4.5 OCT and DGT

In an effort to validate differential game theory as a method to solve for optimal strategies, the same dynamic models and initial starting positions were modeled in Optimal Control Theory (OCT) and Differential Game Theory (DGT). The initial position of the agents are listed in Table 7. For the simulations, the optimal control theory solver was treated as a black box.
The scenarios selected for comparison are Scenario 3 and Scenario 7 as both scenarios can be modeled as a one-sided maximization optimization problem. The figures for this section are listed in the Appendix.

Scenario 3.

For Scenario 3, both T and D are seeking to maximize the separation distance following the optimal strategy. With one variable to be optimized as a maximum for the T and D team, OCT and DGT results were compared for the 10 different initial starting positions as shown in Table 9 to find the difference between the two solutions. The results from the OCT and DGT were compared by:

$$\%\ \text{difference} = \frac{|\text{OCT distance} - \text{DGT distance}|}{\text{DGT distance}} * 100 \tag{98}$$

and since there is no definitive correct answer, the absolute difference is normalized. The result is chosen as a figure of merit to show the percent difference between the two solutions. The OCT A-T separation distance results are greater than the DGT results. The figures are listed in the Appendix.

Table 9. **Results from OCT and DGT for Scenario 3**

Scenario 3	Position 1	Position 2	Position 3	Position 4	Position 5
OTC	12.6843	5.4077	13.8034	12.2759	14.0854
DGT	12.5438	5.2169	13.7261	12.0526	13.9679
% difference	1.1205	3.6565	.5637	1.8527	.8410
	Position 6	Position 7	Position 8	Position 9	Position 10
OTC	4.9982	3.6010	3.3961	2.1872	2.7179
DGT	4.6813	3.3807	3.2014	2.0289	2.4960
% difference	6.7704	.6072	6.0825	7.8036	8.8903

Scenario 7.

In Scenario 7, T is running the optimal strategy while D and A are following the sub-optimal strategy where $Y = T_Y$. OCT can solve for the optimal strategy as T is the only agent seeking to maximize the separation distance with the optimal strategy. The results are shown in Table 10. Again the OCT results have a greater separation distance than the DGT results.

Table 10. **Results from OCT and DGT for Scenario 7**

Scenario 7	Position 1	Position 2	Position 3	Position 4	Position 5
OTC	12.7885	5.2014	13.9489	12.2461	14.2190
DGT	12.7569	5.1895	13.9149	12.2157	14.1804
% difference	0.2476	0.2289	0.2445	0.2490	0.2723
	Position 6	Position 7	Position 8	Position 9	Position 10
OTC	4.7951	3.3540	3.1591	1.9457	2.4309
DGT	4.7806	3.3444	3.1563	1.9422	2.4287
% difference	0.3052	0.2859	0.0873	0 .1809	0.0924

Summary.

In this chapter, the results of the active target defense scenario are presented. Initially, the assumptions of the simulations were defined. The first set of results cover the case where the Target (T) is initially in the Defender (D) territory. The next set of results is the case when T is on the orthogonal bisector. The third set of results are when the Apollonius circle intersects the orthogonal bisector. In the fourth set of results, T was placed where the Apollonius circle does not intersect the orthogonal bisector. The next case to be presented is the case where T is static. The final case presented is the results where differential game theory and optimal control theory are simulating the active target defense scenario.

V. Analysis and Conclusion

5.1 Introduction

The contents of this chapter contains the conclusion of the simulations presented in Chapter IV. Initially, the conclusions from the cases where T is mobile are presented. Next, the cases when T is static are presented. Finally, a comparison of Optimal Control Theory (OCT) and Differential Game Theory (DGT) is presented in reference to two selected scenarios.

5.2 Mobile Target

Simulation, Results Scenario 1.

In Scenario 1, all three agents are utilizing the quartic equation solution Y, thereby yielding the optimal strategies. With all agents employing optimal strategies for the three cases where: T is in D territory; on the orthogonal bisector of $\overline{AD}$; and in T territory, the results serve as a benchmark. The I-T separation at termination is presented in Table 11. The result of all agents operating with optimal strategies, T and D have achieved the optimal maximum separation distance, and A has achieved the optimal minimum separation distance.

Table 11. Cost/payoff summary for Scenario 1

		Scenario 1		
Case 1	12.3562	T optimal	D optimal	A optimal
Case 2	4.5820	T optimal	D optimal	A optimal
Case 3	.8222	T optimal	D optimal	A optimal

Simulation Results, Scenario 2.

In Scenario 2, the strategy of agents T and D is based on the quartic solution Y and A's strategy is a sub-optimal strategy based on the current location of T, that is Y= T_Y. The sub-optimal strategy employed by means A maintains situational awareness of D at T. The expectation is with A employing a sub-optimal strategy and D and T employing the optimal strategy, the final separation distance will be greater than the benchmark distance. Differential Game Theory assumes all players are acting optimally to achieve their respective goals. In this scenario, A selected a sub-optimal strategy. During the simulation, D and T are able to capitalize on A's selection of a sub-optimal strategy and increase the I-T separation distance. Indeed, the results in Table 12 show that there is an increase in the final separation distance. The result is in favor of D and T, as expected.

Table 12. Cost/payoff Summary for Scenario 2

	Bench mark	Realized	Scenario 2		
Case 1	12.3562	13.1065	T optimal	D optimal	A sub-optimal
Case 2	4.5820	4.8946	T optimal	D optimal	A sub-optimal
Case 3	.8222	.8314	T optimal	D optimal	A sub-optimal

Simulation Results, Scenario 3.

In Scenario 3 agents the strategy of agents T and D is formulated with the quartic equation solution Y, whereas and A employs the LOS pursuit strategy. The LOS strategy does not have situational awareness of D, and A heads straight for T and ignores D's approach. Table **??** shows the final distance is increased over the benchmark. Again, since A selected a sub-optimal strategy, D and T are able to increase

the I-T separation distance. The conclusion is this strategy combination favors D and T, as expected.

	Bench mark	Realized	Scenario 3		
Case 1	12.3562	12.4532	T optimal	D optimal	A LOS
Case 2	4.5820	4.9060	T optimal	D optimal	A LOS
Case 3	.8222	.9695	T optimal	D optimal	A LOS

Table 13. Cost/payoff Summary for Scenario 3

Simulation Results, Scenario 4.

For Scenario 4, A's strategy is the optimal strategy, and D and T strategy is the sub-optimal strategy. In this scenario, A is expecting D and T to behave optimally, but the strategy selection is sub-optimal. Since D and T have selected a sub-optimal strategy, A is able to take advantage of the sub-optimal selection. The exptation for this scenario is A should be able to take advantage of D and T not operating optimally, and decrease the I-T separation distance. Table 14 shows that the final distance is less than the benchmark. Thus, it can be concluded the strategy combinations favors A.

Table 14. Distance summary for Scenario 4

Bench mark			Scenario 4		
12.3562	Case 1	12.1032	T sub-optimal	D sub-optimal	A optimal
4.5820	Case 2	4.5075	T sub-optimal	D sub-optimal	A optimal
.8222	Case 3	.6204	T sub-optimal	D sub-optimal	A optimal

Simulation Results Scenario 5.

In Scenario 5, A and T follow the strategy the optimal strategies, and D follows the sub-optimal strategy. With D selecting the sub-optimal strategy, A is able to improve his ability to avoid D as D is not employing the optimal strategy. Since A takes advantage of D's sub-optimal strategy choice, A is able to decrease the I-T separation distance. Table 15 shows that the final distance for the three scenarios. The conclusion is the strategy favors A, which is the expected outcome.

Table 15. Distance summary for Scenario 5

Bench mark			Scenario 5		
12.3562	Case 1	12.1457	T optimal	D sub-optimal	A optimal
4.5820	Case 2	4.4471	T optimal	D sub-optimal	A optimal
.8222	Case 3	.7842	T optimal	D sub-optimal	A optimal

Simulation Results Scenario 6.

For Scenario 6, A and D chose the optimal strategy, and T chose the sub-optimal strategy. In this scenario, T is not following the optimal strategy, whereas D and A are following the optimal strategy. With D following the optimal strategy, D intercepts A as expected, but A is able to decrease the I-T separation distance since T is not following the optimal strategy. Table **??** shows that the final distance is less than the benchmark and the outcome favors A. The conclusion is the strategy favors A, as expected.

Bench mark			Scenario 6		
12.3562	Case 1	12.2092	T sub-optimal	D optimal	A optimal
4.5820	Case 2	4.5106	T sub-optimal	D optimal	A optimal
.8222	Case 3	.5651	T sub-optimal	D optimal	A optimal

Table 16. Distance summary for Scenario 6

Simulation Results Scenario 7.

The results in Scenario 7 do not follow the trend seen in the previous six scenarios, T followed the optimal strategy, and D and A employed sub-optimal strategies. In Case 1 and Case 2, T takes advantage of the A's sub-optimal strategy choice and increases the final separation distance over the baseline. Case 3 does not follow the trend. The expectation is T should increase the I-T separation distance, however this is not the outcome. Table 17 shows that the final distance is not greater than the benchmark in all three cases.

Table 17. Distance summary for Scenario 7

Bench mark			Scenario 7		
12.3562	Case 1	12.7581	T optimal	D sub-optimal	A sub-optimal
4.5820	Case 2	4.7612	T optimal	D sub-optimal	A sub-optimal
.8222	Case 3	.8002	T optimal	D sub-optimal	A sub-optimal

With the outcome for Case 3 not following the trend, further investigation into the outcome required testing of additional initial positions for T. Table 18 shows the positions tested. The initial positions of A and D were held constant, and T was moved from D territory, then to the orthogonal bisector of $\overline{AD}$, and finally moved in

to A territory. Given the condition where T is in D territory or on the orthogonal bisector , T's choice of the optimal strategy based on the quartic equation solution is the best choice. When T is past the boundary condition, the quartic equation solution no longer optimizes the approach strategy. This finding was not within the scope of the experimentation and therefore not pursued. Further research can be performed in exploration of the boundary condition.

Table 18. Position summary for Scenario 7 investigation

	T position	D position	A position	Baseline distance	Scenario distance
Bisector	(0,8)	(-8,0)	(8,0)	4.5802	4.7612
A territory	(0.5,8)	(-8,0)	(8,0)	4.1517	4.2677
A territory	(1,8)	(-8,0)	(8,0)	3.6282	3.7749
A territory	(2,8)	(-8,0)	(8,0)	2.6836	2.7895
A territory	(3,8)	(-8,0)	(8,0)	1.7469	1.8126
A territory	(3.5,8)	(-8,0)	(8,0)	1.2333	1.2765
A territory	(3.75,8)	(-8,0)	(8,0)	1.0262	1.0371
A territory	(4,8)	(-8,0)	(8,0)	0.8222	0.8002

Simulation Results Analysis.

The percentage results from Chapter IV are listed below. By comparing the benchmark distance in Scenario 1 to the remaining scenario distances, there no distinct pattern that developed that favors any one strategy combination over any other combination as shown in Table 19. The expectation was that one scenario would consistently have an increased I-T separation distance. The results in the table show there is no scenario that results in better I-T separation distance. For example, Position 1 Scenario 2 has a separation percentage greater than the remaining scenar-

ios. However in Position 7 Scenario 6, the separation percentage was greater that the remaining scenarios. The conclusion there does not appear to be a pattern or relationship between initial positions and final I-T separation distance.

Table 19. Position percentages

	Scenario 1	Scenario 2	Scenario 3	Scenario 4	Scenario 5	Scenario 6	Scenario 7
Position 1	0	6.07	0.79	2.05	1.70	1.19	3.25
Position 2	0	5.15	1.74	5.38	2.18	4.14	2.63
Position 3	0	6.10	0.35	1.32	0.85	1.32	1.83
Position 4	0	6.43	3.16	1.33	1.57	2.08	4.51
Position 5	0	6.63	1.73	0.85	0.64	0.85	2.99
Position 6	0	6.86	2.70	1.59	5.16	1.52	3.95
Position 7	0	3.81	1.54	6.86	5.58	9.42	1.52
Position 8	0	4.59	2.23	7.54	11.22	7.54	2.39
Position 9	0	5.75	36.51	1.84	2.23	4.67	1.94
Position 10	0	7.26	4.11	12.06	4.93	12.06	4.24
Position 11	A captures T	A captures T	A captures T	A captures T	A captures T	A captures T	A captures T

5.3 Static Target Analysis

For Case 1 when T is located in D territory, distance separation distance are relatively close for each starting position. In the first starting location, the distances are close except when A chose a LOS approach. Since A chose a LOS approach and ignored the approach of D, D was able to increase the I-T separation distance. In Case 2, A won the scenario even though A is captured by D. Both D and A have a capture circle. A successful capture occurred when A fell in the capture circle of D. However, since T fell in A's capture circle, A won as T did not ultimately avoid capture. For Case 3, A won each scenario as T could not cross the orthogonal bisector.

5.4 Comparison of OCT and DGT

Two case were selected to compare Optimal Control Theory (OCT) and Differential Game Theory (DGT). The cases compared are Scenario 3 where both T and

D working cooperatively, and Scenario 7 where T is optimal and D and A are sub-optimal. To give the two methodologies a variety of starting positions, the initial positions are listed in Table 6 and contain rotations and translations between the realistic space and the reduced state space. For the OCT modeling, the players' sub-optimal strategies are known in advance, whereas DGT modeling is with the assumption that all players are following the optimal strategy. Since the strategies are known in advance for the OCT solution, the expectation is OCT will give a greater final separation distance than DGT.

Scenario 3.

In Scenario 3, the T and D team objective was to maximize the I-T separation distance by following the optimal strategy, with A following a sub-optimal strategy. With one scenario defined as a maximization problem for the T and D team, OCT and DGT results were compared for the 10 different initial starting positions (shown in Table. 6) to find the difference between the two solutions. The maximum percent difference between the the two solutions in this scenario is less than 9%. The OCT results have a greater separation distance distance over DGT, which is expected.

Scenario 7.

For Scenario 7, T's objective is to maximize the I-T separation distance with D and A following sup-optimal strategies. As in the previous scenario, this was defined as a maximization problem for the T, OCT and DGT results were compared for the 10 different initial starting positions (shown in Table. 6) to find the difference between the two solutions. The maximum percent difference between the the two solutions in this scenario is less than 1% . The OCT results have a greater separation distance distance over DGT, which is expected.

Summary.

In this chapter, the conclusions of the simulations were presented. The chapter started with an analysis of the mobile target cases. Next, the static target cases were discussed. Finally a comparison between OCT and DGT were presented, and conclusions were made about the results.

VI. Conclusions and Future Research

6.1 Conclusions

The goal of this research was to develop a method of deriving guidance laws based on positional information and incorporating feedback for a three agent active defense scenario. After the proposed guidance laws were developed, they were tested via simulation against combinations of guidance laws that were optimal and sub-optimal. In the case where the Attacker (A) is minimizing the Intercept-Target (I-T) distance while the Target (T) and Defender (D) are maximizing the I-T distance and all agents followed the optimal strategies, Differential Game Theory (DGT) solved for the min-max I-T distance. When D and T chose the optimal strategy against A with a selection of non-optimal strategy, the end result was a final separation distance that favors D and T. When T and D select a combination of sub-optimal strategies while A selects the optimal strategy, the final separation distance favors A. Two scenarios were chosen as test cases to compare the results from DGT and Optimal Control Theory (OCT). The scenarios selected were; T and D employed the optimal strategy against A employing an LOS strategy (Scenario 3); and the scenario where D and A both chose sub-optimal strategies with T chose optimal strategies (Scenario 7) . These two scenarios were chosen because OCT can solve the problem as a maximization problem for the I-T distance, and gives validity to differential game theory as a tool that can solve one sided optimal control problems. The result is both methods arrived at solutions that are up to 92% of each other. The conclusion is DGT can solve optimization problem, for both maximization and minimization-maximization problems.

Future Research.

Differential Game Theory can be employed to solve a diverse array of problems. The fundamental geometry established based on low fidelity models, higher fidelity models can be developed that incorporate flight dynamics and environmental effects. With robust models, the possibility of testing the guidance laws can lead to conducting tests on ground vehicles and later flight testing. Other scenarios to be explored is the geometric relationships when A and D having different speeds. Additional scenarios to considered is given a static target, and determining the best positioning of the defender based on the direction of the attacker. An extension of the static target case is also the concept of the differential coastal defense game where the target is not a static point target but rather a polygon or a plane. In these types of static target games, elements to be explored is the optimal behavior of the attacker and the defender where they have same speeds or different speeds.

Appendix A.

1.1 Position 1

This section contains the plot for the positions where rotations and translations are introduced between the reduced state and the realistic space. These plot were generated using Matlab as teh program to run the simulations.

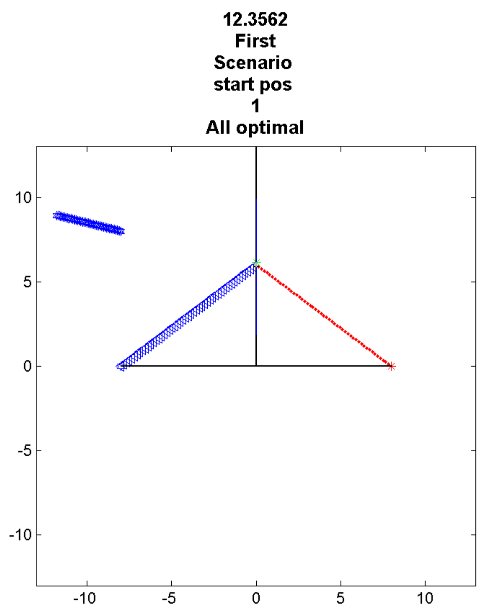

Figure 67. Position 1, Scenario 1

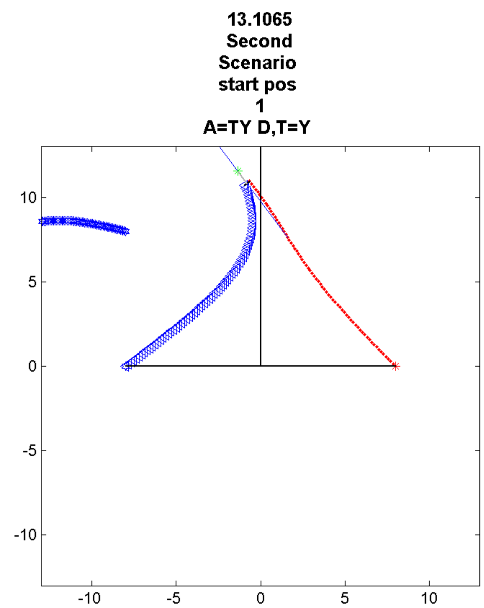

Figure 68. Position 1, Scenario 2

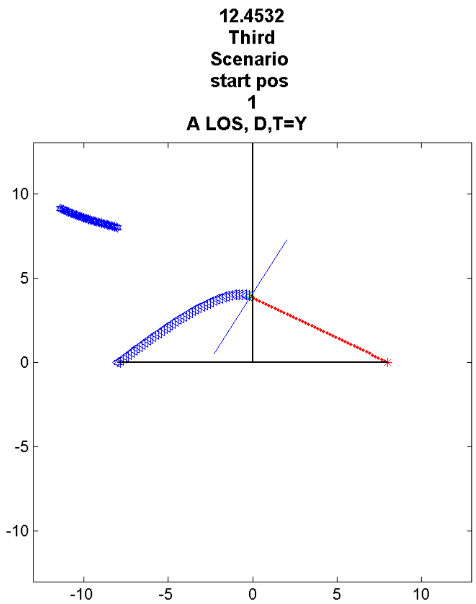

Figure 69. Position 1, Scenario 3

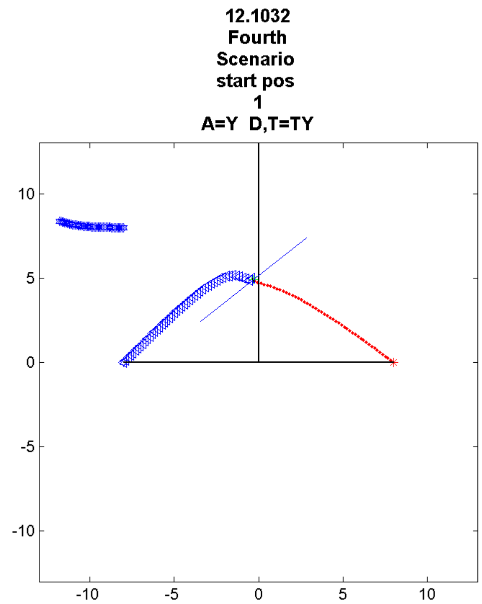

Figure 70. Position 1, Scenario 4

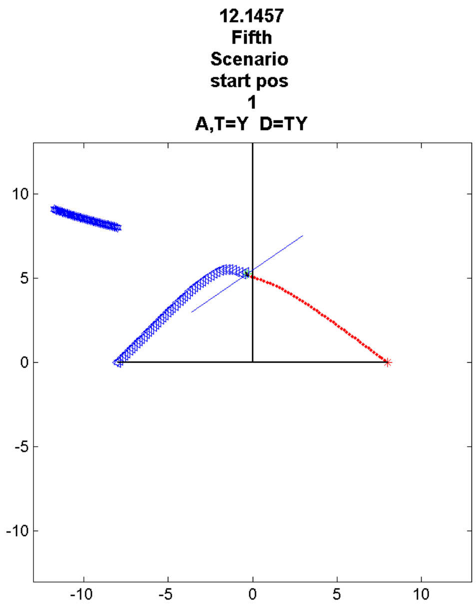

Figure 71. Position 1, Scenario 5

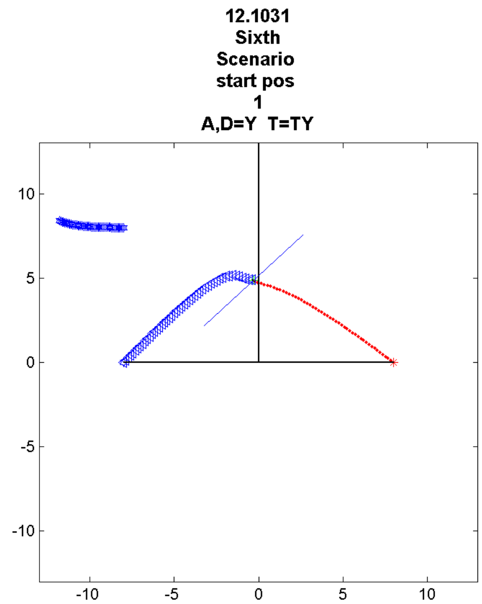

Figure 72. Position 1, Scenario6

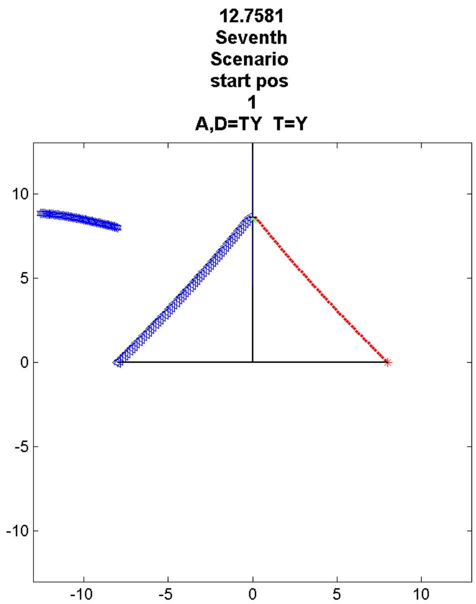

Figure 73. Position 1, Scenario 7

Appendix B.

2.1 Position 2

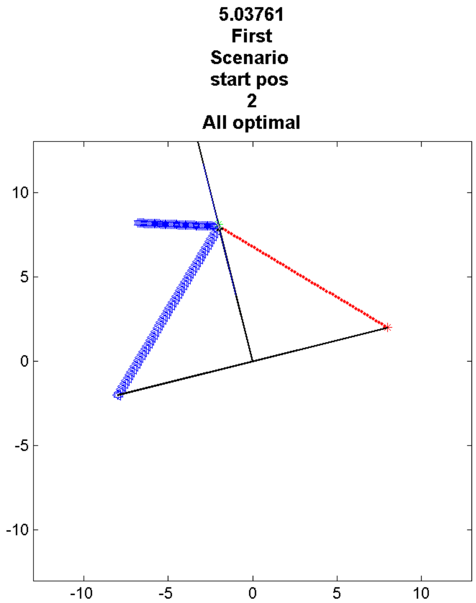

Figure 74. Position 2, Scenario 1

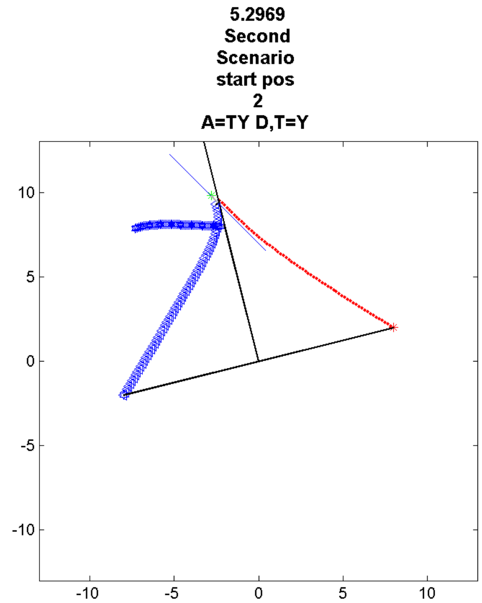

Figure 75. Position 2, Scenario 2

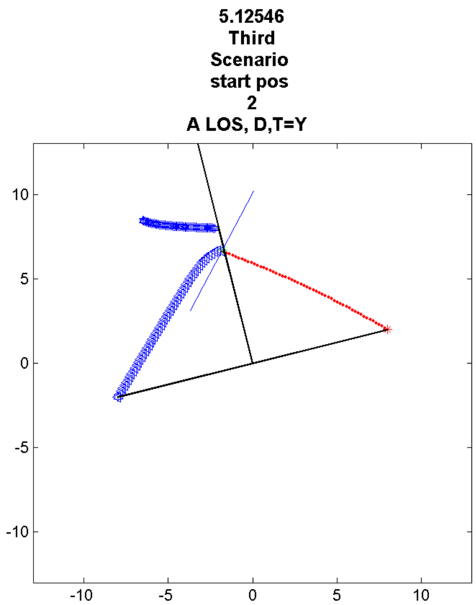

Figure 76. Position 2, Scenario 3

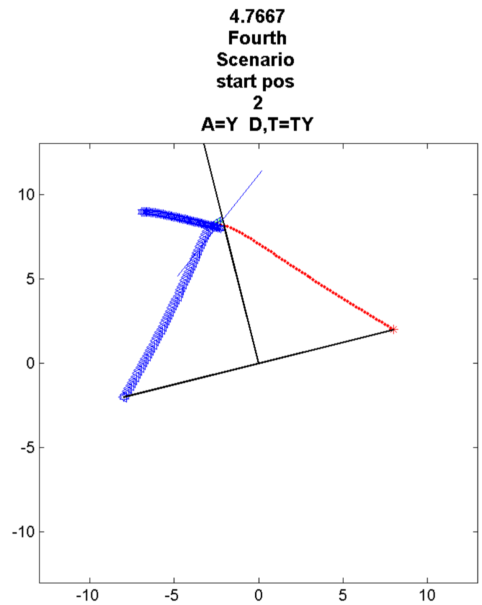

Figure 77. Position 2, Scenario 4

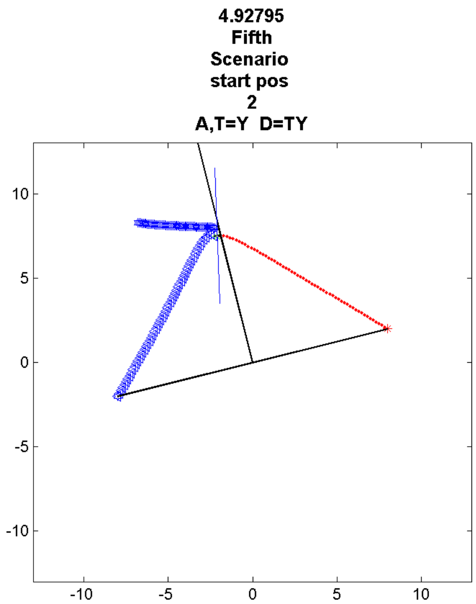

Figure 78. Position 2, Scenario 5

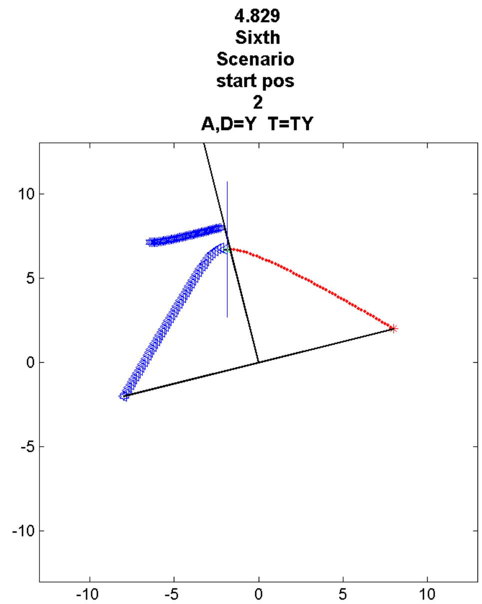

Figure 79. Position 2, Scenario 6

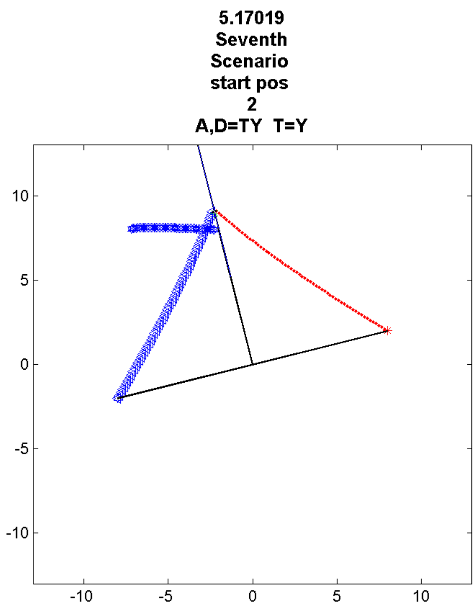

Figure 80. Position 2, Scenario 7

Appendix C.

3.1 Position 3

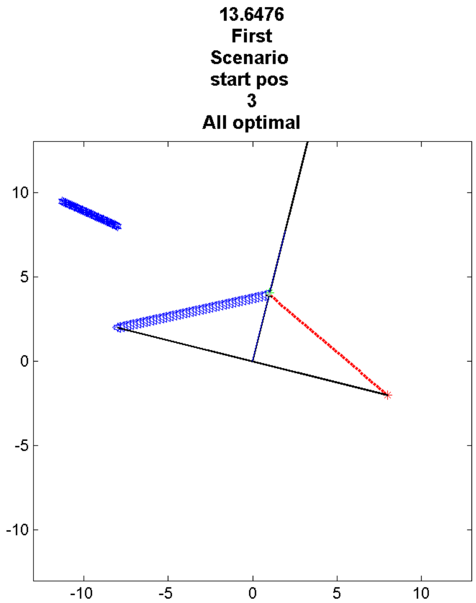

Figure 81. Position 3, Scenario 1

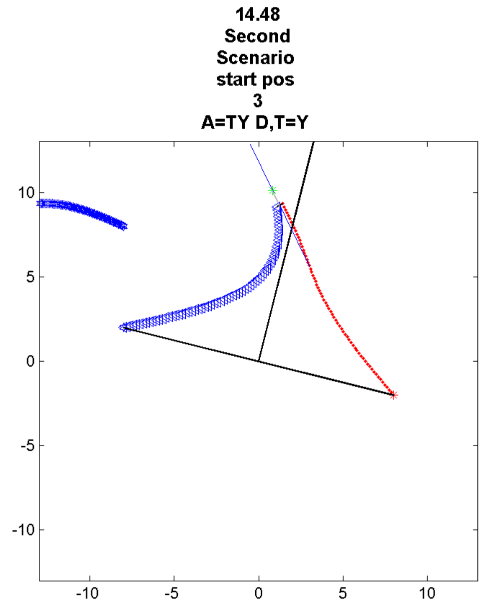

Figure 82. Position 3, Scenario 2

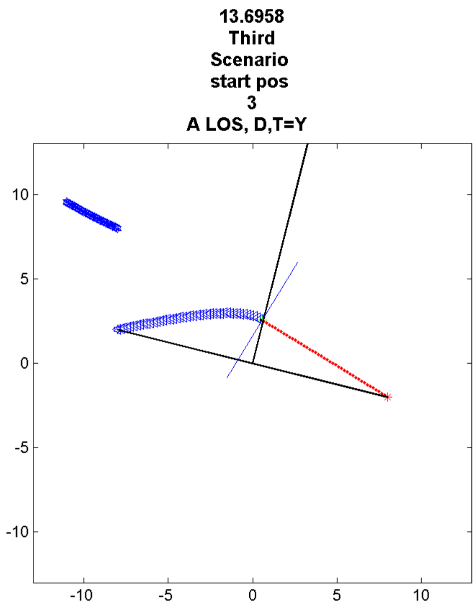

Figure 83. Position 3, Scenario 3

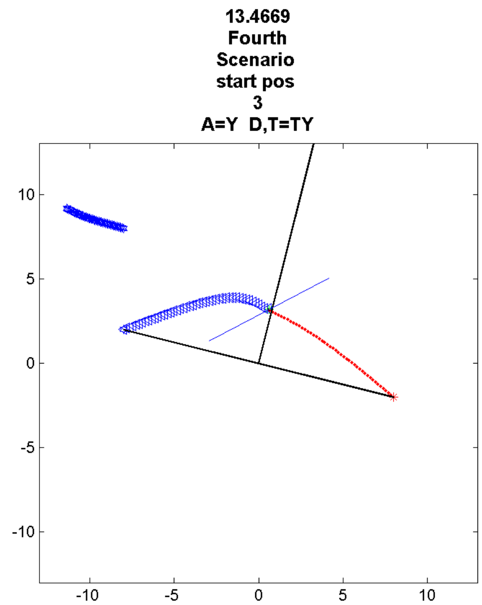

Figure 84. Position 3, Scenario 4

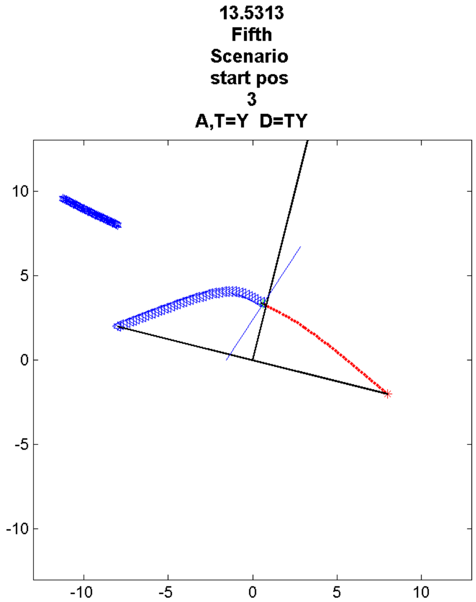

Figure 85. Position 3, Scenario 5

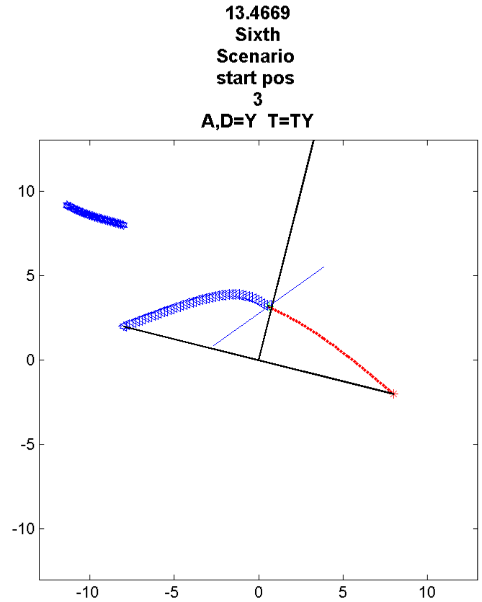

Figure 86. Position 3, Scenario 6

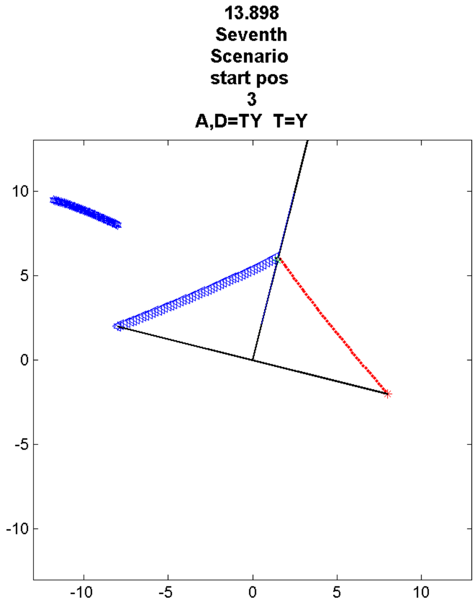

Figure 87. Position 3, Scenario 7

Appendix D.

4.1 Position 4

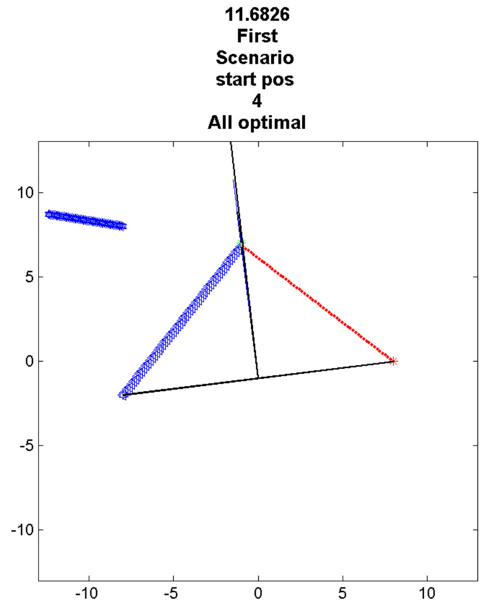

Figure 88. Position 4, Scenario 1

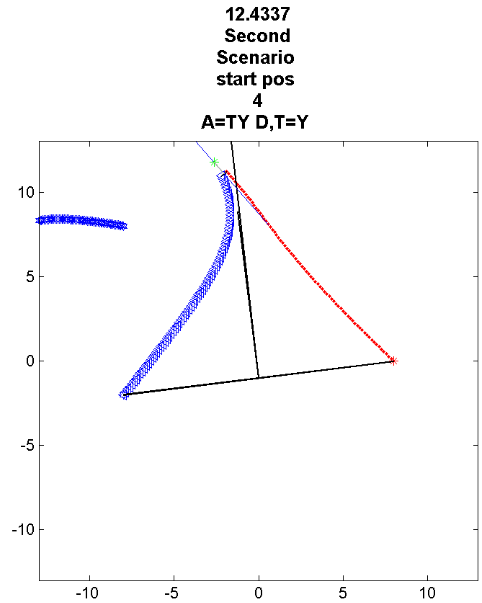

Figure 89. Position 4, Scenario 1

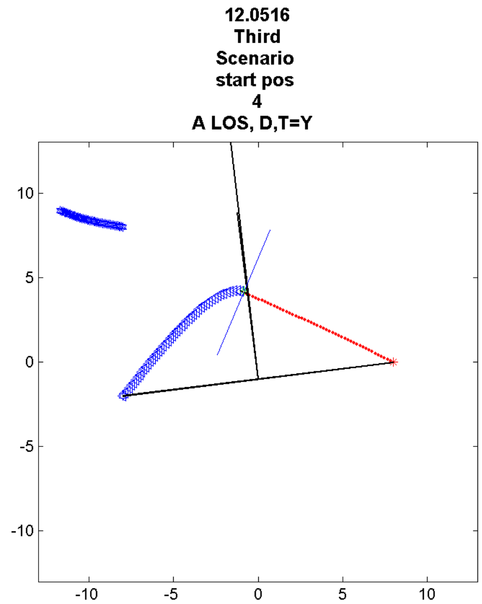

Figure 90. Position 4, Scenario 3

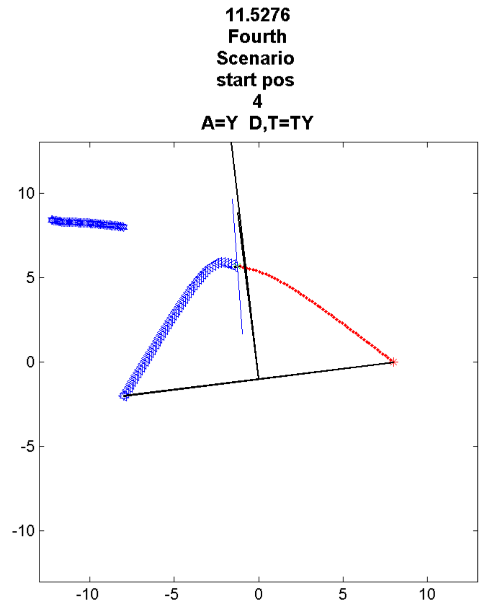

Figure 91. Position 4, Scenario 4

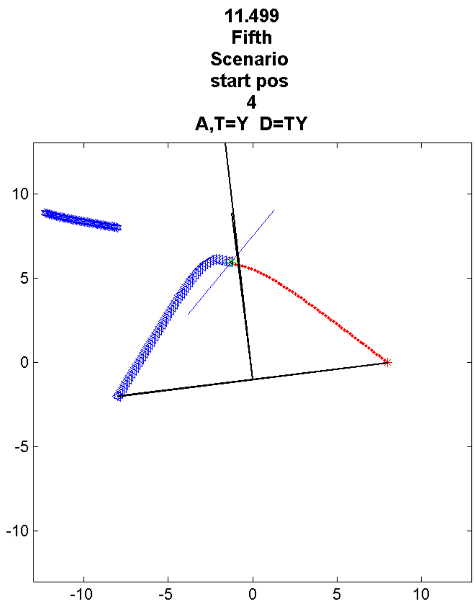

Figure 92. Position 4, Scenario 5

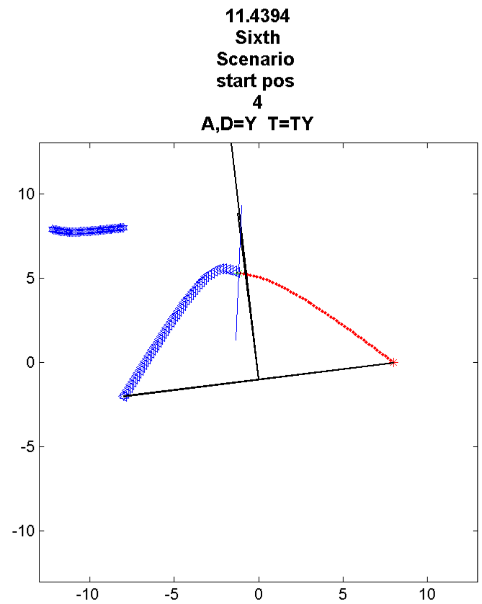

Figure 93. Position 4, Scenario 6

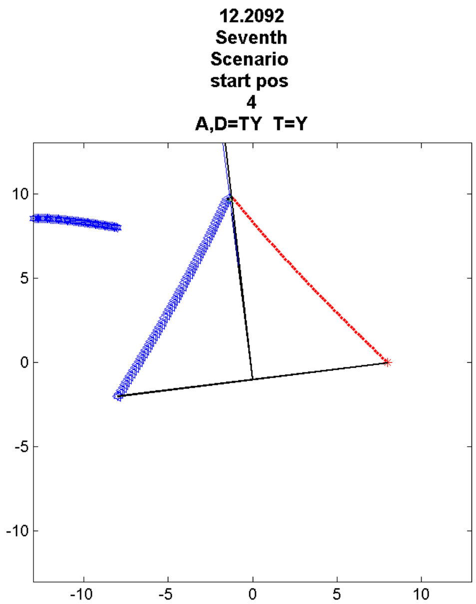

Figure 94. Position 4, Scenario 7

Appendix E.

5.1 Position 5

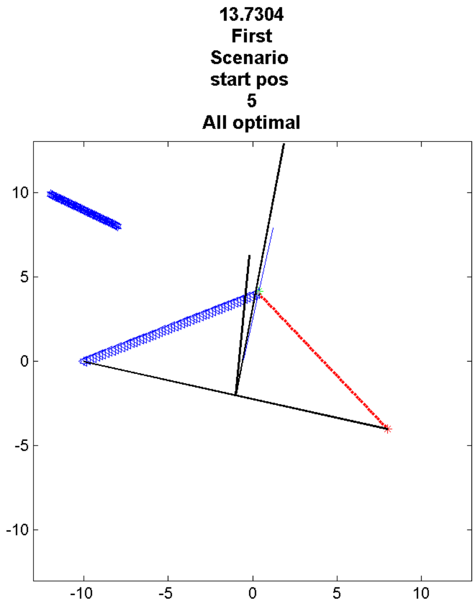

Figure 95. Position 5, Scenario 1

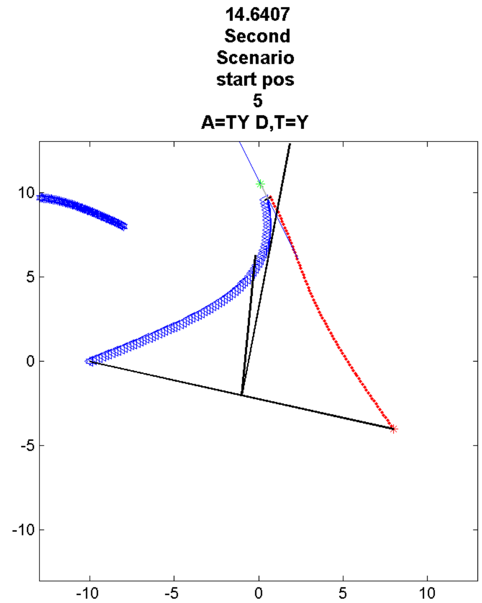

Figure 96. Position 5, Scenario 2

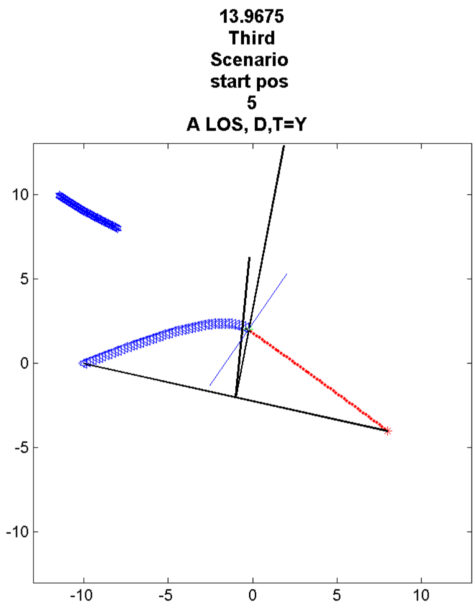

Figure 97. Position 5, Scenario 3

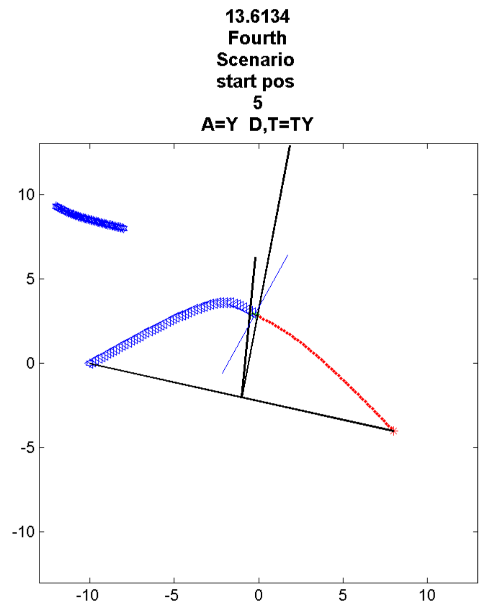

Figure 98. Position 5, Scenario 4

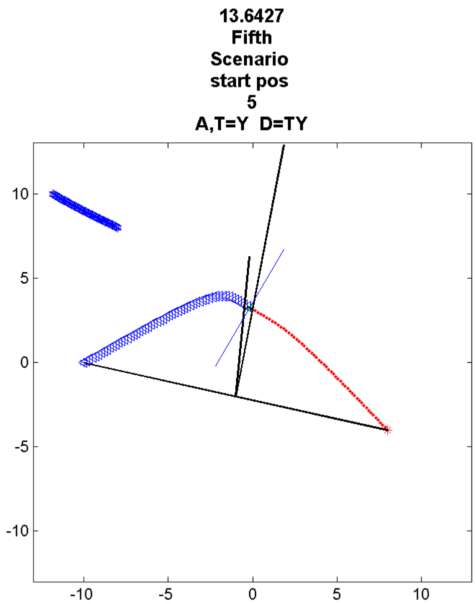

Figure 99. Position 5, Scenario 5

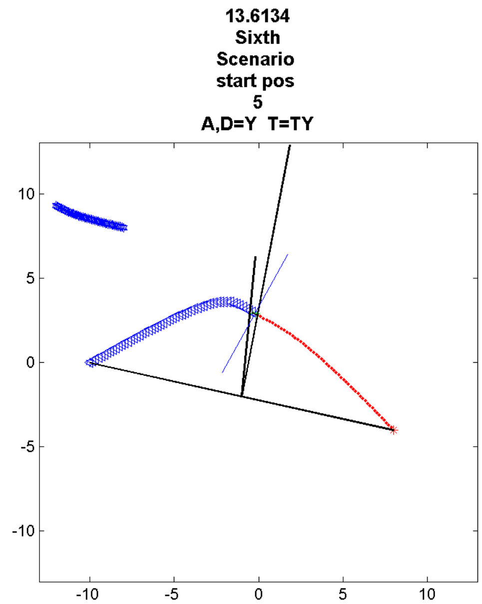

Figure 100. Position 5, Scenario 6

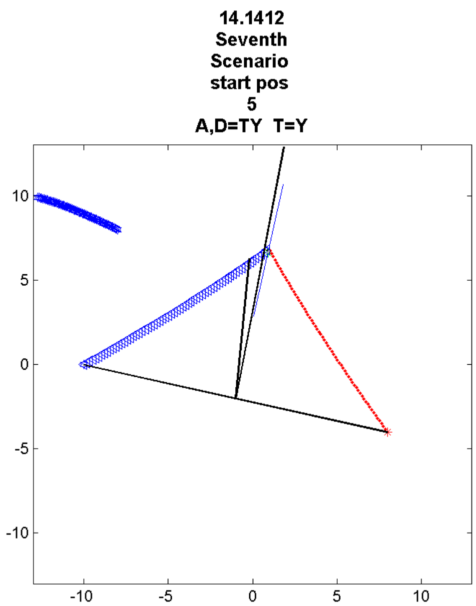

Figure 101. Position 5, Scenario 7

Appendix F.

6.1 Position 6

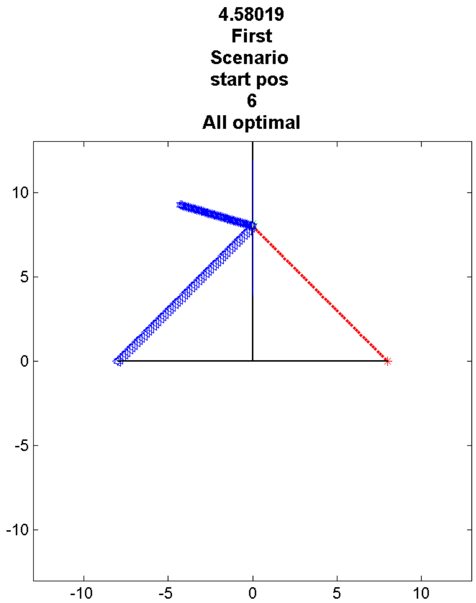

Figure 102. Position 6, Scenario 1

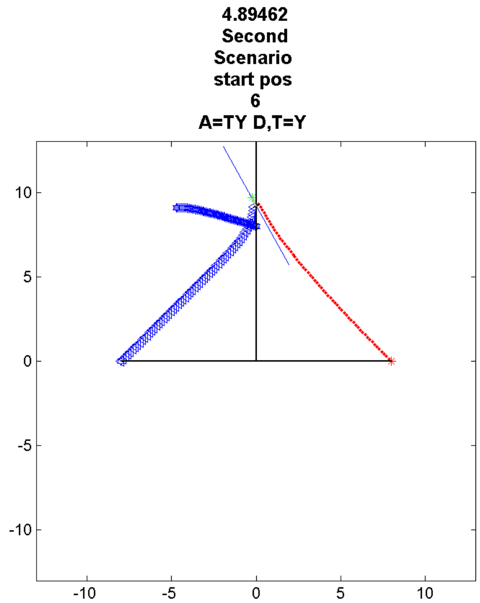

Figure 103. Position 6, Scenario 2

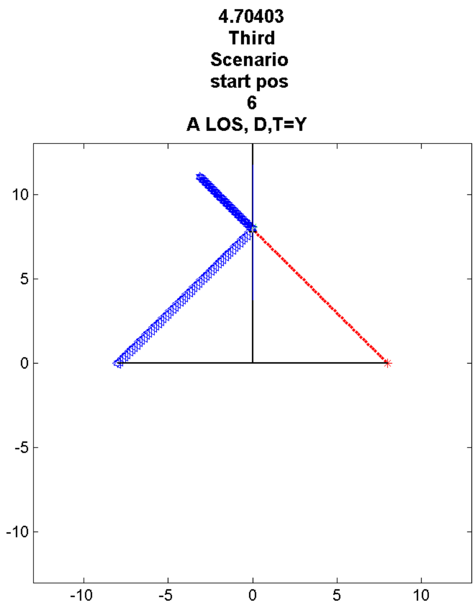

Figure 104. Position 6, Scenario 3

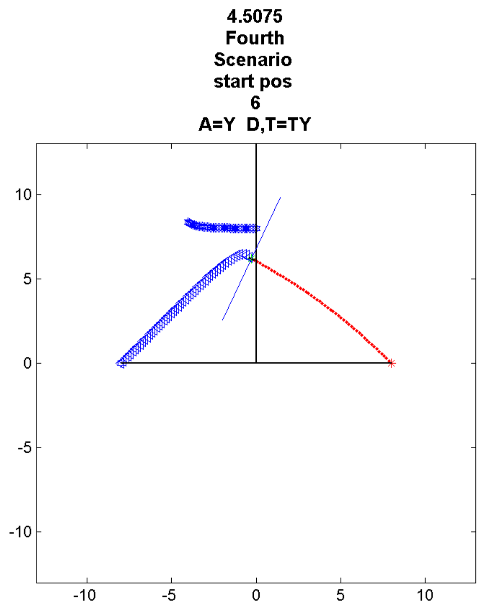

Figure 105. Position 6, Scenario 4

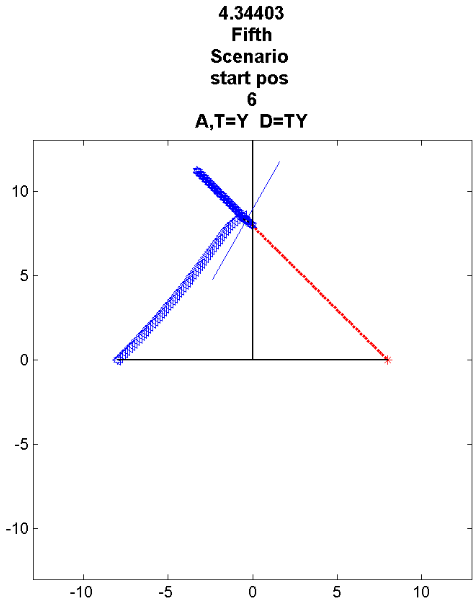

Figure 106. Position 6, Scenario 5

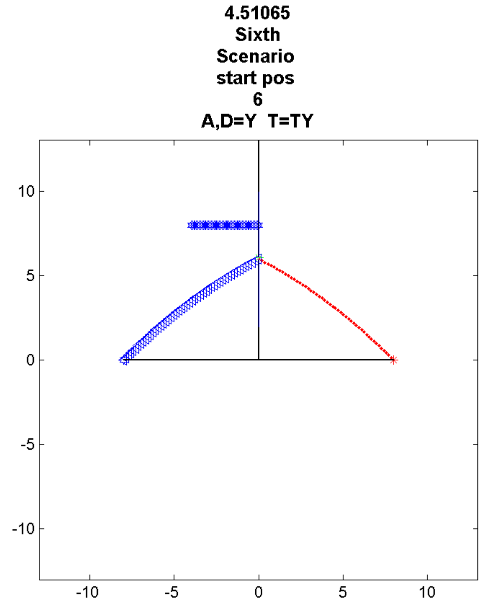

Figure 107. Position 6, Scenario 6

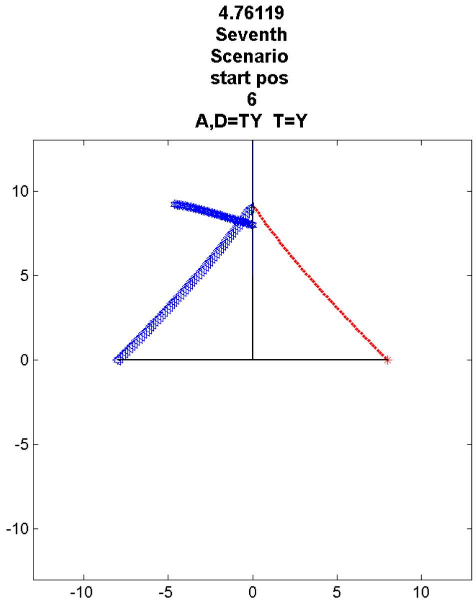

Figure 108. Position 6, Scenario 7

Appendix G.

7.1 Position 7

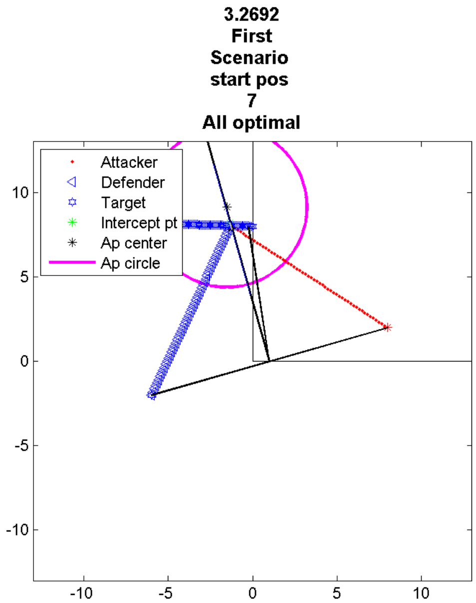

Figure 109. Position 7, Scenario 1

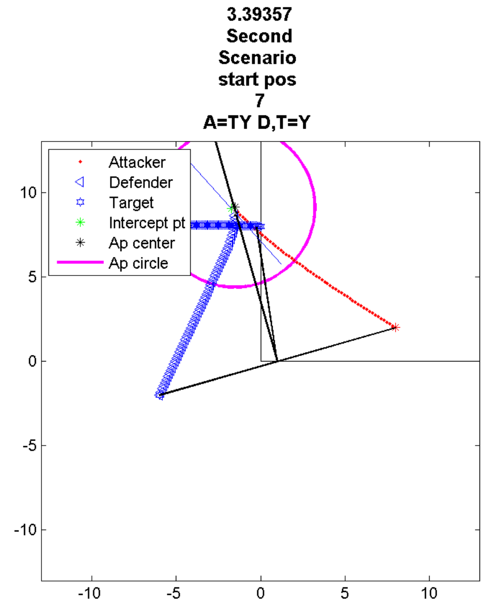

Figure 110. Position 7, Scenario 2

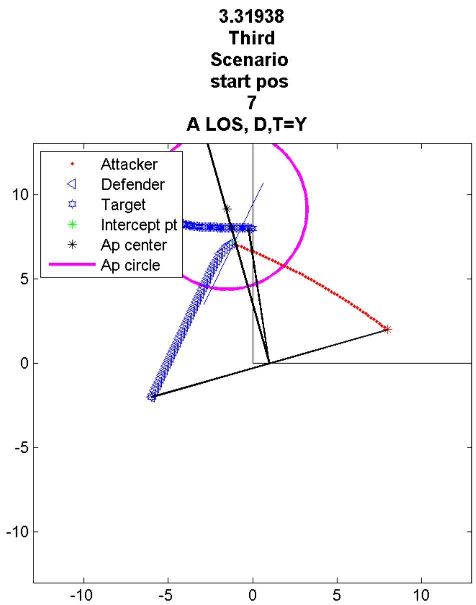

Figure 111. Position 7, Scenario 3

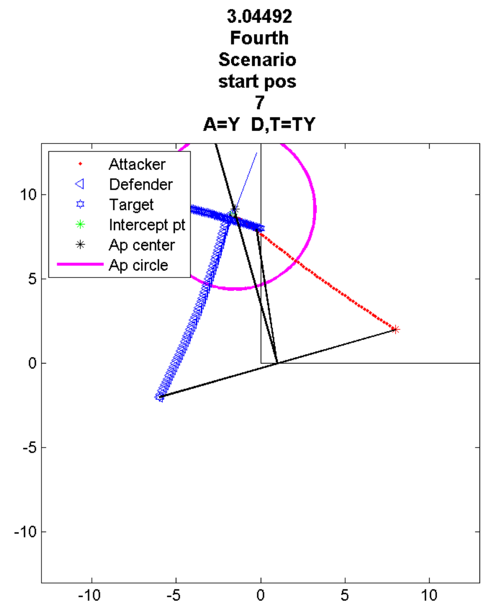

Figure 112. Position 7, Scenario 4

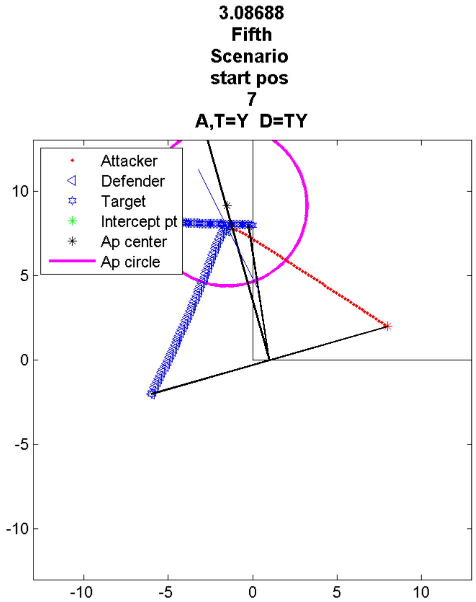

Figure 113. Position 7, Scenario 5

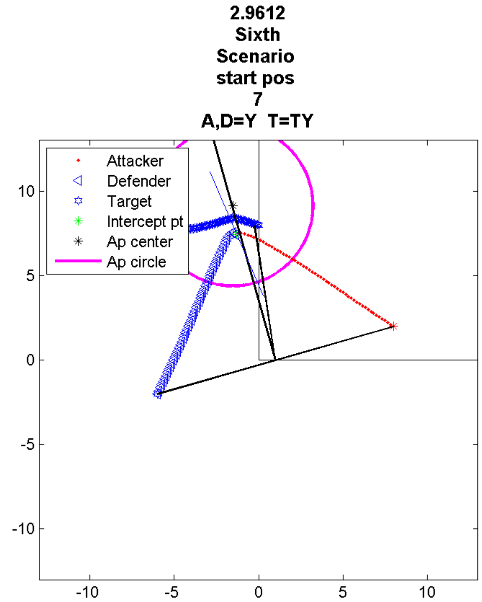

Figure 114. Position 7, Scenario 6

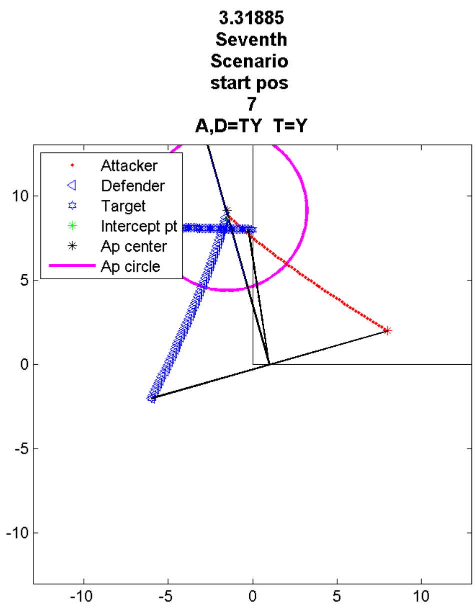

Figure 115. Position 7, Scenario 7

Appendix H.

8.1 Position 8

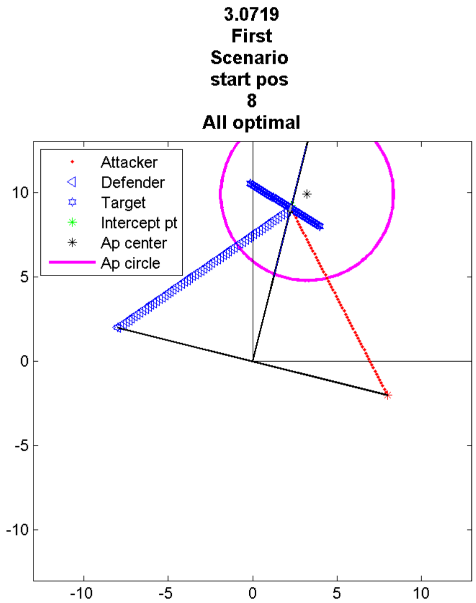

Figure 116. Position 8 Scenario 1

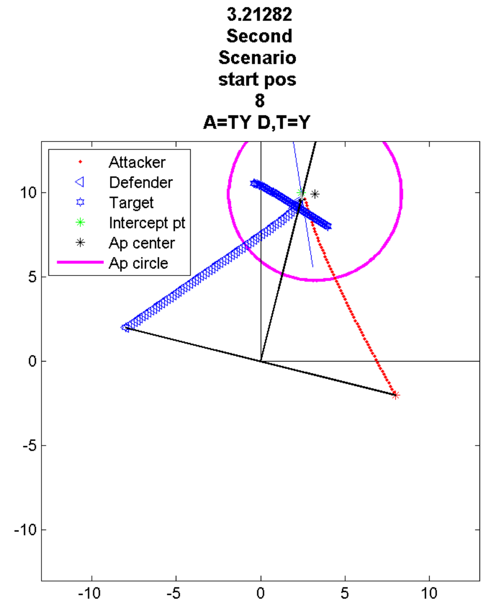

Figure 117. Position 8, Scenario 2

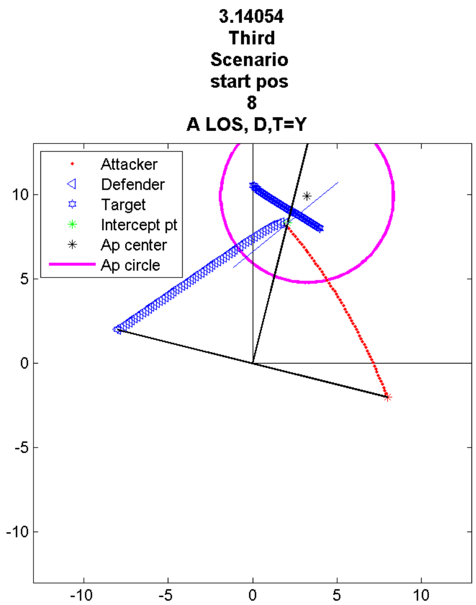

Figure 118. Position 8, Scenario 3

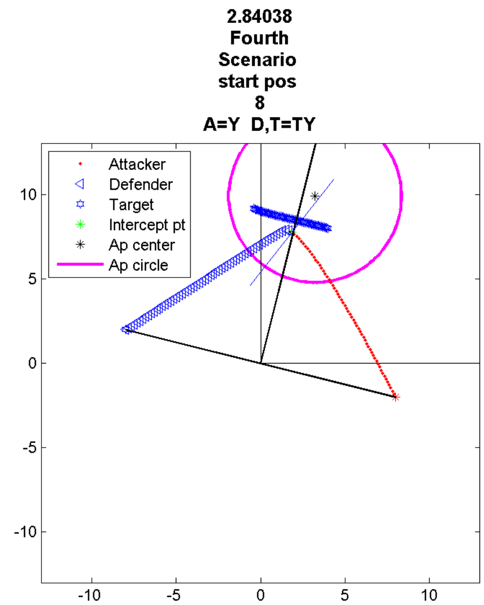

Figure 119. Position 8, Scenario 4

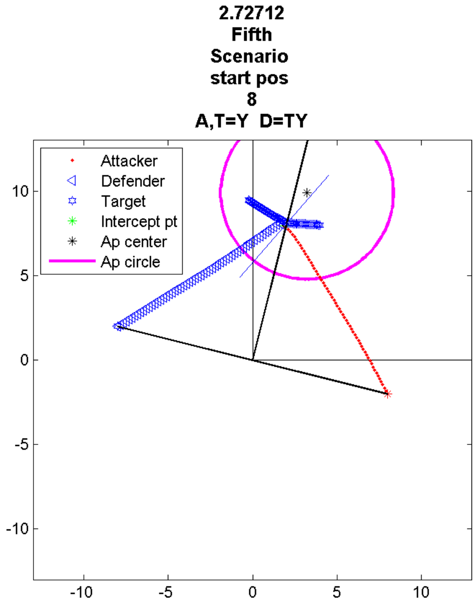

Figure 120. Position 8, Scenario 5

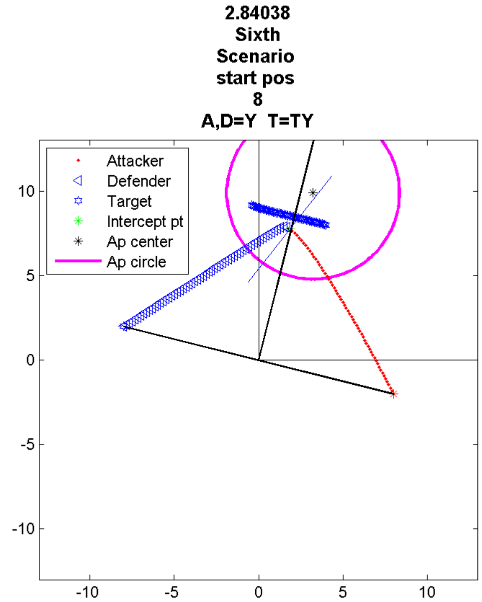

Figure 121. Position 8, Scenario 6

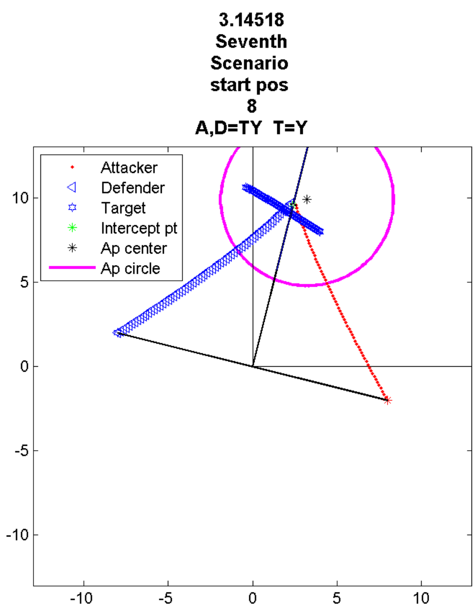

Figure 122. Position 8, Scenario 7

Appendix I.

9.1 Position 9

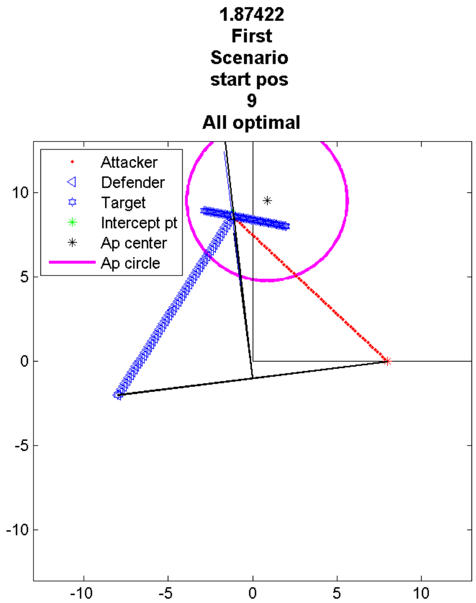

Figure 123. Position 9 Scenario 1

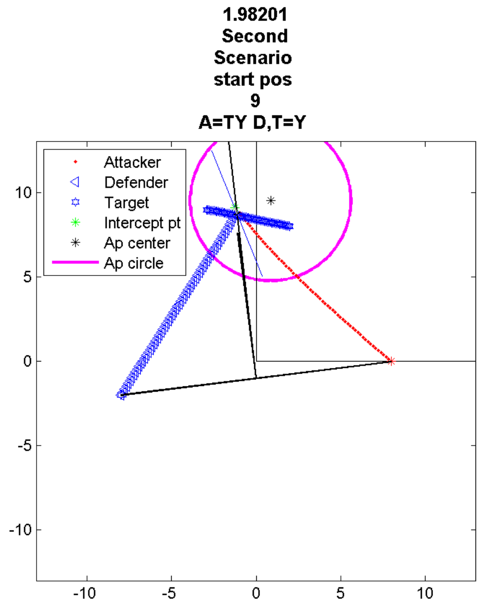

Figure 124. Position 9, Scenario 2

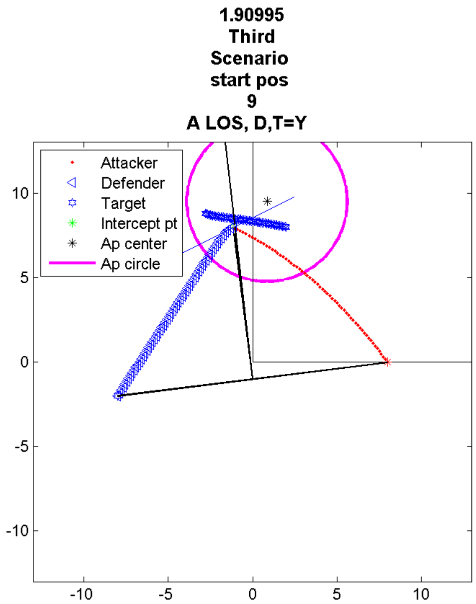

Figure 125. Position 9, Scenario 3

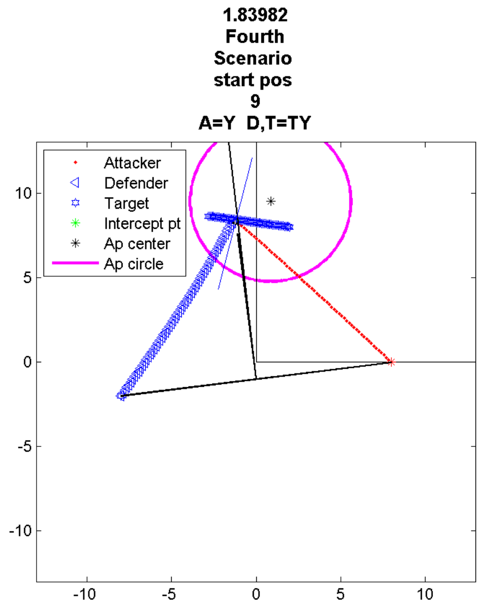

Figure 126. Position 9, Scenario 4

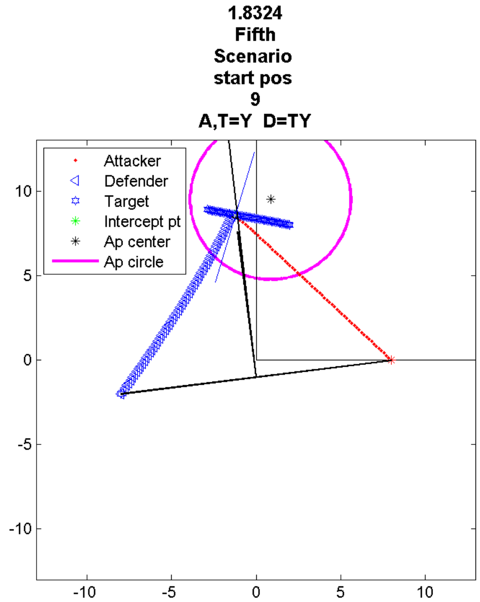

Figure 127. Position 9, Scenario 5

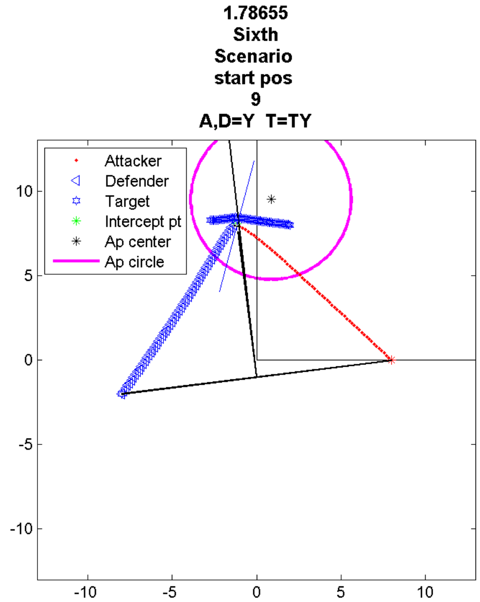

Figure 128. Position 9, Scenario 6

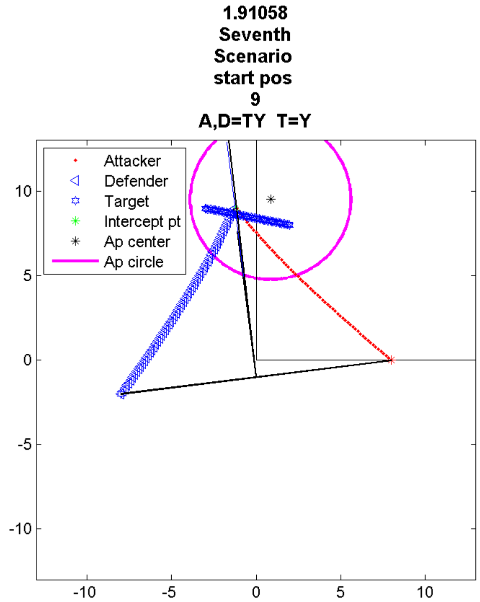

Figure 129. Position 9, Scenario 7

Appendix J.

10.1 Position 10

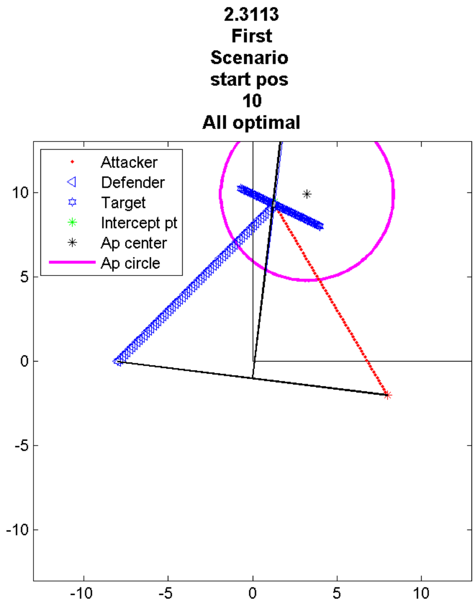

Figure 130. Position 10 Scenario 1

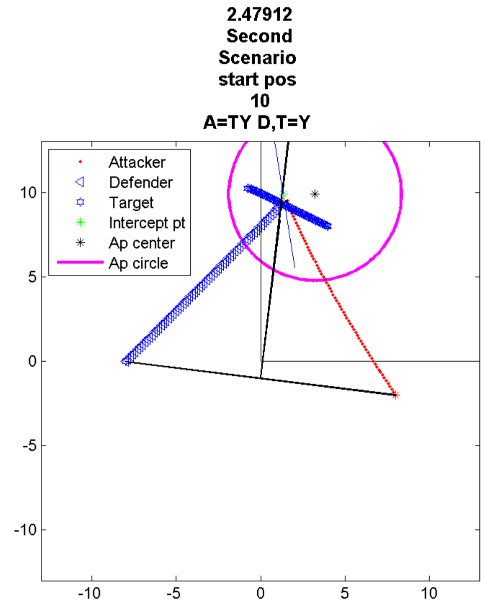

Figure 131. Position 10, Scenario 2

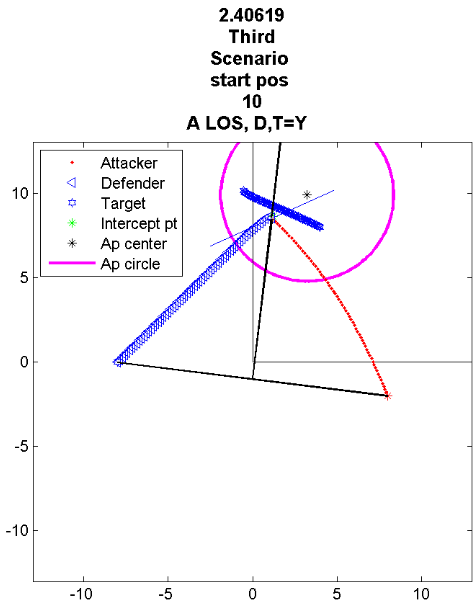

Figure 132. Position 10, Scenario 3

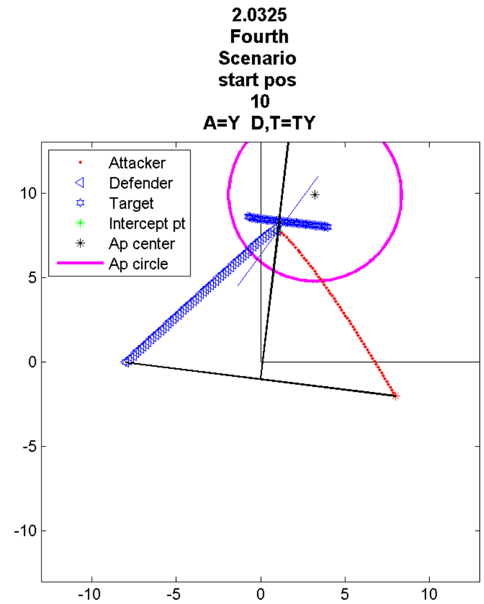

Figure 133. Position 10, Scenario 4

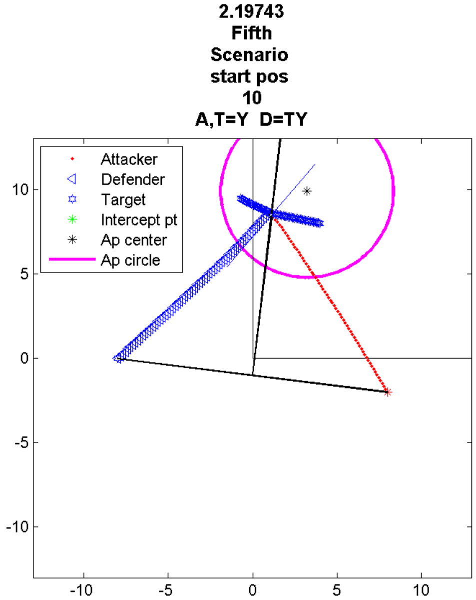

Figure 134. Position 10, Scenario 5

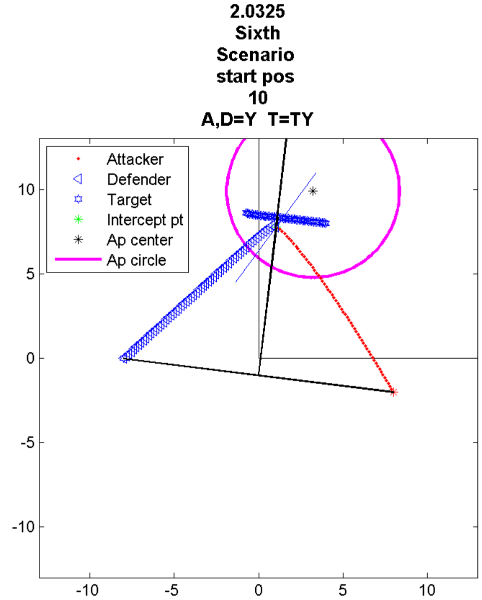

Figure 135. Position 10, Scenario 6

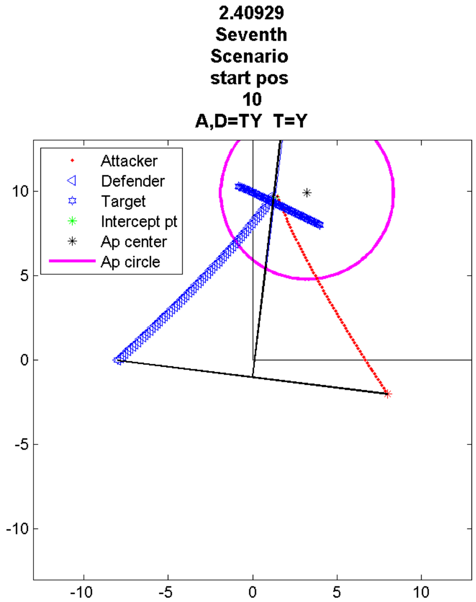

Figure 136. Position 10, Scenario 7

Appendix K.

11.1 Position 11

For the initial position of T, there is no strategy combination where D can aid T. T is captured by A at the boundry of the Apollonius circle.

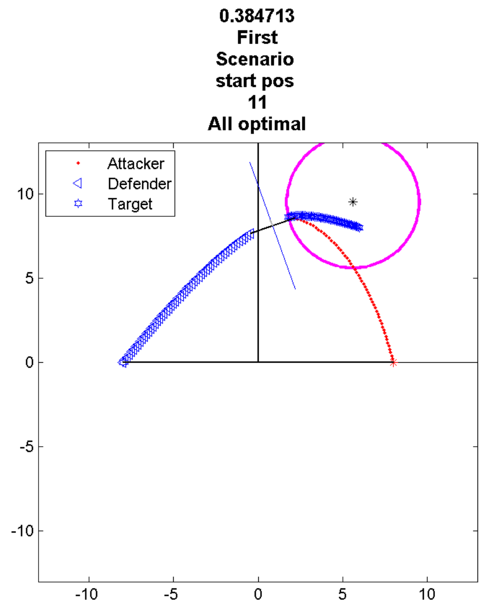

Figure 137. Position 11 Scenario 1

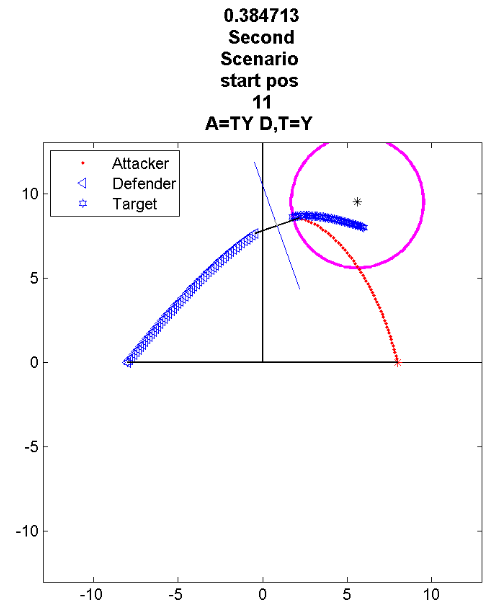

Figure 138. Position 11, Scenario 2

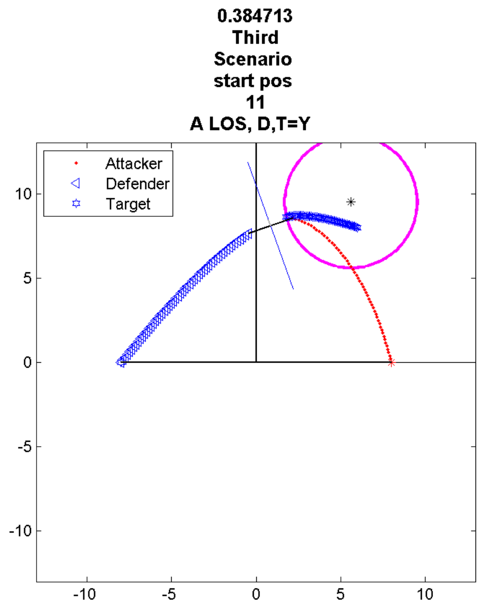

Figure 139. Position 11, Scenario 3

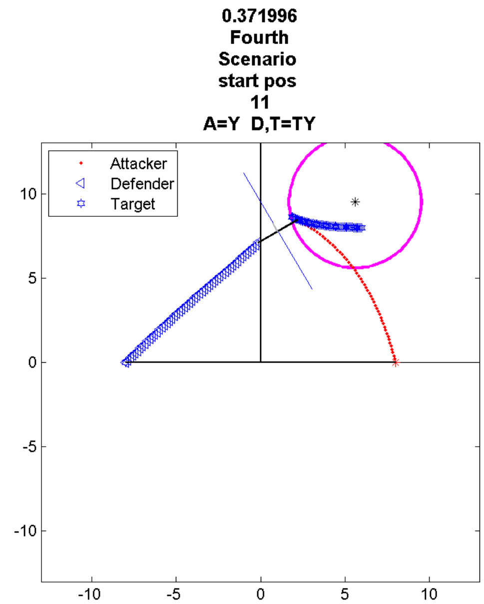

Figure 140. Position 11, Scenario 4

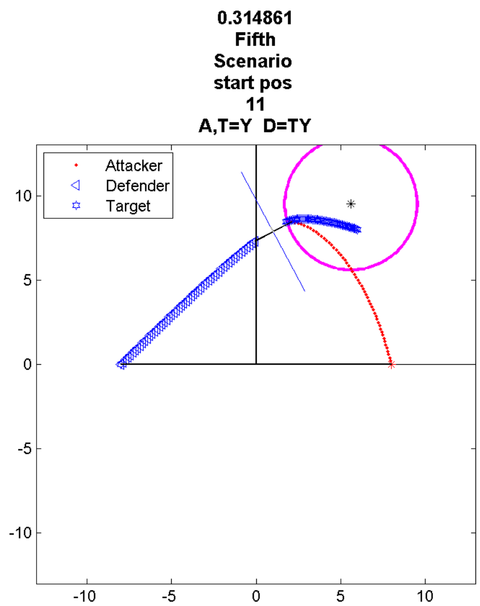

Figure 141. Position 11, Scenario 5

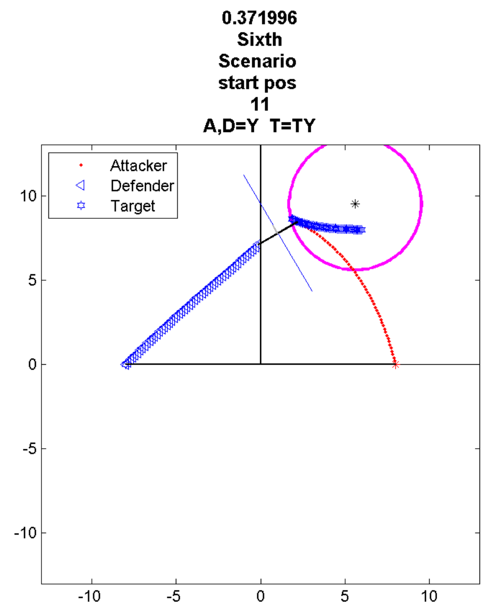

Figure 142. Position 11, Scenario 6

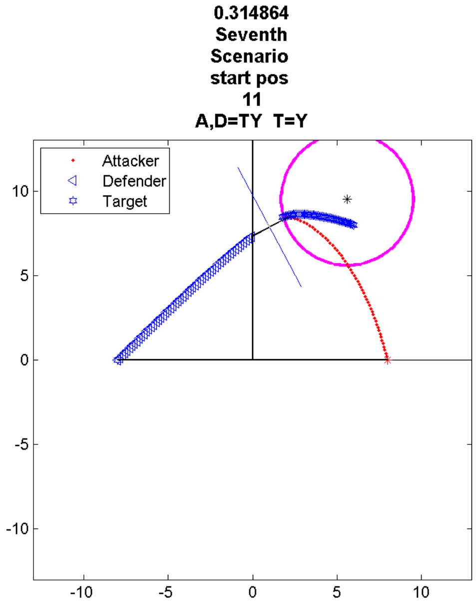

Figure 143. Position 11, Scenario 7

Appendix L.

12.1 DGT and OCT results

This section contains the plot for the Optimal Control Theory and the Differential Game Theory comparison for Scenario 3 and Scenario 7. The plots are of ten different starting positions for both scenarios.

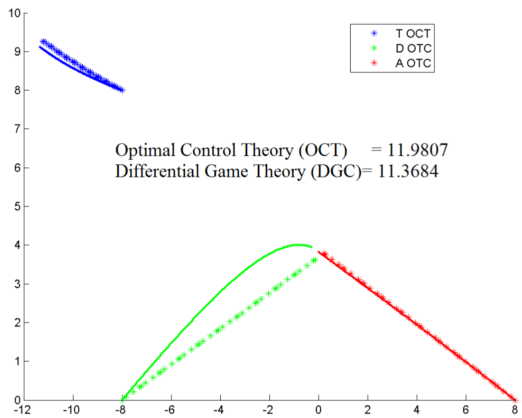

Figure 144. Scenario 3, Position 1

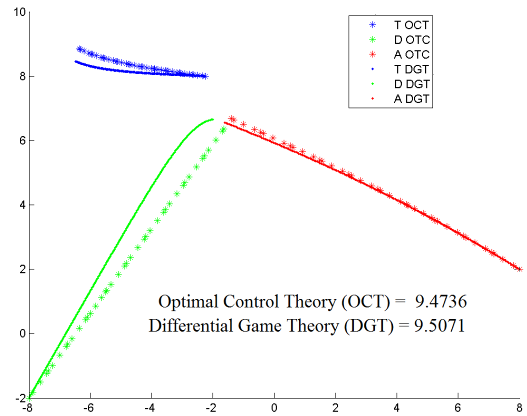

Figure 145. Scenario 3, Position 1

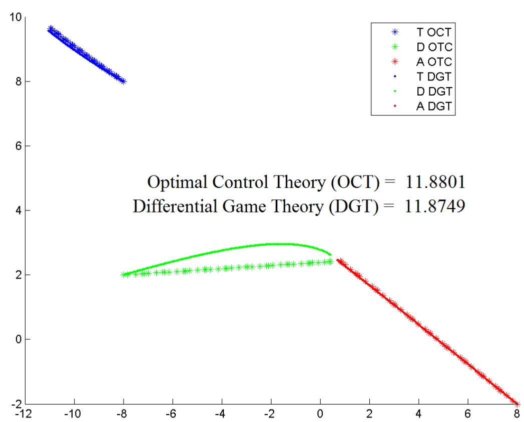

Figure 146. Scenario 3, Position 3

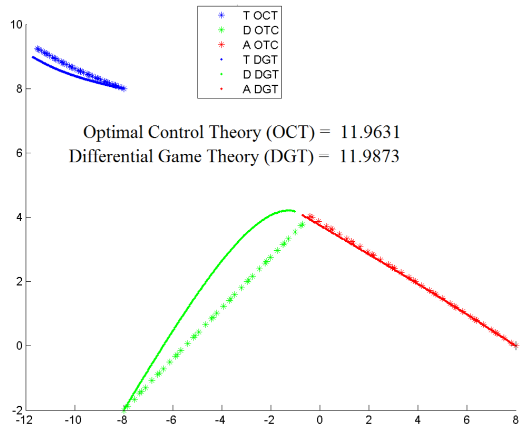

Figure 147. Scenario 3, Position 3

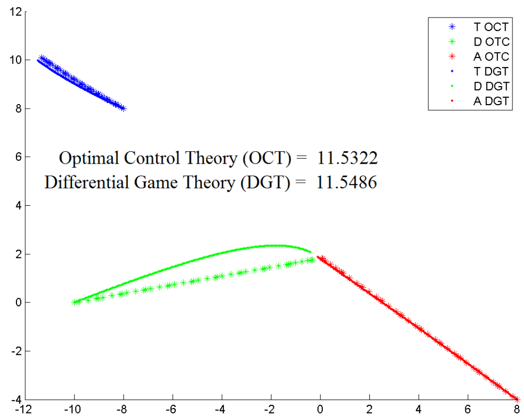

Figure 148. Scenario 3, Position 5

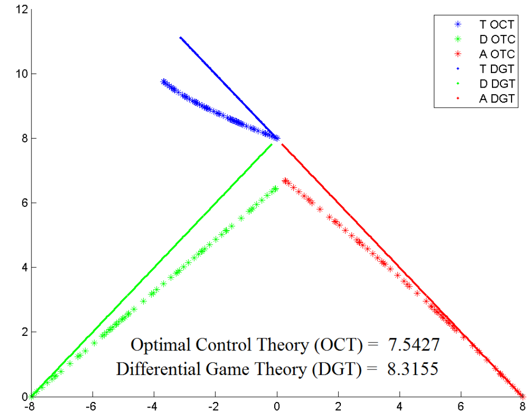

Figure 149. Scenario 3, Position 6

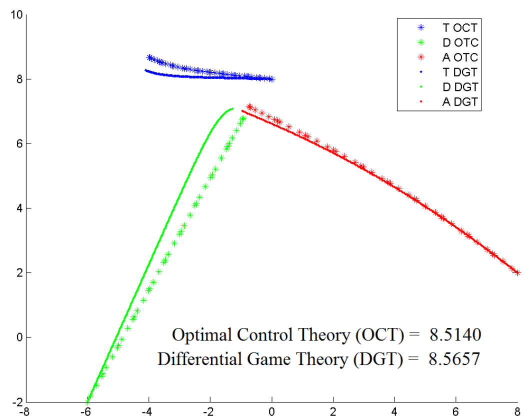

Figure 150. Scenario 3, Position 7

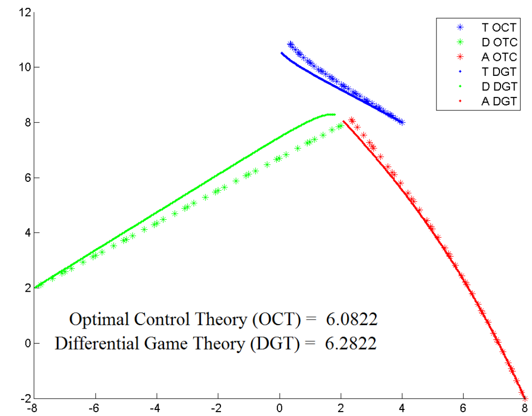

Figure 151. Scenario 3, Position 8

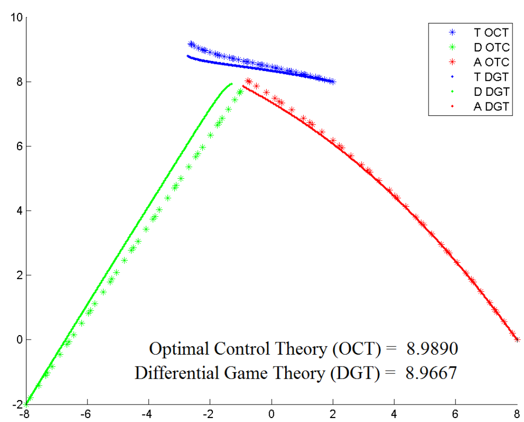

Figure 152. Scenario 3, Position 9

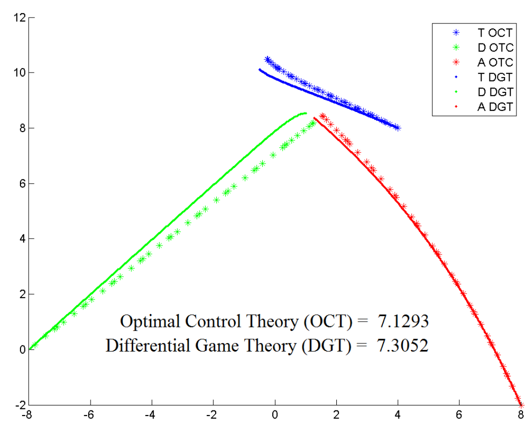

Figure 153. Scenario 3, Position 10

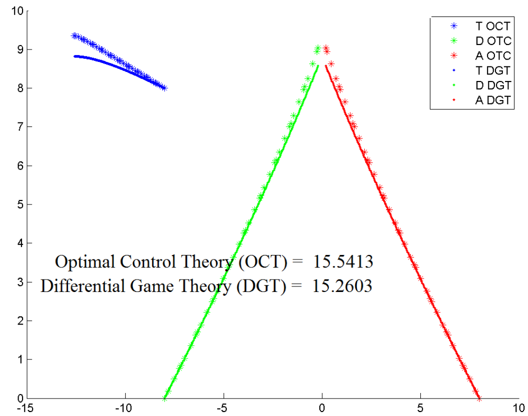

Figure 154. Scenario 7, Position 1

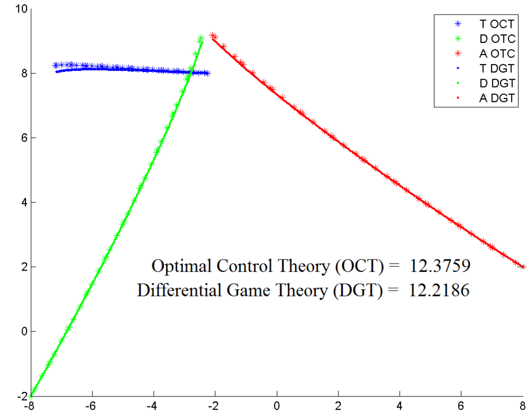

Figure 155. Scenario 7, Position 1

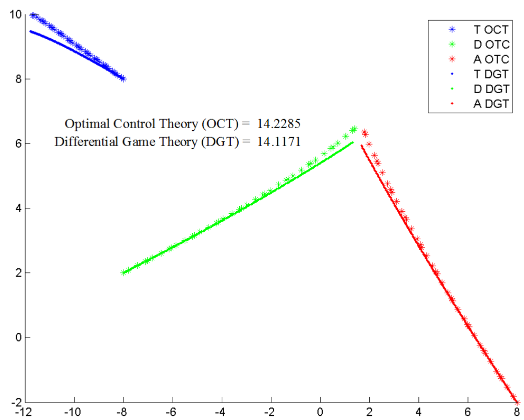

Figure 156. Scenario 7, Position 3

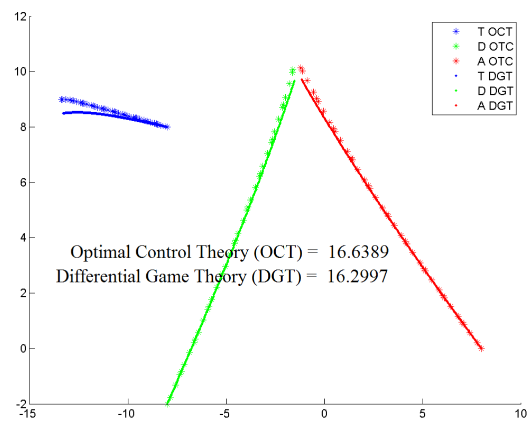

Figure 157. Scenario 3, Position 7

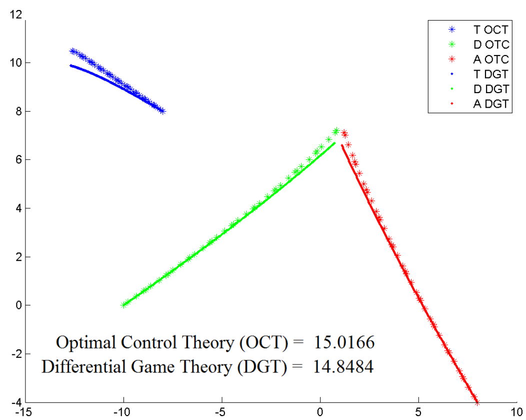

Figure 158. Scenario 7, Position 5

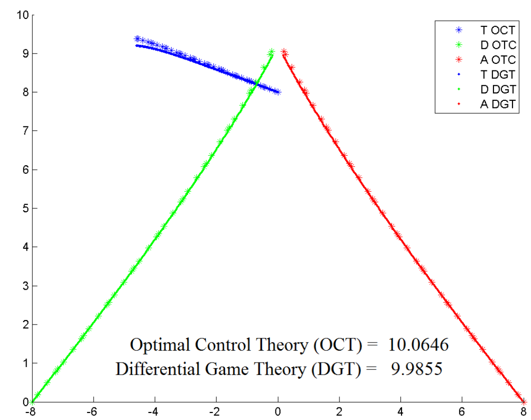

Figure 159. Scenario 7, Position 6

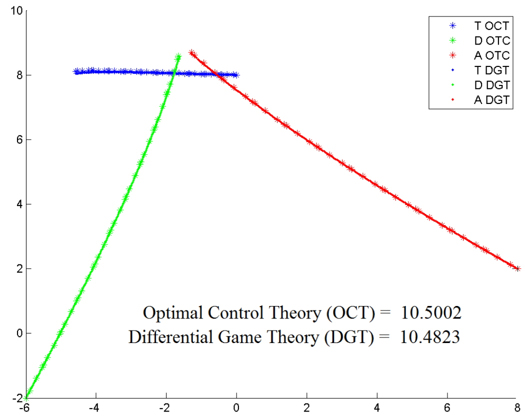

Figure 160. Scenario 7, Position 7

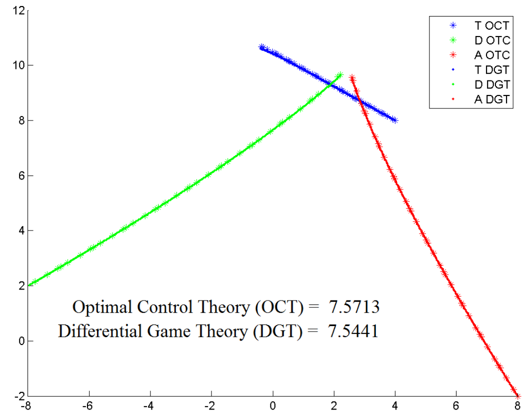

Figure 161. Scenario 7, Position 8

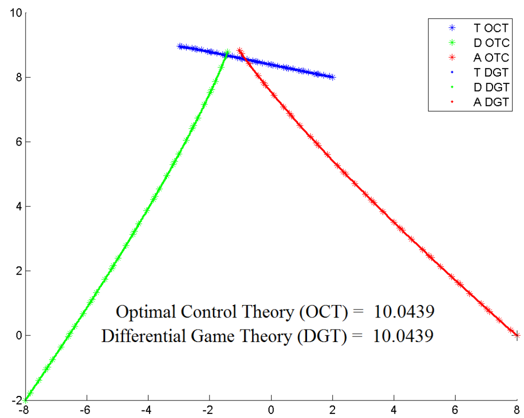

Figure 162. Scenario 7, Position 9

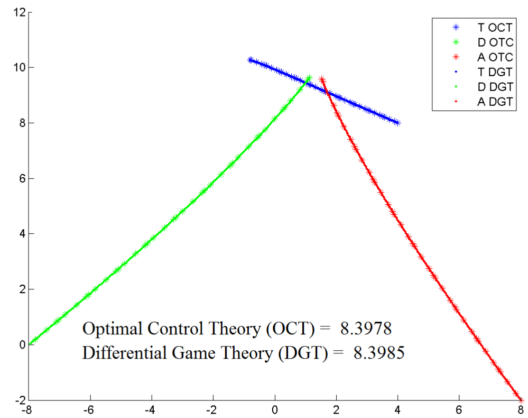

Figure 163. Scenario 7, Position 10

Bibliography

1. Anderson, Gerald M. "Comparison of Optimal Control and Differential Game Intercept Missile Guidance Laws". *Journal of Guidance, Control, and Dynamics*, 4(2):109–115, 1981.

2. Baba, Yoriaki, Makoto Yamaguchi, and Robert M Howe. "Generalized Guidance Law for Collision Courses". *Journal of Guidance, Control, and Dynamics*, 16(3):511–516, 1993.

3. Boyell, RL. "Counterweapon Aiming for Defense of a Moving Target". *Aerospace and Electronic Systems, IEEE Transactions On*, (3):402–408, 1980.

4. Bressan, Alberto. "Noncooperative Differential Games. A Tutorial". *Department of Mathematics, Penn State University*, 2010.

5. Cottrell, Ronald G. "Optimal Intercept Guidance for Short-Range Tactical Missiles". *AIAA Journal*, 9(7):1414–1415, 1971.

6. Fahroo, Fariba. "Dynamics and Control". url-http://www.wpafb.af.mil/library/factsheets/factsheet.asp?id=9196, December 2014. [Online; accessed 15-January-2015].

7. Garber, Vitalij. "Optimum Intercept Laws for Accelerating Targets". *AIAA Journal*, 6(11):2196–2198, 1968.

8. Ho, Yu-Chi, AE Bryson Jr, and Sheldon Baron. "Differential Games and Optimal Pursuit-Evasion Strategies". *IEEE Transactions on Automatic Control*, 10, 1964.

9. Hughes, Robin. "Israel Armor Protection System Revolutionary". *Janes Defense Weekly*, 16, 2005.

10. Isaacs, Rufus. *Differential games: A Mathematical Theory with Applications to Warfare and Pursuit, Control and Optimization*. John Wiley and Sons,Inc, 1965.

11. Kim, BJ. “The circle of Apollonius”. *Mathematics Education Program J. Wilson, EMAT*, 2009.

12. Oyler, Dave W, Pierre T Kabamba, and Anouck R Girard. “Pursuit-Evasion Games in the Presence of a Line Segment Obstacle”. *Proceedings of the53rd IEEE Conference on Decision and Control*, December(15-17), 2014.

13. Patterson, Michael A and Anil V Rao. “GPOPS-II: A MATLAB software for solving multiple-phase optimal control problems using hp-adaptive gaussian quadrature collocation methods and sparse nonlinear programming”. *ACM Transactions on Mathematical Software (TOMS)*, 41(1):1, 2014.

14. Perelman, Andrey, Tal Shima, and Ilan Rusnak. “Cooperative Differential Games Strategies for Active Aircraft Protection from a Homing Missile”. *Journal of Guidance, Control, and Dynamics*, 34(3):761–773, 2011.

15. Prokopov, Oleg and Tal Shima. “Linear Quadratic Optimal Cooperative Strategies for Active Aircraft Protection”. *Journal of Guidance, Control, and Dynamics*, 36(3):753–764, 2013.

16. Ratnoo, Ashwini and Tal Shima. “Line-of-sight Interceptor Guidance for Defending an Aircraft”. *Journal of Guidance, Control, and Dynamics*, 34(2):522–532, 2011.

17. Ratnoo, Ashwini and Tal Shima. “Guidance Strategies Against Defended Aerial Targets”. *Journal of Guidance, Control, and Dynamics*, 35(4):1059–1068, 2012.

18. Rusnak, Ilan. “The Lady, The Bandits, and The Bodyguards–A Two Team Dynamic Game”. *Proceedings of the 16th World IFAC Congress*. 2005.

19. Shima, Tal. "Optimal Cooperative Pursuit and Evasion Strategies Against a Homing Missile". *Journal of Guidance, Control, and Dynamics*, 34(2):414–425, 2011.

20. Shmakov, Sergei L. "A universal method of solving quartic equations". *Int. J. Pure Appl. Math*, 71(2):251–259, 2011.

21. Yamasaki, Takeshi, SN Balakrishnan, and Hiroyuki Takano. "Modified Command to Line-of-Sight Intercept Guidance for Aircraft Defense". *Journal of Guidance, Control, and Dynamics*, 36(3):898–902, 2013.

22. Yuan, Luke Chia-Liu. "Homing and Navigational Courses of Automatic Target-Seeking Devices". *Journal of Applied Physics*, 19(12), 1948.

REPORT DOCUMENTATION PAGE

Form Approved
OMB No. 0704–0188

1. REPORT DATE *(DD–MM–YYYY)*	2. REPORT TYPE	3. DATES COVERED *(From — To)*
26–03–2015	Master's Thesis	Sept 2013 — Mar 2015

4. TITLE AND SUBTITLE

Counter Weapon Control

5a. CONTRACT NUMBER

5b. GRANT NUMBER

5c. PROGRAM ELEMENT NUMBER

6. AUTHOR(S)

Roadruck, Brian J.

5d. PROJECT NUMBER

JON 15G454D

5e. TASK NUMBER

5f. WORK UNIT NUMBER

7. PERFORMING ORGANIZATION NAME(S) AND ADDRESS(ES)

Air Force Institute of Technology
Graduate School of Engineering and Management (AFIT/EN)
2950 Hobson Way
WPAFB OH 45433-7765

8. PERFORMING ORGANIZATION REPORT NUMBER

AFIT-ENG-MS-15-M-056

9. SPONSORING / MONITORING AGENCY NAME(S) AND ADDRESS(ES)

Air Force Office of Scientific Research Mathematics, Dynamic Systems and Control Division
Attn: Tristan Nguyen 875 N Randolph St
Ste 325 Rm 3112
Arlington AFB, VA 22203
COMM 503-426-7796 Email: Tristan.Nguyen@us.af.mil

10. SPONSOR/MONITOR'S ACRONYM(S)

AFMC/AFOSR-RTA

11. SPONSOR/MONITOR'S REPORT NUMBER(S)

12. DISTRIBUTION / AVAILABILITY STATEMENT

DISTRIBUTION STATEMENT A:
APPROVED FOR PUBLIC RELEASE; DISTRIBUTION UNLIMITED.

13. SUPPLEMENTARY NOTES

14. ABSTRACT

In this work, pursuit-evasion differential game theory is applied to the target defense scenario. The targets, attackers, and the defenders positional information is assumed to be known to the players. With positional information, a computational efficient method of strategy synthesis can be derived applying a differential game theory approach. We demonstrate that when non-optimal strategies are employed by one of the players, e.g. Line Of Sight guidance, the outcome will favor the players that employ the optimal strategy given by the solution of the pursuit-evasion differential game.

15. SUBJECT TERMS

Differential Game Theory

16. SECURITY CLASSIFICATION OF: a. REPORT	b. ABSTRACT	c. THIS PAGE	17. LIMITATION OF ABSTRACT	18. NUMBER OF PAGES	19a. NAME OF RESPONSIBLE PERSON
					Dr. Meir Pachter, AFIT/ENG
					19b. TELEPHONE NUMBER *(include area code)*
U	U	U	U	138	(937) 255-3636, x4555; meir.pachter@afit.edu